Assessment of Innovative Downstream Processing Methods for Microalgal β-Carotene Production

Dissertation
zur Erlangung des akademischen Grades

Doktoringenieur
(Dr.-Ing.)

von: Dipl.-Ing. Kristin Ludwig
geb. am: 31. Juli 1986
in: Lutherstadt Wittenberg

genehmigt durch die Fakultät für Verfahrens- und Systemtechnik
der Otto-von-Guericke-Universität Magdeburg

Promotionskommission:
Prof. Dr.-Ing. Evangelos Tsotsas (Vorsitz)
Prof. Dr.-Ing. Kai Sundmacher (Betreuer)
Prof. Dr.-Ing. Anja Drews (Gutachter)
Prof. Dr.-Ing. Stefanie Stute (Gutachter)

eingereicht am: 28. März 2018
Promotionskolloquium am: 15. August 2018

Abstract

In a time characterized by the constantly increasing environmental impact of industrial activities and a rising demand for food and energy, a more effective exploitation of biomass as well as alternative production strategies are asked for. One potential approach to meet these challenges is the cultivation of microalgae. Since decades, the producers of biomass and high-value products complement the product portfolio of chemical and agriculture industry. So far, only a few species are used commercially. Moreover, there is a great potential of process optimization to enhance the performance of several process steps in microalgal production and getting more competitive compared to conventional production plants. Especially the optimization of the downstreaming route bears the potential to realize huge energy and cost savings.

The present work evaluates several innovative approaches for the downstream route of industrial β-carotene production with *Dunaliella salina* based on experimental efforts and a profitability analysis. Therefore, a realistic reference process scheme is introduced providing a benchmark for comparison with the investigated process alternatives. The reference process is characterized by the biomass and product generation in open ponds, a dewatering step using centrifugation and a pigment extraction unit by the organic solvent hexane.

Aiming for the reduction of the high cost of centrifugation energy, flocculation was examined as potential preconcentration method of *D. salina*. So far, flocculation is primarily used to separate a liquid product from waste particles. To assess its applicability for β-carotene production, diverse strategies were analyzed, namely flocculation by cationic metal ions by means of metal salt addition or electrolysis as well as flocculation by pH increase. Among all investigated flocculants, $FeCl_3$ and NaOH performed most effective. However, with respect to interactions of the flocculant with other process steps, NaOH revealed inhibitory effects on medium recycling and product extraction yields. The calculation of energy demands and operating costs demonstrated, that flocculation is not a favorable preconcentration strategy for *D. salina* biomass.

In addition, supercritical CO_2 ($scCO_2$) extraction was compared with conventional hexane extraction. According to pilot scale examinations, a parameter set-up using 500 bar and 70 °C results in the most efficient extraction. Moreover, the addition of 10% ethanol as entrainer of the solvent stream significantly increased the product yield. The calculation of the techno-economic properties indicated a higher energy consumption of $scCO_2$ which is however compensated by lower solvent costs. Thereby comparable β-carotene production costs to the reference method with hexane were estimated. The green solvent $scCO_2$ and its co-solvent ethanol are rated to be more environmental friendly and more appropriate for application in the food and medical sector. Accordingly, $scCO_2$ is recommended for the extraction of the pigment from *D. salina* biomass.

Finally, the potential of mild hydrothermal liquefaction (mHTL) to valorize biomass remnants after β-carotene extraction was discussed. The large carbohydrate fraction of the residuals was recovered in the aqueous reaction phase already at hydrolysis conditions. Here, the main-product was a glucose-rich solution which was successfully applied as carbon source of diverse microorganisms with biotechnological relevance. The techno-economic analysis indicated the beneficial effect of a process plant expansion by the unit of mHTL on the overall process economic. It was demonstrated, that a low energy input allows the production of a valuable by-product and an optimal exploitation of the biomass waste in the process. With these findings, first steps were done towards the realization of a holistic biorefinery concept which creates an economic as well as ecologic added-value in the β-carotene process.

In conclusion, the underlying thesis highlights the optimized interaction of experimental and techno-economic analyses for the realistic assessment of innovative technologies in marine biotechnology. Triggered by the application of the species-specific experimental data, a reliable evaluation of the potential of all investigated downstreaming techniques as well as the consideration of interactions between process units were possible. With that, a new evaluation concept was introduced and successfully verified based on the example of industrial β-carotene production.

Zusammenfassung

In einer Zeit von steigender Umweltbelastung infolge industrieller Aktivitäten und zunehmender Nahrungsmittelknappheit ist die effektive Ausnutzung nachwachsender Rohstoffe und die Etablierung alternativer Produktionskonzepte unabdingbar geworden. Ein möglicher Ansatz diesen Problembereich zu adressieren, ist die industrielle Kultivierung von Mikroalgen. Diese Produzenten von Biomasse und hochpreisigen Gütern ergänzen nunmehr seit Jahrzehnten das Produktportfolio konventioneller Prozesse aus Landwirtschaft und chemischer Industrie. Jedoch werden derzeit nur wenige Mikroalgen-Spezies industriell genutzt. Zudem existiert ein enormer Optimierungsbedarf der einzelnen Prozessschritte, um bestehende und zukünftige Produktionsanlagen wettbewerbsfähig zu gestalten und Algen als gängige Produktionsorganismen zu etablieren. Bei der Umsetzung dieser Vision kann vor allem die Verwendung geeigneterer Methoden der Downstream Prozessroute zu beträchtlichen Einsparungen von Kosten und Energiebedarfen führen.

In der vorliegenden Arbeit werden innovative Alternativen für die Aufarbeitungsstrecke industrieller β-Carotin Produktion durch die grüne Mikroalge *Dunaliella salina* experimentell analysiert und auf ihre Wirtschaftlichkeit vor dem Hintergrund des Gesamtprozesses bewertet. Dazu wird zunächst ein realitätsnahes Referenzprozessschema vorgestellt, das als Vergleichsgrundlage der untersuchten Methoden dient.

Mit dem Ziel, die hohen Erntekosten durch Zentrifugation zu reduzieren, wurde als erstes die Flockung als potentielle Vorkonzentrationsmethode untersucht. Um die Anwendbarkeit der Methode im β-Carotin-Prozess zu bewerten, wurden unterschiedliche Flockungsstrategien analysiert: die Flockung mithilfe multivalenter Metall-Kationen durch Zugabe von Metallsalzen oder die Anwendung von Elektrolyse sowie die Flockung durch pH-Wert Erhöhung. Des Weiteren konnte der Einfluss dieses Prozessschrittes auf andere Schritte im Gesamtprozess gezeigt werden. Unter allen Flockungsmitteln erwiesen sich $FeCl_3$ und NaOH als besonders effektiv. Dabei wirkte sich letzteres negativ auf den Mediumrecycle, als auch auf die β-Carotin Extraktion aus. Die Kalkulation des Energiebedarfes und der Betriebskosten

bestätigte die Untauglichkeit der Flockung als Vorkonzentrationsstrategie in der *D. salina* Produktion.

Im nächsten Schritt wurde die überkritische CO_2 ($scCO_2$) Extraktion mit der konventionellen Hexan-Extraktion verglichen. In einer experimentellen Studie im Pilotmaßstab stellten sich die Betriebsparameter 500 bar und 70 °C als vielversprechend dar. Zudem verbesserte der Zusatz von 10% Ethanol als Kosolvent die Produktausbeute merklich. Die finale Bewertung der Methode durch die Berechnung von Energieverbräuchen und Operationskosten ergab, dass die Nutzung von $scCO_2$ zwar höhere Energiekosten aber vergleichbare Prozesskosten zum Referenzlösungsmittel Hexane verursacht. Das grüne Lösungsmittel und sein Kosolvent werden aufgrund ihres weniger umweltschädlichen Charakters als nachhaltiger und unbedenklicher beim Einsatz im Nahrungsmittel- und Medizinsektor eingestuft. Somit empfiehlt sich sein Einsatz bei der β-Carotin Extraktion algaler Biomasse.

Im letzten Teil der Arbeit wurde die milde hydrothermale Verflüssigung als potentielles Verfahren zur Aufwertung vorhandener Restbiomasse im Prozess diskutiert. Der hohe Kohlenhydratgehalt der Restbiomasse konnte bereits unter Hydrolysebedingungen effektiv in das wässrige Reaktionsprodukt extrahiert werden. Dabei wurde hauptsächlich Glukose gebildet, die in Form der wässrigen Phase als Kohlenstoffquelle verschiedener Produktionsorganismen der Biotechnologie eingesetzt werden konnte. Die techno-ökonomische Analyse ergab, dass sich diese Prozesserweiterung vorteilhaft auf die Prozess-Ökonomie auswirken kann. Zum einen kann durch einen geringen Energieaufwand ein wertvolles Nebenprodukt hoher Relevanz für den Markt erzeugt werden; zum anderen erlaubt die Methode eine optimale Verwertung der Restbiomasse. So wurden erste Schritte in Richtung eines Bioraffinerie-Konzeptes realisiert, welches sowohl einen ökologischen als auch ökonomischen Mehrwert erzielen kann.

Zusammenfassend betrachtet, veranschaulicht die vorliegende Arbeit das optimale Zusammenspiel experimenteller Analysen mit techno-ökonomischer Betrachtungen zur realitätsnahen Bewertung innovativer Prozessstrategien in der Algenbiotechnologie. Durch Integration der spezies-spezifischen experimentellen Daten konnten die tatsächlichen Potentiale der einzelnen Methoden im Hintergrund des Gesamtprozesses eingeschätzt und Abhängigkeiten zwischen den Verfahrensschritten berücksichtigt werden. Hierfür wurde ein neues Evaluierungskonzept vorgestellt, das erfolgreich am Beispiel der industriellen β-Carotin Produktion verifiziert werden konnte.

Acknowledgements

In this thesis I present most of my work I have conducted from October 2011 – December 2017 as an employee at the Max Planck Institute for Dynamics of Complex Technical Systems and Otto von Guericke University Magdeburg, Germany.

First and foremost, I would like to express my gratitude to Prof. Dr.-Ing. Kai Sundmacher for the challenging topic, the trust and scientific freedom in letting me explore and contribute to the research field of microalgae biotechnology. I am very grateful for his support and demands on a wide range of activities, including publications, conference contributions, student supervisions and teaching. My special thanks goes to Dr. Liisa Rihko-Struckmann for all the time spent on the supervision of my thesis and for her readiness for scientific discussion.

I further express my gratitude to Prof. Dr.-Ing. Stephanie Stute and Prof. Dr.-Ing. Anja Drews for accepting the invitation to peer review my thesis. Additionally, I would like to thank Prof. Ami Ben-Amotz for providing some helpful information of his *D. salina* production site in Israel and the team of the Fraunhofer CBP in Leuna for supporting my $scCO_2$ extraction experiments.

Much gratitude goes to Melanie Fachet and Robert Flassig. I do not only value the helpful discussions, your continuous support and shared knowledge, but also the great moments we had working together. I am very grateful for the time I could spend with my colleagues and friends from the Max Planck Institute for Dynamics of Complex Technical Systems and Otto-von-Guericke University Magdeburg. In particular I want to mention Claudia Bednarz, Stefanie Leuchtenberg, Philipp Erdrich, Adriana Kozlowski, Ruxandra Rehner, Christiane Rudolf and Peter Schulze.

This work has also benefited from contributions of several lab technicians and engineers. My special thanks go to Saskia Nickel, Anne Christin Reichelt, Bianka Stein and Markus Ikert for their continuous assistance, their motivating and fruitful discussions and their excellent work. Furthermore, I would like to thank Patrick Siegmund and Torsten Schröder for their technical support. In these lines, I would like to thank the mechanical and electric workshop members Detlef Franz, Stefan Hildebrandt, Steve Haltenhof,

Klaus-Dieter Stoll, Reiner Könning and Martin Stengel. This work has also benefited from contributions of several students, which have conducted their study research, bachelor or master thesis within my supervisions. I would like to thank Thomas Fläschel, Kay Eilers, Andreas Eichel, Theresa Lau and Nadine Hellmond for their support and enthusiasm. It was a pleasure to work with all of you.

Finally, I would like to express my gratitude to my family and friends for your motivation, support, trust and love. Special thanks goes to a very special person in my life who contributed in making this work possible. Thank you my dear Stefan for your patience, encouragement and love during these years and for giving me such a wonderful time with our daughter Hilda.

There are so many other persons, unfortunately too many to mention, who supported me during the time as a PhD student. Thank you all.

Contents

Notation

Greek symbols

γ_l^-	Electron donor parameter of the liquid	J m^{-2}
γ_s^-	Electron donor parameter of the particle	J m^{-2}
γ_l^+	Electron acceptor parameter of the liquid	J m^{-2}
γ_s^+	Electron acceptor parameter of the particle	J m^{-2}
γ_l^{AB}	Polar surface component of the liquid	J m^{-2}
γ_s^{AB}	Polar surface component of the particle	J m^{-2}
γ_l^{LW}	Apolar probe liquid surface energy component	J m^{-2}
γ_s^{LW}	Apolar particle surface energy component	J m^{-2}
δ	Solubility parameter	cal$^{0.5}$ cm$^{-1.5}$
ϵ	Dielectric constant of the medium	F m^{-1}
ζ	ζ-potential of the surface	mV
η_E	Extraction efficiency	-
η_{ex}	Heat exchanger efficiency	-
η_f	Dynamic viscosity of a fluid	kg m^{-1} s^{-1}
η_H	Harvesting efficiency	-
η_v	Evaporation efficiency	-
θ	Contact angle	$^\circ$
κ	Debye length	m
λ_{max}	Wavelength at the absorption maximum	nm
μ	Average value	-
$\Delta\nu_i$	Molecular volume of species i	cm^3 mol^{-1}
ν_c	Capacity of the centrifuge	m^3 h^{-1}
ρ	Density	kg m^{-3}
σ	Standard deviation	-
$\Phi_{PSII,max}$	Maximum quantum efficiency of PSII	-
ψ	Surface potential	mV

Latin symbols

A	Hamaker constant	J

A_T	Surface area of mass transfer	m^2
a	Radius of the alga	m
CF	Concentration factor	-
$C_{i,k}$	Mass flow of chemicals	kg d^{-1}
c	β-carotene concentration	mg g_{dw}^{-1}
c_{algae}	Mass concentration of the algae slurry	kg m^{-3}
c_f	Flocculant doses	g kg_{dw}^{-1}
c_{p_i}	Heat capacity of species i	kJ kg^{-1} K^{-1}
c_i	Solute concentration	mol m^{-3}
D_{is}	Diffusion coefficient of solute i into solid s	m^2 s^{-1}
d_e	Effective diameter	m
d_{max}	Maximal diameter of a particle	m
d_{min}	Minimal diameter of a particle	m
d_p	Diameter of a particle	m
E_c	Energy consumption centrifuge	kWh
E_H	Energy consumption electrolysis	kWh kg_{dw}^{-1}
$E_{j,k}$	Energy consumption of utility j in step k	kWh d^{-1}
ΔE_v	Energy of vaporization	cal mol^{-1}
Δe_{v_i}	Energy of vaporization of species i	cal mol^{-1}
e	Electron charge	C
ΔG_{coh}	Free energy of cohesion	J or k_bT
F_0	Minimal fluorescence of dark adapted cells	-
F_m	Maximal fluorescence of dark adapted cells	-
$F_{i,k}^{in}$	Raw material stream of component i in step k	kg d^{-1}
$F_{i,k}^{out}$	Product stream of component i in step k	kg d^{-1}
F_v	Variable fluorescence of dark adapted cells	-
G_E	Electrostatic interaction	J or k_bT
G_{LW}	Lifshitz-Van der Waals interaction	J or k_bT
GR	Gross revenue	USD d^{-1}
G_{tot}	Free energy of interaction	J or k_bT
g	Gravitational acceleration	m s^{-1}
H	Separation distance	m
H_0	Minimum separation distance	m
HHV_{Boie}	Heating value according to Boie (1953)	MJ kg^{-1}
h_i	Specific enthalpy of species i	kJ kg^{-1}
$h_{v_{EtOH}}$	Evaporation enthalpy of EtOH	kJ kg^{-1}
h_1	Fill level suspension	m
h_2	Height of sedimented algae	m
h_m	Measuring height	m
I	Current	A
k_b	Boltzmann constant	J K^{-1}
n_i	Number concentration of ionic species i	m^{-3}
M_{Al}	Molecular mass of aluminum	kg mol^{-1}
m_{Al}	Mass of dissolved aluminum	kg
m_{EtOH}	Mass of EtOH	kg
$\dot{M}_i$	Rate of mass transfer of solute i	mol s^{-1}
m_{dw}	Dry weight of the biomass	kg
m_F	Remaining flocculant mass	kg kg_{dw}^{-1}
m_i	Mass of species i	kg

m_{s_i}	Mass of solvent i	kg
OC	Operating cost (net)	USD d^{-1}
$P_{1,i}$	Price of raw materials	USD kg^{-1}
P_2	Cost of electrical power	USD kWh^{-1}
$P_{3,i}$	Cost of chemicals	USD kg^{-1}
$P_{4,i}$	Cost of waste	USD kg^{-1}
$P_{5,i}$	Sale price of the product	USD kg^{-1}
P_c	Motor power centrifuge	kW
P_{E_i}	Electrical power of compression for solvent i	kJ h^{-1}
p_c	Critical pressure	bar
Q_{h_i}	Heating energy extraction	kJ
Q_{c_i}	Cooling energy extraction	kJ
$Q_{e_{EtOH}}$	Evaporation energy extraction	kJ
$R_{i,kk}$	Recycling stream	kg d^{-1}
S	Relative solubility	-
S_e	Experimental determined solubility	mg g^{-1}
T_b	Boiling point	K
T_c	Critical temperature	K
t	Time (t_0 start time,t_{end} end time)	min
t_E	Extraction time	h
V	Volume	m^3
v_p	Sedimentation velocity of a particle	m s^{-1}
$W_{i,k}$	Waste stream	kg d^{-1}
y_{max}	Maximum extraction yield	-
z	Extraction distance	m
z_i	Charge number of ionic species i	-

Abbreviations

BHT	Butylated hydroxytoluene
EPA	Eicosapentaenoic acid
CCAP	Culture Collection of Algae and Protozoa
CER	Constant extraction rate
COP	Coefficient of performance
DHA	Decosahexaenoic acid
DLVO	Derjaguin-Landau-Verwey-Overbeek
DMF	Dimethylformamide
DMSO	Dimethyl sulfoxide
EDTA	Ethylenediaminetetraacetic acid
EtOH	Ethanol
FDA	Fluorescein diacetate
GC	Gas chromatography
GRAS	Generally regarded as safe
HEPES	4-(2-hydroxyethyl)-1-piperazineethanesulfonic acid
HPLC	High performance liquid chromatography

HMF	Hydroxylmethylfurfural
IC	Ion chromatography
ICP-OES	Inductively coupled plasma optical emission spectrometry
LCA	Life cycle assessment
MeOH	Methanol
MTBE	Methyl tert-butyl ether
NTB	Natural Beta Technology
OD	Optical density, absorption
PAM	Pulse amplitude modulation
PBR	Photobioreactor
PSII	Photosystem II
PUFA	Polyunsaturated fatty acids
SCF	Supercritical fluid
SCFE	Supercritical fluid extraction
$scCO_2$	Supercritical carbon dioxide
SAG	Culture Collection of Algae at Goettingen University
STR	Stirred tank reactor
TAG	Triacylglyceride
THF	Tetrahydrofuran
TEA	Techno-economic assessment
UV/Vis	Ultraviolet visible

List of Figures

LIST OF FIGURES

List of Tables

LIST OF TABLES

1

Introduction

1.1 Motivation of the thesis

Nowadays, the global demand for green products and renewable resources is growing steadily as fossil feedstocks are running out and people ask for an environmentally aware lifestyle. Biomass for feed and food is replacing petroleum as energy source which raises its global demand. Biotechnological production of microalgae became an essential alternative to satisfy these needs. They have the great potential to produce a variety of interesting products for the nutrition, pharmaceutical and cosmetic industry by the biochemical conversion of the inexhaustible resources sunlight and carbon dioxide (Borowitzka, 2013; Griehl & Bieler, 2011; Mobin & Alam, 2017; Wijffels *et al.*, 2010). Furthermore, microalgae are also intensively discussed as alternative feedstock of CO_2-neutral second-generation biofuels production (Carriquiry *et al.*, 2011). One great advantage of microalgae is their ability to populate non-agricultural areas which avoids the undesired competition with arable cropland. So far, an annual algae biomass generation of more than 10.000 tonnes is estimated with a growing tendency (Benemann, 2008).

Nevertheless, there are still drawbacks in microalgal based processes needed to be overcome to be more competitive with conventional industrial production approaches. Primarily, the cost of production has to be reduced (Koller *et al.*, 2012). A great potential of improvements is given by the downstream processing, accounting for 50-80% of the overall production costs (Molina Grima *et al.*, 2003). However, in the past years extensive research and development was done especially in the direction of upstream processes such as the design of photobioreactor or genetic engineering (overview in Vandamme (2013)).

Most commercial microalgae based processes have been established in the 1970s–1990s (Richmond, 2007). Since then, great scientific efforts have been devoted to the discovery of further promising production strains as well as the development of innovative techniques for algal cultivation and processing. Accordingly, an increase of the

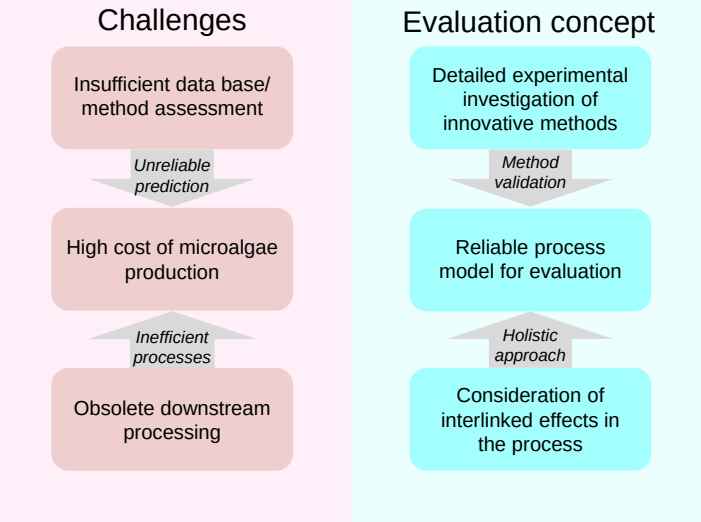

Figure 1.1: Challenges in the field of microalgae production addressed by the evaluation concept of the present thesis.

performance of existing production sites or the development of new production processes are still relevant issues in microalgal biotechnology. To evaluate such state of the art technologies, techno-economic assessment has been established as an efficient tool (Quinn & Davis, 2015). Every microorganism strain requires an individual processing concept regarding cultivation and product recovery to achieve optimal product quantity and quality. However, most of these techno-economic studies were done without the consideration of the individual species properties (overview in Ribeiro & Silva (2013)). The predictions may help to roughly understand the potential of commercial microalgae production but do not allow reliable statements about the benefits and feasibility of a specific investigation. Furthermore, most of the published microalgae process analyses are dealing with the production of biofuels (e.g. Davis *et al.* (2011); Delrue *et al.* (2012); Lundquist *et al.* (2010) or (Benemann & Oswald, 1996)) whereas the potential of high-value products is rarely discussed.

In addition, the experimental studies in the field of microalgae processing are usually focused only on the efficiency of the applied techniques. Less work is done in analyzing the impacts of a certain method on other up- or downstream steps in the overall production chain (t Lam *et al.*, 2018). However, these dependencies are needed to be identified before moving from lab- to full-scale installations.

Commercial β-carotene production by the green microalga *D. salina* is used as a case study to address all the above-mentioned issues (see also Fig. 1.1) in the present work. There are diverse factors provoking a challenging downstream processing of the alga. For

example, the extremely low cell densities reached in production scale entail a complex and cost-intensive dewatering procedure. Moreover, the pigment extraction is done by conventional organic solvents which can be critical regarding the product quality losses caused by solvent residues. Hitherto, there is no beneficial use of remnant biomass after the main-product extraction (Harvey, 2017). As the remnant accounts for up to 90% of the generated biomass, potential by-products are wasted in the industrial process. Taking a closer look at all these challenges, the great improvement potential of the β-carotene process becomes apparent making the process interesting for the underlying case study.

1.2 Research aims of the thesis

The objectives of the current study are:

1. to develop an evaluation platform by means of an overall process model which can be applied for the assessment of innovative downstream processing methods in microalgal production, especially for the aforementioned β-carotene production by *D. salina*,
2. to identify potential downstream processing methods for the dewatering, the product extraction and the residual biomass exploitation,
3. to find optimal parameter set-ups for the identified methods and uncover their effects on other process units,
4. to incorporate the results in the overall process model for the calculation of the energetic and economic footprints of the alternative process routes and
5. to quantify uncertainties of the used data by means of Monte Carlo simulations.

1.3 Structure of the thesis

This document consists of seven chapters. Starting with Chapter 2, a brief overview of the state of the art methods used in the up- and downstream paths of microalgae farming is presented. Furthermore, existing microalgal products are presented and the alga of interest, *D. salina*, is introduced. In Chapter 3 the reference process model for β-carotene production is developed and verified. This model was used as evaluation platform of the investigated downstream methods discussed in Chapter 4 to Chapter 6. Each of these chapters is composed of one section explaining the motivation and theoretical background of the individual downstream processing approaches, one section providing the applied experimental and theoretical methods as well as one section for the results and final conclusion, respectively. In particular, Chapter 4 presents flocculation as possible preconcentration approach for *D. salina* biomass. Experimental and theoretical approaches of colloid process engineering such as DLVO theory are applied to the algal system to evaluate the preconditions of flocculation. In addition, a number

of flocculation strategies are examined under the consideration of diverse assessment criteria. In Chapter 5, a more economic and environmentally friendly pigment extraction technique is searched for. Therefore, supercritical carbon dioxide extraction is compared with conventional organic solvent extraction. The issue of residual biomass valorization is addressed in Chapter 6. Here, a novel application of mild hydrothermal liquefaction is introduced. Furthermore, a potential by-product of the β-carotene production process and its field of application are identified. Each of these chapters incorporates an operating energy and cost prediction based on the developed model to rationally compare the investigated downstream alternatives with the conventional techniques. The thesis ends with some concluding remarks in Chapter 7 which also comprises several challenges and tasks that remain in the downstream processing of microalgal biomass and its assessment.

2

Industrial production of microalgae based commodities

In the present chapter a brief overview of industrial microalgae farming is provided. Therefore, the currently used process options of the individual up- and downstream units are explained and microalgae based products are summarized. The green microalga *D. salina* is introduced as organism of great biotechnological relevance. More detailed background information of the applied downstream techniques in the present thesis is provided in Chapter 4-6.

2.1 Production train in microalgal biotechnology

Algal based production processes are characterized by different process units schematically illustrated in Fig 2.1. The upstream cultivation step aims for biomass generation and product formation. On the downstream route harvesting and drying are followed by product extraction. In many cases, the algal biomass itself accounts for the product which makes further processing steps redundant. However, if certain cell components represent the targeted products, extraction is essential resulting in a product fraction and a fraction of residual biomass. To work in an economically and ecologically viable way, it is important to consider all product streams and insert recycling loops. Therefore, the utilization of biomass remnant as well as the water and solvent recycle are envisaged aims of every sustainable process.

2.1.1 Types of cultivation

Most commonly, microalgae are cultivated under photoautotrophic conditions, meaning that solar light and CO_2 are used as substrate for biomass generation. As depicted in Figure 2.2, several cultivation systems are currently available to provide these conditions. In particular, there are the open systems e.g. raceway ponds, pools or natural shallow lakes with culture depths not higher than 30 cm and the closed photobioreactors (PBRs) e.g. simple bags, tubes or flat panels. These cultivation systems can be

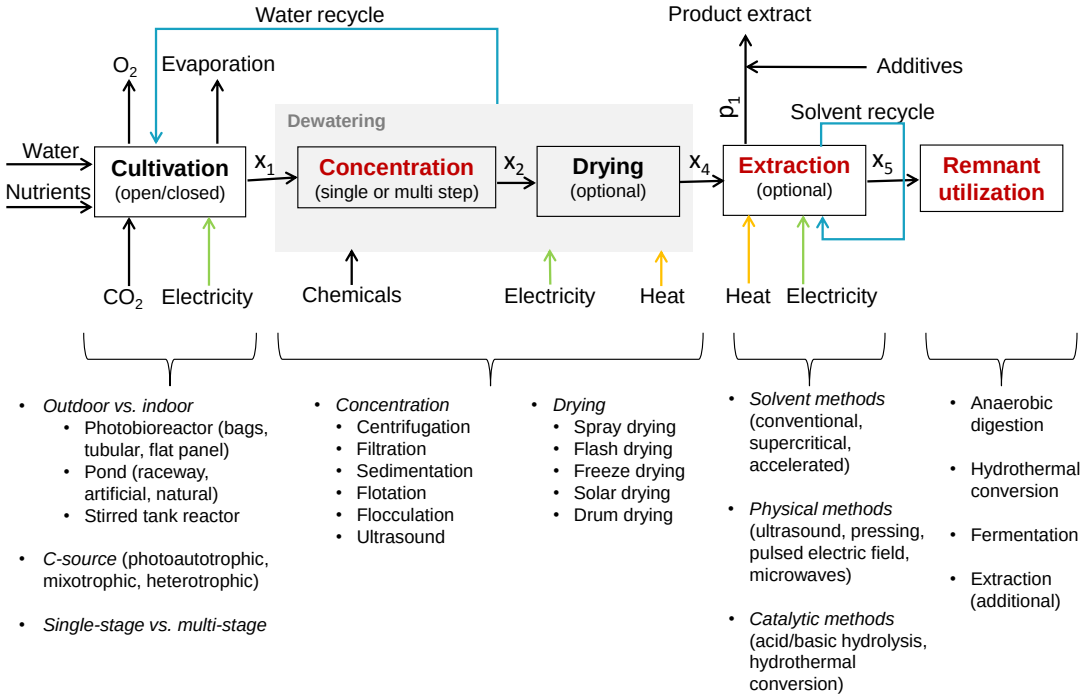

Figure 2.1: State of the art technologies for the different process units within an industrial microalgae production train. Mass cultivation of microalgae is usually divided in four process steps: cultivation, dewatering, product extraction and the utilization of biomass remnants. Red marked process units are investigated more closely in the present thesis.

operated outdoor, exposed to natural environment or indoor, in greenhouses or closed rooms illuminated by artificial light sources.

Figure 2.2: Types of closed (flat panel, tubular and bags) and open (shallow lakes, raceway ponds and pools) reactors for phototrophic mass cultivation of microalgae.

All options entail their own advantages and drawbacks. For example, the open ponds are less expensive to install and operate as well as more easily scalable than closed systems (Richardson *et al.*, 2012). However, open pond systems bear a significantly higher risk of predators and contamination (Chaumont, 1993). Furthermore, their area demand is higher and the area productivity significantly lower compared to that of closed systems (Wijffels *et al.*, 2010). Consequently, lower biomass concentrations were reached in open ponds coming along with higher dewatering costs. Open systems are reasonable for stable polycultures or extremophilic monocultures in terms of pH, salinity or temperature (Koller *et al.*, 2012). So far, this cultivation strategy is the most common one due to economic reason. Nevertheless, only few species are stable and industrially exploited under the open cultivation conditions (Bajpai *et al.*, 2014). Closed systems are more justified for high-value products to compensate higher operating and installing costs (Chaumont, 1993). They have low evaporation and CO_2 losses accompanied with a higher level of control (Posten & Schaub, 2009; Wang *et al.*, 2012).

Special cases of microalgae mass cultivation are the mixotrophic and heterotrophic cultivations. In heterotrophic cultivations organic carbon sources such as glucose, acetate or glycerol are used to produce biomass and high-value products under the exclusion of light. Here, the cultivation occurs in stirred tank reactor vessels (STR) which are commonly used in biotechnology. Heterotrophic cultivations achieve up to 25-fold increased biomass yields compared to the photoautotrophic ones (Morales-Sánchez *et al.*, 2017). In contrast, mixotrophic culturing in closed PBR combines the phototrophic growth on sunlight and inorganic carbon with the heterotrophic growth on an organic carbon source (Zhan *et al.*, 2017). Both approaches are feasible especially for the production of high-value products such as polyunsaturated fatty acids, pigments, vitamins,

polysaccharides or antioxidants (Barry *et al.*, 2016).

A lot of microalgae-derived products are generated more efficiently under nutrient starvation or other abiotic stress conditions (e.g. light intensity, pH, temperature, salinity). In most cases, these stressors inhibit cell growth and thereby biomass production. To overcome the incompatibility of simultaneous biomass and product generation, multi-stage processes are recommended. In the first stage, biomass production is done by applying optimal growth conditions. In the second stage, the generated biomass is transferred to the stress condition to initiate product accumulation (Borowitzka & Borowitzka, 1990; Koller *et al.*, 2012).

2.1.2 Dewatering concepts

After the production of microalgal biomass, one or more concentration steps are necessary prior to further processing (see Figure 2.1). Dewatering is challenging and expensive due to the relatively low cell concentration, the small cell size and density and the large amount of culture broth needed to be processed. Up to 20-30% of the overall production costs account for the biomass recovery (Molina Grima *et al.*, 2003), meaning that the choice of an optimal harvesting strategy significantly impacts the entire product economy. The real dewatering costs are determined by the species, the culture conditions and the desired final biomass slurry concentration.

Sedimentation, filtration, flotation, flocculation and centrifugation are well-established and frequently used for industrial microalgae dewatering (Pittman *et al.*, 2011). Figure 2.3 schematically illustrates these harvesting concepts. Among all dewatering approaches, sedimentation is the simplest one. Here, the culture broth is pumped into a sedimentation tank or pond and allowed to settle down by gravity to be concentrated to 1.5-5 wt% (Lundquist *et al.*, 2010). The above-mentioned properties of microalgae (low density and small cell sizes) entail slow sedimentation velocities. Therefore, it is reasonable to accelerate the velocity by e.g. centrifugation or flocculation. Centrifugation uses centrifugal acceleration to separate the algal particles and the culture broth. The efficiency of this approach is determined by the type of centrifuge, the physical properties of the algal cells and the operating conditions. Currently, centrifugation is the preferred method for algal cell recovery because it is highly efficient (η_H>95%), proceeds fast and can be applied for most microalgae species (Pittman *et al.*, 2011). Furthermore, high final biomass concentrations of 15-25 wt% can be achieved (Uduman *et al.*, 2010). Nevertheless, centrifugation as single harvesting step is energy and cost intensive and might be more appropriate as a second dewatering step after preconcentration (Davis *et al.*, 2011).

Flocculation can be used to preconcentrate the biomass by cell coagulation which facilitates the sedimentation process. More precisely, particle agglomerates are bigger in size and weight leading to enhanced sedimentation velocities (Vandamme *et al.*, 2013). However, particles in suspension are stable due to their negative surface charge which

prevents self-agglomeration. Flocculants such as metal salts, polymers or microbial products can disrupt the stable system by charge neutralization or dispersion and initiate the formation of flocs (more information on flocculation is provided in Section 4.2).

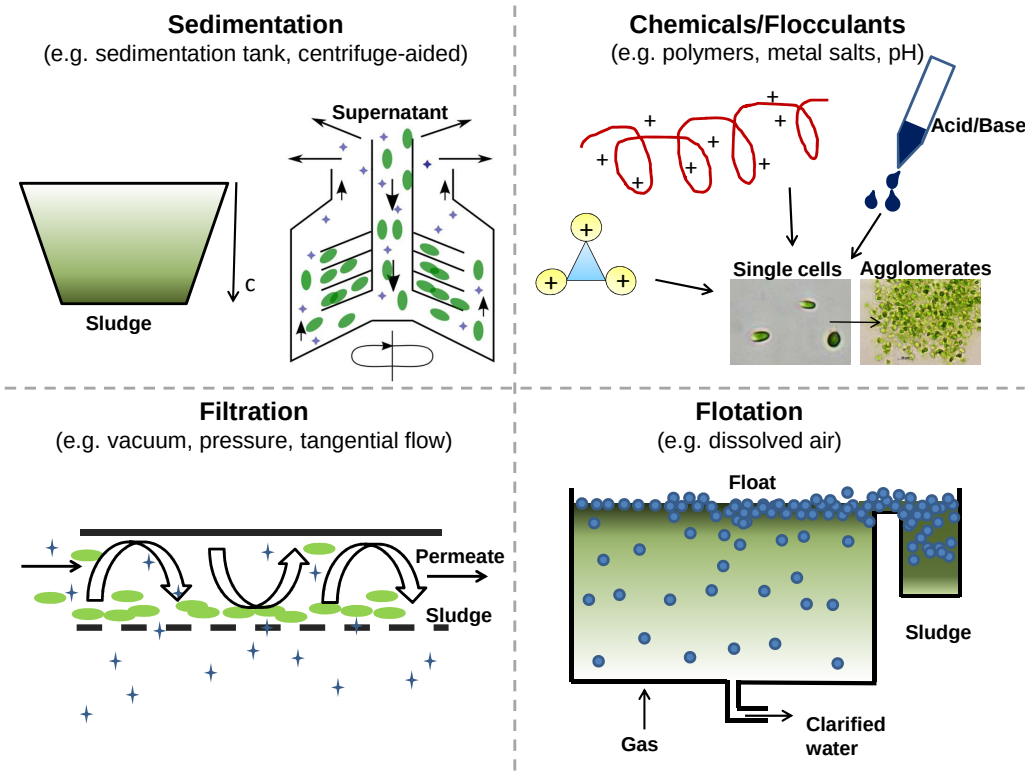

Figure 2.3: Schematic illustration of commercially used dewatering techniques in microalgae production processes.

Another concept of preconcentration is the application of flotation by gas bubble buoyancy which is useful in particular for small algae cells (Uduman *et al.*, 2010). Gas bubbles produced by pressure or electrolysis are passed into the culture broth, attach to the algae particles and carry them to the suspension surface. The generated float on the surface can be removed by e.g. filtration or sedimentation. In addition, the transfer of the suspension through filters which are permeable for the medium but impermeable for the algae particles is also a possible dewatering method. Different filtration techniques are proposed for microalgae harvesting such as vacuum filtration, tangential flow filtration, membrane micro filtration and ultra filtration. In all approaches either gravity, vacuum, pressure or centrifugal force is used as driving force (Pittman *et al.*, 2011). Ultrasonic harvesting uses the effect that algal cells agglomerate at the nodal point of standing acoustic waves which accelerated the particle sedimentation (Petrick *et al.*, 2013).

A further dewatering step in form of drying could be necessary, if a higher biomass concentration is required for the product extraction. Drying is one of the most energy consuming steps in the production of algal products. Therefore, extraction methodologies working with wet biomass slurry are needed. Currently, the extraction of lipids and pigments are mostly done from dried biomass to achieve high yields and product qualities (Mäki-Arvela *et al.*, 2014). The simplest and most economical way to get dried biomass is solar drying. Here, the preconcentrated slurry is exposed to sunlight allowing the evaporation of water. However, the duration of drying is strongly determined by the weather condition and not suitable for pigment-containing biomass which might be bleached out under sun irradiation. Besides this, spray drying, drum drying, freeze drying and flash drying are much faster approaches to dewater the algal biomass. They are applied for high-value products to compensate their high energy costs (Molina Grima *et al.*, 2003; Petrick *et al.*, 2013).

2.1.3 Product extraction

In most cases, it is necessary to disrupt the dried cells prior to the extraction step in order to ease the product release. Currently, mechanical (e.g. homogenizers, bead mills, ultrasounds and pulsed electric field) as well as non-mechanical (e.g. osmotic shock, freezing, enzymes, acid or base treatment) techniques can be used depending on the strength of cell wall and the targeted product (Mata *et al.*, 2010; Polikovsky *et al.*, 2016). In general, the efficiency of a certain extraction approach is influenced by several factors, namely the composition of the targeted product, the algal species and its growth conditions, the used harvesting technique and the required degree of dewatering (Barry *et al.*, 2016). Accordingly, every product requires its own optimal extraction strategy.

Several extraction approaches are already applied in industrial microalgae production routes (see Figure 2.1 and Section 5.2 for more details). Conventional extraction by means of organic solvents is widely used for the recovery of non-polar lipids or lipophilic compounds from dried algal biomass. The most common organic solvents are hexane, hexane-isopropanol or chloroform-methanol (Molina Grima *et al.*, 2003). Accelerated solvents are organic solvents which are applied at pressures and temperatures above the boiling point (Barry *et al.*, 2016). By using accelerated solvents an improvement of the extraction time, the efficiency and the solvent-to-biomass ratio can be achieved (Denery *et al.*, 2004). Nowadays, high valuable products such as pigments or polyunsaturated fatty acids are extracted by green solvents like supercritical fluids (Casas Cardoso *et al.*, 2012). Here, the positive properties of an organic solvent are accompanied by the rapid diffusion velocity of a gas. Furthermore, a nearly complete solvent separation and recovery is possible by simple decompression of the solvent (Palma *et al.*, 2013).

Next to the solvent extraction approaches, also physical procedures are applied for the product recovery. Pressing by oil-mills is the simplest form to recover the oil fraction of algal biomass. During pulse electric field extraction the cell membrane permeability increases for internal metabolites by the generation of pores whereas ultrasonic-assisted

extraction is used to recover compounds through induced cavitation (Das, 2015). In addition, the microwave-assisted extraction is based on the change of cell membrane properties caused by electromagnetic waves (Palma *et al.*, 2013). Moreover, enzymatic treatment and hydrothermal liquefaction are both feasible for wet biomass extraction which would eliminate a costly drying step. In the first procedure, the enzymatic decomposition of the cell wall increases the release of cell components. In contrast, liquefaction uses water as reactant to convert wet biomass under high temperature and pressure conditions into lipophilic bio-crude, a hydrophilic aqueous phase and other components.

2.1.4 Utilization of biomass remnant

After the main-product is recovered, a biomass remnant remains as a potential feedstock to produce further by-products and thus, to realize a more sustainable biorefinery concept. The residual biomass can be used in numerous of different applications depending on its biochemical composition. A brief overview of the expectable products from microalgal remnants is provided in Figure 2.1 and Figure 2.4. In principle, carbohydrate-

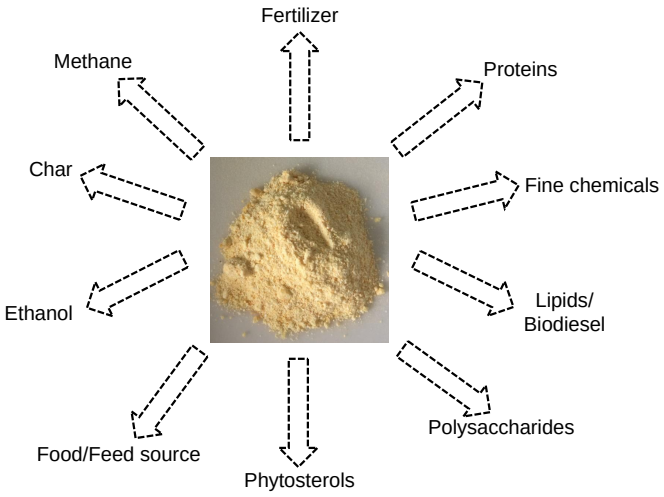

Figure 2.4: Possible products derived from microalgal biomass remnant.

rich biomass waste can be converted via anaerobic digestion or fermentation to produce energy carriers such as methane, bio-ethanol or hydrogen (Orosz & Forney, 2008). The final product is determined by the used fermentation process. Anaerobic digestion constitutes a set of biomass degradation processes conducted by different microorganisms under the exclusion of oxygen to generate biogas (Zhu, 2014). The remnant of the digestion can be processed to recover fertilizers (Benemann *et al.*, 2011). For the production of bio-ethanol or hydrogen, anaerobic fermentation of the biomass by fungi or bacteria can be applied (Harun *et al.*, 2010b). Besides bio-reforming processes also chemical

techniques are feasible to exploit the remnant. Thus, the recovery of additional valuable components such as phytosterole or certain proteins can be realized by a second tailor-made extraction step. Moreover, thermo-chemical processes e.g. gasification, pyrolysis, torrefaction or hydrothermal liquefaction can be employed to produce biofuels but also further valuable components (for more details see Section 6.2).

2.2 Commercial applications of microalgae

2.2.1 Products from microalgae

The term microalgae comprises all prokaryotic and eukaryotic microorganisms which are able to grow photoautotrophically. To be more precise, photoautotrophic growth is provoked by the assimilation of sunlight, water and carbon dioxide to generate biomass, which is equal to terrestrial plants. However, the cultivation of microalgae has some significant advantages compared to that of terrestrial plants (Griehl & Bieler, 2011), namely: a higher area productivity, an increased efficiency of CO_2 sequestration, a possible application of waste water and flue gas, the possibility to be cultivated in extreme environments and non-arable land and the generation of lignocellulose-free biomass.

Accordingly, they are promising production organisms in biotechnology which are not competing with agriculture production areas. Nevertheless, less than 1% of about 30,000 known microalgae species are industrially exploited so far (Mata *et al.*, 2010). Due to the heterogeneous physiology within the microalgae group, they provide a multifaceted product portfolio, as exemplary given in Table 2.1. The ability to accumulate high amounts of triacylglycerides (TAGs) makes them potential biofuel producers. Moreover, the environmental impact of microalgal biofuels is significantly lower than that of conventional ones (Das, 2015). Today, most targeted commodities traded on the global market are high-value compounds for the nutrition, cosmetic and health care sectors (Spolaore *et al.*, 2006). They comprise pigments, antioxidants, polyunsaturated fatty acids (PUFAs) and sterols, different polysaccharides and proteins. In addition, great research efforts are currently devoted to the healing power of secondary metabolites for e.g. Alzheimer disease, cancer or HIV (Griehl & Bieler, 2011).

The microalgal biomass itself is regarded as health-promoting in human nutrition and therefore offered as powder, tablets or capsules. *Chlorella vulgaris*, *Spirulina platensis*, *Dunaliella salina* and *Scenedesmus spp.* are the species which are mainly farmed for this purpose (Pulz & Gross, 2004). Furthermore, microalgae biomass is an ingredient of numerous commercial available foods such as snacks, bread, noodles as well as beverages (Spolaore *et al.*, 2006). In addition, 30% of the overall produced biomass is used for animal feed in order to enrich milk, eggs, meat or fish with the healthy ingredients of microalgae (Lum *et al.*, 2013; Spolaore *et al.*, 2006). Essential for the good reputations of microalgae biomass are the immune-promoting, antimicrobial, antiviral, antioxidative, antitumoral and cholesterol-lowering activities described for certain algal

compounds (Guedes *et al.*, 2011). Therefore, also extracted components or substance classes such as the PUFA or pigment fractions were used as healthy additive in food or cosmetic products. Nowadays, there is a growing demand for these green products. Especially, PUFAs like eicosapentaenoic acid (EPA) or docosahexaenoic acid (DHA) and pigments in form of β-carotene, astaxanthin or lutein provide an enormous market growth worldwide. For example the global carotenoid market is expected to reach 1.3 billion USD in 2018 (Yaakob *et al.*, 2014). Carotenoids are applied as coloring substances or antioxidants. Among the lipid compounds, also sterols are interesting algal products with bioactive properties which are in great demand in the nutraceutical and pharmaceutical industry (Ibañez & Cifuentes, 2013).

Table 2.1: Commercial products from diverse microalgae species.

Product	**Species**	**Reference**
Biomass	*Chlorella vulgaris*	(Pulz & Gross, 2004)
	Spirulina platensis	(Pulz & Gross, 2004)
	Scenedesmus spp.	(Borowitzka, 2013)
	Dunaliella salina	(Borowitzka, 2013)
Pigments andAntioxidants		
β-carotene	*Dunaliella bardawil*	(Borowitzka & Borowitzka, 1990)
	Dunaliella salina	(Ben-Amotz, 1999)
Astaxanthin	*Haematococcus pluvialis*	(Borowitzka, 2013)
	Chlorella zofingiensis	(Del Campo *et al.*, 2007)
Lutein	*Chlorella pyrenoidosa*	(Plaza *et al.*, 2009)
	Chlorella zofingiensis	(Del Campo *et al.*, 2007)
	Chlorella protothecoides	(Del Campo *et al.*, 2007)
Fucoxanthin	*Phaeodactylum tricornutum*	(Borowitzka, 2013)
	Isochrysis galbana	(Cuellar-Bermudez *et al.*, 2015)
Fatty acids		
Eicosapentaenoic acid	*Phaeodactylum tricornutum*	(Guedes *et al.*, 2011)
	Nannochloropsis spp.	(Cuellar-Bermudez *et al.*, 2015)
Docosahexaenoic acid	*Phaeodactylum tricornutum*	(Cuellar-Bermudez *et al.*, 2015)
Phytoterols (C28, C29)	*Chlorella spp.*	(Ibañez & Cifuentes, 2013)
Polysaccarides		
Sulfated polysaccharides	*Rhodella spp.*	(Borowitzka, 2013)
	Porphyridium spp.	(Plaza *et al.*, 2009)
	Chlorella pyrenoidosa	(Plaza *et al.*, 2009)
β-1,3-glucan	*Chlorella vulgaris*	(Spolaore *et al.*, 2006)
Proteins		
Phycobiliproteins	*Spirulina platensis*	(Plaza *et al.*, 2009)

A diverse range of different polysaccharides can be found in algae biomass. However, so far the conventional sugars derived from microalgae are badly received from the market owing to cheaper alternatives from plants and macroalgae (Borowitzka, 2013). Nevertheless, there are still some special polysaccharides such as unsulfated polysaccharides (e.g. hebrenoid) which were found to have antithrombotic and antinflammatory actions making them relevant as pharmaceutical (Das, 2015). Another example in the

group of polysaccharides is β-1,3-glucan produced by the green microalga *Chlorella vulgaris*. The molecule is known to be an immune system activator, a reducer of blood lipids and a scavenger of free radicals (Spolaore *et al.*, 2006). In the molecule class of proteins, phycobiliproteins are rated as promising products. Aside antioxidative and immunomodulation activity, this extracted molecule type from the blue alga *S. platensis* possess different properties which are attractive for medical application (Plaza *et al.*, 2009).

2.2.2 *Dunaliella* - a green microalga with specific properties

Dunaliella salina is one of the first microalgae which was exploited for industrial application. The genus *Dunaliella* was firstly discovered by Teodoresco in 1905 and belongs to the phylum *Chlorophyta*, the order *Volvocales* and the family *Polyblepharidaceae* (Teodoresco, 1905). So far, over 20 unicellular and motile biflagellate microalgae species are associated to this genus. *Dunaliella* is found in hypersaline environments such as shallow brine lakes and tolerates salt concentrations between 0.5-5.5 M (Ramos *et al.*, 2011). Already Teodoresco (1905) reported the fast adaptively of its algal cell morphology to changing osmolarity. This property is supported by a flexible and elastic cell membrane and the lack of a rigid cell wall (Tafreshi & Shariati, 2009). The adaption is done by varying the intracellular glycerol concentration (Ben-Amotz, 1999). By withstanding harsh environmental conditions e.g. the high salt concentrations, the cultivation can occur nearly free from predators. Merely, some halobacteria species are able to populate the same natural habitats making the cultivation predestined for open pond conditions (Ben-Amotz & Avron, 1990).

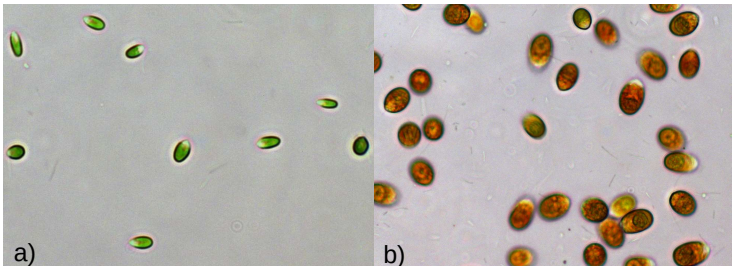

Figure 2.5: *D. salina* cells under a) normal growth or b) abiotic stress conditions to initiate carotenogenesis.

The most interesting property of *Dunaliella* for industrial application is the ability to generate large amounts of high valuable β-carotene. The pigment is produced as a response of high solar irradiation and nitrogen deprivation (see Figure 2.5b). It is accumulated together with TAGs in the lipid granules within the chloroplast thylakoids. β-carotene is used as colorant, provitamin A, antioxidant and sun protector (Ben-Amotz & Avron, 1983; Ramos *et al.*, 2011). Due to the variety of applications,

the global β-carotene market is increasing and expected to reach 334 million USD in 2018 (Yaakob *et al.*, 2014). Natural β-carotene by *D. salina* is composed of a mixture of 41% 9-cis, 42% all-trans and 10% 15-cis β-carotene. With this composition a more healthy effect is provided compared to that of the synthetically produced all-trans form (Ben-Amotz, 1999; Tafreshi & Shariati, 2009). The natural form contributes with 20-30% to the global β-carotene market (Borowitzka, 2013).

Concentrations up to 14 wt% are described for the species *D. salina* and *D. bardawil* visible also by the change of their oval, green phenotypes into round, reddish ones as depicted in Figure 2.5 (Ben-Amotz *et al.*, 1991; Borowitzka & Borowitzka, 1990). With that, *Dunaliella* is the most important producer of natural β-carotene and subject of immense industrial and academic efforts. The industrial production of the microalga started 1986 in USA, Israel and Australia near the sea in natural formed shallow lakes or simple raceway ponds (Ben-Amotz & Avron, 1989; Borowitzka & Borowitzka, 1990). Today, annual biomass production reaches over 1200 t and the number of production sites is increased by producers in Spain, India, Taiwan, Japan, Hawaii and China (Del Campo *et al.*, 2007; Griehl & Bieler, 2011). Next to pigments extracts, also the dried biomass powder is used for human purpose but also applied to feed aquacultures (Richmond, 2007).

2 INDUSTRIAL PRODUCTION OF MICROALGAE BASED COMMODITIES

3

Assessment of microalgae based production processes

The present chapter briefly introduces the commonly used assessment approaches of microalgal biotechnology. Furthermore, an overall process scheme of microalgal β-carotene production is developed, based on process data from literature, real production plants and experimental work. The process model was used as assessment platform to calculate energy and operating costs of the individual downstream techniques investigated in this thesis. For this reason, the model was individually extended or adapted (see Chapter 4-6) to simulate different process scenarios based on Monte-Carlo simulations. The following chapter refers to the model originally published in Pirwitz *et al.* (2015a).

3.1 Economic and sustainability assessment of microalgae based production processes

The design of sustainable and economically viable bio-processes is an envisaged aim in research and industry. Lots of the existing microalgae production processes are economically feasible only due to the high market values of the underlying products. Nevertheless, there is still potential to improve their performance with respect to economy and environmental compatibility. Furthermore, also new bio-processes require a detailed theoretical assessment prior to installation. Consequently, an assessment platform is needed, allowing the evaluation of new or modified process steps within the overall process train. Different assessment strategies are available in dependency of the desired evaluation criteria.

In general, techno-economic assessment (TEA) has been established to be an efficient assessment tool for state of the art technologies in microalgal industry (Benemann & Oswald, 1996; Lundquist *et al.*, 2010). The approach combines conventional systems engineering process modeling with economic calculations (Quinn & Davis, 2015). Initially, a detailed process scheme composed of all modules and streams of the overall

process must be provided. In the next step, technical understanding of the process is included by the calculation of mass and energy balances to estimate product yields and energy demand. Afterwards, the capital and operating costs can be derived enabling the estimation of e.g. selling prices. Capital costs comprise e.g. cost of land, equipment, facilities and indirect expenditures while operating costs include cost of labor, maintenance, raw materials and utilities (Sun *et al.*, 2011). Accordingly, TEA is a powerful tool to identify the economic viability and technical challenges of a particular process step or the overall process. In microalgae based production processes, every process unit can be realized by various processing techniques (see Figure 2.1). To find the most cost-effective process route for a specific product, superstructure based optimization is a commonly used approach (Rizwan *et al.*, 2015).

A measure of the overall sustainability character of an underlying process is provided by life cycle assessment (LCA). Here, the environmental impact of microalgal production can be evaluated by the consideration of the energy demand and emissions of all processes within the production system (Frank *et al.*, 2013; Quinn & Davis, 2015). The key criteria within a LCA are given by: Net energy ratio, global warming potential and the energy return of investment (Quinn & Davis, 2015). This methodology is especially appropriate for the comparison of the sustainability character of different production scenarios.

Nowadays, most published process analyzes of microalgal processes are focused on the production of biofuels (see Ribeiro & Silva (2013) for a literature overview). For example, a detailed process analysis was done by Delrue *et al.* (2012), using an economic, sustainability and energetic model for the comparison of various methodologies for microalgae bio-diesel production. A major disadvantage of usual process models is the incorporation of organism-unspecific assumptions. However, each microalgae strain is characterized by its own specific properties regarding e.g. growth rate, environmental requirement, product content and downstream behavior. Consequently, simply applying standardized assumptions might entail unrealistic calculations for a specific microalgae production process. Furthermore, microalgal process models frequently use over-optimistic forecasts for the area productivity and product yields. For the evaluation of the feasibility of bio-process a more reliable and realistic data base is essential.

3.2 Development of a process scheme for industrial microalgal β-carotene production

In the following sections a techno-economic process model is developed as base line scenario to reliably assess the process variations investigated in the present thesis. The process is characterized by three main units: a cultivation unit for biomass generation and β-carotene accumulation in ponds, a multi-step harvesting unit accounting for the dewatering procedures of the algal biomass and an extraction unit for the recovery of β-carotene (see Figure 3.1). So far, no residual biomass treatment is considered in

industrial β-carotene production. To be more realistic, algae based process data from large scale provided by literature or industry is partly used in the model. Whenever possible, real data for the β-carotene production by *D. salina* were incorporated in the process analysis. The used parameters of the underlying process model are summarized in Table 3.1. A detailed explanation of the parameter is given in Sections 3.2.1-3.2.5.

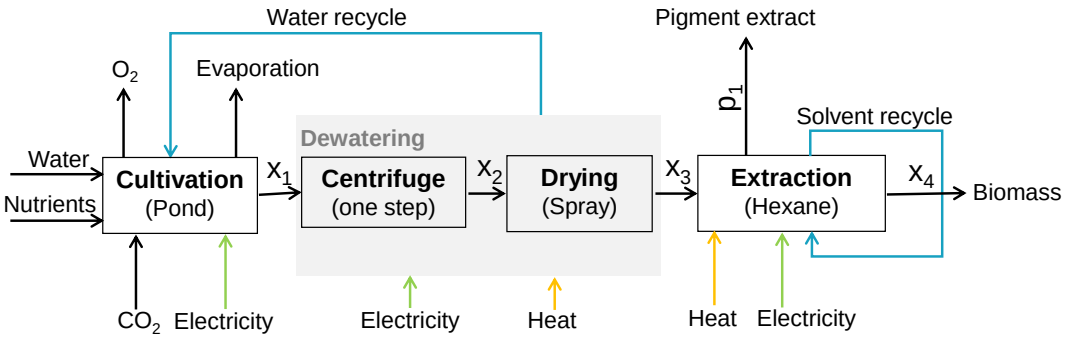

Figure 3.1: Reference process of industrial β-carotene production by *D. salina*. The process system is divided into three groups of process units; namely the biomass and product generation, the dewatering including a centrifugation and a drying step and the n-hexane extraction of the product.

3.2.1 Cultivation conditions

The considered process illustrated in Figure 3.1 was assumed to be located in coastal areas close to the sea. With that, natural reservoirs of NaCl and water are freely available. Since carotenogenesis requires high sun irradiation, the surrounding climate was taken as Mediterranean. Thus, a simulation of comparable cultivation conditions to existing production sites in Israel or Australia was provided. Therefore, the annual average temperature was oriented towards the production site in Hutt Lagoon, Western Australia (Moulton *et al.*, 1987); the origin of the used strain CCAP 19/18 and was set to 19.8 °C. For the calculation of gross annual production costs, the domestic taxes and the cost of manpower were taken into account using industrial data of the *D. salina* open pond plant in Israel (NBT Ltd.). Therefore, costs of 5,000 and 50,000 USD ha^{-1} a^{-1} are assumed, respectively (Ben-Amotz, 2008).

The growth of *D. salina* was simulated to be operated in raceway ponds at 330 d a^{-1} (Davis *et al.*, 2011). The ponds are characterized by a depth of 0.2 m and a total production area of 10 ha. Based on the work of Lundquist *et al.* (2010), a paddle wheel velocity of 0.25 m s^{-1} with an energy consumption of 574 kWh d^{-1} was applied for culture mixing. According to industrial process data from NBT Ltd. an algae growth rate of 2 g_{dw} m^{-2} d^{-1} was presumed (Ben-Amotz, 2008), leading to a gross biomass production of 200 kg_{dw} d^{-1}. A final cell concentration of 300 mg_{dw} L^{-1} was defined to be present in the pond which refers to real process data published by Curtain &

Snook (1983). The β-carotene content of the cells was expected to be 5 wt% of the cell dry weight (dw), similar to the extraction results of *Dunaliella* biomass from the open pond plant in Western Australia and India (Sources of biomass: Nutra-Kol and Denk Ingredients GmbH). To achieve optimal growth conditions, the raceway pond is actively fed with CO_2 and nutrients, whereas the CO_2 and nutrient consumption were calculated based on the stoichiometric equation of algae biomass according to Bailey Green *et al.* (1996): $C_{106}H_{181}O_{45}N_{16}P$. The demand of the nutrients $(NH_4)_3PO_4$ and NH_3 was calculated considering an excess of 10% for the blow-down and loss of nutrients further downstream. Under the assumption of a complete medium recycling after dewatering, a reusability of 5% nutrients was expected. The CO_2 uptake in the algae was expected to be 85% effective. CO_2 delivery occurs with a blower consuming 0.025 kWh m^{-3} (Verrecht *et al.*, 2010). The daily energy consumption of the blower was estimated considering a CO_2 density of 2.23 kg m^{-3} at an average process temperature of 19.8 °C and a delivery pressure of 1.22 bar, as proposed by Lundquist *et al.* (2010).

3.2.2 Water supply and pumping

Recycled water from the harvesting step was supplied for medium preparation considering a blow-down of 5%. For the compensation of blow-down and evaporation losses, make-up water was assumed to be taken from the nearby sea. Furthermore, natural evaporation and rainfall were taken into account using weather data from the existing *D. salina* production site in Hutt Lagoon (Australia) to simulate realistic conditions. For this purpose, evaporation and rainfall values of 2445 mm a^{-1} and 449.7 mm a^{-1} (Nowicki *et al.*, 2009) were applied to estimate the average net evaporation rate of 5.5 mm d^{-1}. The cost of sea water cleaning by filtration and chlorination was set to 0.54 USD m^{-2} according to data from the NBT Ltd. plant in Israel (Ben-Amotz, 2008). Pumping work of recycled and make-up water as well as the transport of microalgae suspension through the process units was supposed to be done by conventional waste water pumps. Therefore, an energy demand of 0.016 kWh m^{-3} was used, adopted from the work of Verrecht *et al.* (2010).

3.2.3 Dewatering procedure

The downstream route typically found in microalgae process analysis is composed of a multi-step harvesting procedure (Davis *et al.*, 2011; Delrue *et al.*, 2012; Sun *et al.*, 2011; Weschler *et al.*, 2014). Most commonly, dewatering is initiated by a simple sedimentation step without the addition of flocculants. As demonstrated in the preliminary results obtained in this thesis, *D. salina* has an insufficient settling efficiency of less than 40% within one day (see Appendix Figure A.1). Thus, this subunit was not implemented and centrifugation was directly used for cell harvesting in the simulated process. Therefore, a daily harvesting volume of 667 m^3 was supposed to be pumped into the centrifuge. This volume corresponds to the daily biomass yield of 200 kg (see Section 3.2.1).
A harvesting efficiency η_H of 95% was used for the centrifugation step, provided by Prof. Ami Ben-Amotz from NBT Ltd. Israel (personal communication with Prof. Ben-

Table 3.1: Parameters incorporated in the process model.

Parameter	Value	Unit
Location data		
Man power cost	5,000	USD ha^{-1} a^{-1}
Domestic tax	50,000	USD ha^{-1} a^{-1}
Temperature	19.8	°C
Cultivation period	330	d a^{-1}
Pond depth	0.2	m
Production area	10	ha
Evaporation	2445	mm a^{-1}
Rainfall	449.7	mm a^{-1}
Water treatment cost	0.54	USD m^{-2}
Cultivation		
Species	CCAP 19/18	
Growth rate	2	g_{dw} m^{-2} d^{-1}
β-carotene content	5	%
Cell concentration	0.3	g_{dw} L^{-1}
Nutrient blow down	10	%
Water blow down	5	%
Nutrient recycle	5	%
CO_2 uptake efficiency	85	%
NaCl concentration	24	%
Harvesting volume	667	m^3 d^{-1}
Downstream processing		
Harvesting efficiency	95	%
Post-harvest concentration	100	g_{dw} L^{-1}
Drying efficiency	99	%
Post-drying concentration	900	g_{dw} L^{-1}
Extraction efficiency	95	%
Loss of solvent	1	%
Equipment		
Paddle wheel velocity	0.25	m s^{-1}
Paddle wheel energy demand	574	kWh d^{-1}
Blower energy consumption	0.025	kWh m^{-3}
Pump energy consumption	0.016	kWh m^{-3}
Centrifuge capacity	85	m^3 h^{-1}
Centrifuge motor power	75	kW
Dryer energy consumption	1.31	kWh $kg_{H_2O}^{-1}$
Extractor energy consumption	0.00035	kWh kg_{dw}^{-1}
Heater extraction energy consumption	1.5	kWh kg_{dw}^{-1}

Amotz, 2014). Consequently, 95% of the applied biomass obtained in the cultivation step can be recovered by centrifugation. The dewatering approach was supposed to reach a final biomass concentration of 10 wt% which is a typical value in microalgae processes (Ben-Amotz, 2008; Molina Grima *et al.*, 2003). The energy demand of the centrifuge was estimated from Equation 3.1 (adopted from Xu *et al.* (2011)) by using the technical data of the Westfalia separator SSE 400 with a capacity of 85 $m^3\ h^{-1}$ and a motor power of 75 kW:

$$E_c = \frac{m_{dw} \cdot P_c}{c_{algae} \cdot \nu_c} \tag{3.1}$$

where E_c is the energy in kWh required by the centrifuge, m_{dw} is the dry weight of *D. salina* needed to be processed in kg, c_{algae} is the mass concentration of the algae slurry in kg m^{-3}, ν_c is the capacity of the centrifuge in $m^3\ h^{-1}$ and P_c is the motor power of the centrifuge in kW. As a last dewatering step, drying was expected to reach a final biomass concentration of 90%. According to Ben-Amotz & Avron (1989), spray drying, freeze-drying and drum drying is appropriate for *Dunaliella* biomass, resulting in a comparable quality of the biomass powder and stability of the pigment. For this reason, a spray-drying unit similar to the plant in Israel (Ben-Amotz, 2008) was used for process simulation, consuming 1.31 kWh $kg_{H_2O}^{-1}$ (Baker & McKenzie, 2005). The loss of biomass during spray drying was assumed to be 1%.

3.2.4 Extraction

After the dewatering procedure, the main product β-carotene can be extracted by different ways (see Section 2.1.3). Conventional extraction with non-polar organic solvents such as n-hexane is feasible due to the high extraction efficiencies of at least 95% (Ruane, 1974). Based on simulations of bio-oil extraction with n-hexane from microalgae biomass at 60 °C by Delrue *et al.* (2012), electric power requirements of 1.3 kWh kg_{dw}^{-1} were applied for the heater and 0.00035 kWh kg_{dw}^{-1} for the extractor, respectively. This also considers the energy demand of the heater needed for the recovery of the solvent. Solvent recovery was assumed to be 99% effective. Adopted from the patent of Ruane (1974), a relation of 10:1 hexane:algae slurry was assumed for the solvent to biomass ratio.

3.2.5 Implementation and statistics

To assess the economics of the production route in the underlying study, the mass and energy flows were calculated using the mentioned parameters. Mass flows refer to the in and out flows of the process as schematically illustrated in Figure 3.2. Energy flows account for the direct energy consumption within the individual process units. All data above are derived from published works, own experimental results or personal communications with experts in the field. The developed process model was implemented in Matlab (MathWorks) and can be generally expressed by the following equations:

$$OC = \sum_{i,k} P_{1,i}(F_{i,k}^{in} - \sum_{l} R_{i,k+l}) + \sum_{j,k} P_2 E_{j,k} + \sum_{i,k} P_{3,i} C_{i,k} + \sum_{i,k} P_{4,i}(W_{i,k} - R_{i,k}) \tag{3.2}$$

$$GR = \sum_{i,k} P_{5,i} F_{i,k}^{out} \tag{3.3}$$

with OC as net operating costs. $P_{1,i}$, P_2, $P_{3,i}$ and $P_{4,i}$ are the costs of the raw materials $F_{i,k}^{in}$, the consumed energy $E_{j,k}$ of utility j (e.g. pump, centrifuge, heater) the needed chemicals $C_{i,k}$ as well as the waste and recycling streams $W_{i,k}$ and $R_{i,k}$. The gross revenue GR considers the sales price $P_{5,i}$ of component i in the product stream $F_{i,k}^{out}$. Index i refers to mass components in the flow (e.g. water, biomass, pigment), whereas k accounts for the process steps.

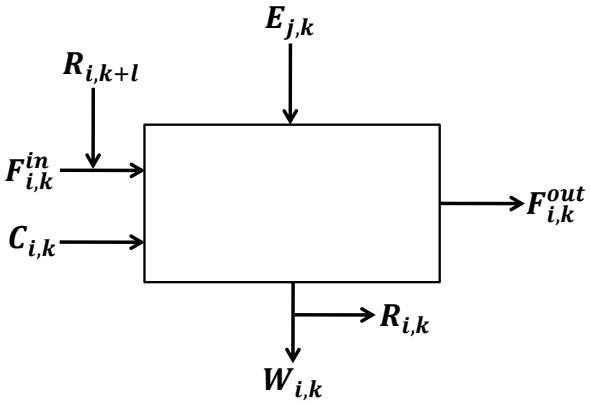

Figure 3.2: Schematic illustration of the mass and energy flows in the used process model.

For the consideration of uncertainties of all parameter values used in the energy and cost analysis, Monte Carlo simulations were applied using 5×10^5 independent normally distributed samples. The variances were defined in dependence of the individual parameter sources. In particular, a variance of $\sigma^2_{\text{parameter}} = (\frac{0.25}{3}\mu_{\text{parameter}})^2$ was applied for parameters derived from literature which are three standard deviations corresponding to 25% of the nominal parameter. A variance of $\sigma^2_{\text{parameter}} = (\frac{0.1}{3}\mu_{\text{parameter}})^2$ was used for parameters which are specific for *D. salina*. For the determined experimental parameters, the actual observed experimental variances were used. Thus, the sampling intervals with their specific upper and lower limits of each parameter were defined.

3.2.6 Reliability of the process model

The process model depicted in Figure 2.1 was used as reference case of subsequent investigations. The results of the process analysis clearly demonstrate the reliability of the used assumptions in the developed model. To be more precise, the estimated total annual process costs of 181,603 ± 19,330 USD a^{-1} are nearly identical to the 180,000 USD a^{-1} reported from the real industrial *D. salina* production process in Israel (Sun *et al.*, 2011) which is identical in area size and productivity to the reference case. Furthermore, the overall biomass production cost calculated to be

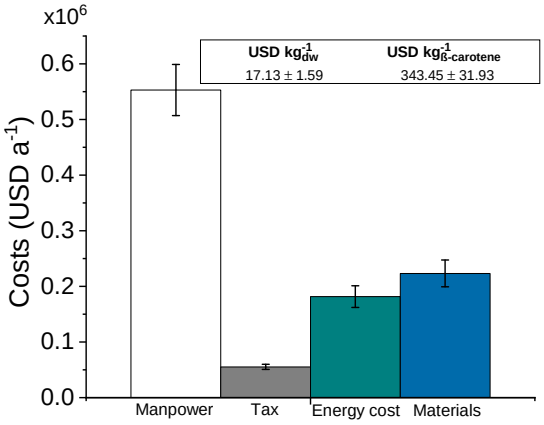

Figure 3.3: Annual operating costs for the production of β-carotene with *D. salina*. Costs are composed of manpower cost, tax, operating costs for energy and raw materials cost. Error bars account for one standard deviation from the average value based on Monte Carlo simulation to consider the uncertainties of experimental and literature data.

17.13 $\pm$ 1.59 USD kg_{dw}^{-1} biomass are almost the same to the value of 17 USD kg_{dw}^{-1} biomass, published for the mentioned production site (Ben-Amotz, 2008). Accordingly, the techno-economic estimates of the process model seem to be realistic, allowing the application of the evaluation concept for the assessment of innovative downstream processes for β-carotene production with *D. salina* in the following chapters of the present thesis.

4

Flocculation as potential preconcentration step of *D. salina*

The present chapter is dedicated to the investigation of flocculation as possible harvesting step within the *D. salina* downstreaming chain. The theoretical feasibility of flocculation is addressed by the characterization of its physico-chemical properties. Therefore, theoretical and experimental methods established for colloid process engineering are transferred to the algal system. In addition, different chemical and physical flocculation strategies are experimentally investigated. For the assessment of flocculation as innovative harvesting approach, different assessment criteria are taking into account, e.g. the reusability of separated culture medium or the product yield. Finally, the calculation of operating energy and costs is done to compare all flocculation attempts with the conventional harvesting technique centrifugation. This chapter involves methods and results published in Pirwitz *et al.* (2015a) and Pirwitz *et al.* (2015b).

4.1 Motivation

One of the main challenges of industrial microalgae farming is the downstream processing of the biomass. The downstream processing can account for 50-80% of total production costs, depending on the biochemical properties of the product and the required product purity (Molina Grima *et al.*, 2003). Since the algal biomass concentration achieved in production scale is only in the range of 0.5-5 g L^{-1}, large amounts of water needs to be processed for cell separation (Vandamme *et al.*, 2013). Consequently, high energy input is needed to dewater the biomass prior to product extraction. Due to the harsh environmental conditions during β-carotene production by *D. salina* in open ponds, even lower cell concentrations of 300 mg_{dw} L^{-1} are reached (Curtain & Snook, 1983).

The small size and low density of *D. salina* and most other microalgae are unfavorable for the application of simple gravity sedimentation to concentrate the biomass. Thus, the harvesting of microalgae cultures is primary done by centrifugation, since it

works highly efficient for nearly all industrial strains (Pittman *et al.*, 2011). However, the biomass dewatering by single step centrifugation is costly and energy consuming which is especially problematic for low-value products such as biofuels (Molina Grima *et al.*, 2003). A more energy-saving harvesting strategy would lead to an improved overall process economy, also for the high-value products. To make microalgae based processes more competitive compared to conventional production processes, alternative dewatering concepts are becoming highly relevant. One promising concept is the extension of the dewatering route by a preconcentration step prior to centrifugation. This can be realized by diverse techniques e.g. flotation, filtration or flocculation (see Section 2.1.2 for more details).

Flocculation is a well-established technology for the separation of waste particles and impurities from large volumes of a liquid product. The technique is used particularly in the brewing and paper industry as well as the water treatment (Vandamme *et al.*, 2013). In algal based production processes, the application of flocculation follows another concept. Here, the generated algae flocs are the product itself whereas the surrounding aqueous medium needs to be separated as waste. Due to the gentle character of this approach it seems highly promising for the preconcentration of the fragile microalga *D. salina*. The high saline environment of *D. salina* could possibly have a positive effect on the physical agglomeration properties of the alga and increase the flocculation efficiencies (Duan & Gregory, 2003). Since every flocculation approach is accompanied by its own benefits and drawbacks, a detailed assessment of each technique is needed, focused on not only the economics and efficiencies but also on its interactions with other process steps e.g. product extraction or medium recycle.

4.2 Theoretical background

4.2.1 Physico-chemical surface properties of microalgae

Most particles in natural aquatic resources are negatively charged in suspension. In the case of suspended microalgae this charge is provoked by the complex composition of their surfaces. Different binding sides for metal cations and protons originated from lipids, polysaccharides and proteins are located in the plasma membranes and cell walls of the microorganisms (Hong & Brown, 2006). The deprotonations of carboxylates at pH 4-6, phosphates at pH 7-8 and hydroxyl groups at pH 9-10 from these binding sites mainly contribute to their negative surface charges (Brady *et al.*, 2014). To reach neutrality, positively charged counter ions are attracted by the microalgal surface, leading to the formation of a surrounding electrostatic double layer (see Figure 4.1a). The double layer is characterized by a dense layer of counter ions directly located at the particle surface (stern layer) and a more distant diffuse counter ion layer called slipping plane. A measure of the overall particle surface charge is given by the ζ-potential. As illustrated in Fig 4.1, the ζ-potential is the electric potential at the slipping plane of a suspended particle. It can be used for the control of coagulation. In microalgal particle

suspensions a ζ-potential between -8 mV and +2 mV effectively induce cell coagulation (Henderson *et al.*, 2006).

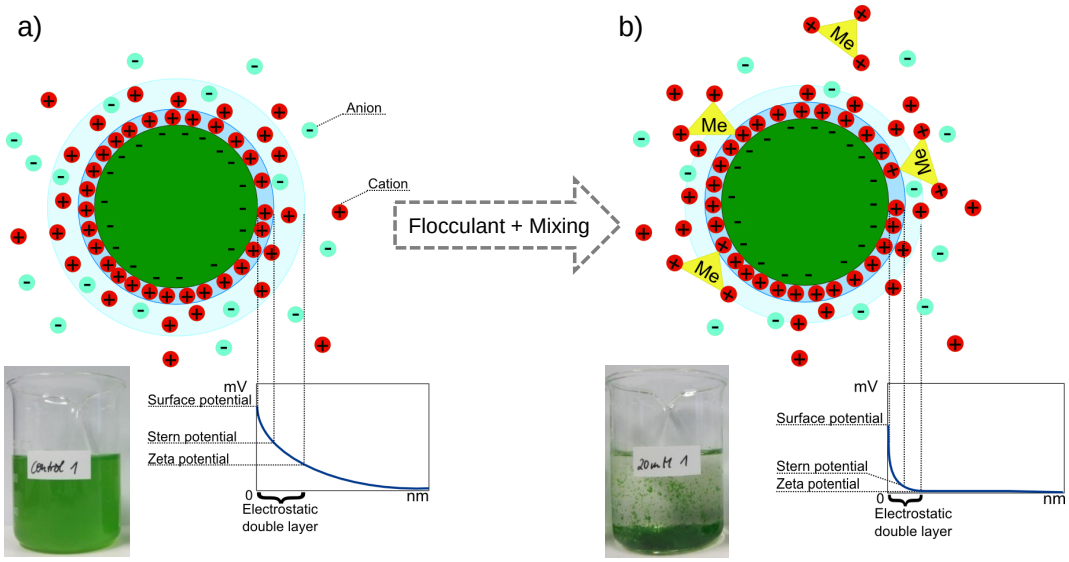

Figure 4.1: Schematic illustration of microalgae surface potentials of a) single cells and b) coagulated cells in suspension. Cell coagulation is eased by the help of flocculants e.g. trivalent metal cations.

In general, different physico-chemical interactions can influence particle adhesion or agglomeration, namely the Lifshitz-Van der Waals interaction, the electrostatic interaction, the hydrophobic interaction and the Brownian motion. Lifshitz-Van der Waals forces are based on the electric moment of electrons in an atom which induces a counter electric moment in another atom. Their impact is relatively weak but extends to long range distances (>50 nm). These interactions are mainly of attractive nature (Martienssen, 2001). With decreasing distance of particles (10-20 nm) electrostatic interactions become predominant. Due to the negative net surface charge of most particles in suspension, these forces are mainly repulsive resulting in stable single cell suspensions (Vandamme *et al.*, 2013). At shorter distances an attraction and agglomeration of particles can occur by short range electrostatic forces (2-10 nm), driven by the different character of local charges on the particle surfaces. Furthermore, the hydrophobic properties of a particle influence its agglomeration behavior. Thus, hydrophobic functional groups on the microorganism surface can locally overcome the hydrogen bond of its surrounding aqueous medium (short range interaction of <2 nm). For distances lower than 1 nm, specific interactions such as ionic or hydrogen bonds as well as receptor-ligand interactions become prevalent (Martienssen, 2001).

For cell harvesting purposes in microalgae production it is necessary to overcome the energy barrier of the stable single cell suspension and ease the formation of flocs. Therefore, the addition of a flocculation aid (see Figure 4.1b and Section 4.2.4) can lead to an increase of the ζ-potential close to zero. The repulsive interaction declines which leads to a higher probability of particles attraction by Lifshitz-Van der Waals forces.

4.2.2 DLVO theory

The interactions of a particle with increasing distance to another particle or surface can be described as change of the free enthalpy of the particle G_{tot} according to the Derjaguin-Landau-Verwey-Overbeek (DLVO) theory of colloid stability (see Figure 4.2). In general, colloids are small dispersed particles which are suspended in a liquid or gas. The particles have their size in nanometer or micrometer scale. Thus, microalgae can also be denoted as colloids and the classical DLVO theory is applicable. The underlying free energy of interaction G_{tot} is described by the sum of the interaction energies given by Lifshitz-Van der Waals interactions G_{LW} and electrostatic interactions G_E in dependence of the separation distance H. In this theory, short range interactions are not considered (Bos *et al.*, 1999):

$$G_{tot}(H) = G_{LW}(H) + G_E(H) \tag{4.1}$$

with

$$G_{LW}(H) = -\frac{AR}{12H} \tag{4.2}$$

and

$$G_E(H) = 2\epsilon\pi\psi^2 ln[1 + \exp(-\kappa H)] \tag{4.3}$$

where A is the strain-dependent Hamaker constant in J, derivable from contact angle measurements and R is the particle radius in nm. The cells are assumed to be spherical. ϵ is the dielectric constant of the medium in F m^{-1} and ψ is the surface potential in mV which can be calculated from ζ-potential measurements. Negative ζ-potential values entail a repulsive electrostatic force whereas positive ones are accompanied by attractive interactions. The inverse Debye length or double layer thickness of the particle κ can be described by following equation:

$$\kappa = \sqrt{\frac{e^2}{\epsilon k_b T} \sum z_i^2 n_i} \tag{4.4}$$

with e representing the electron charge ($1.602 \cdot 10^{-19}$ C), z_i the charge number and n_i the number concentration of the ionic species i in the solution.

Due to the fact that 1 k_bT ($\approx 4.05 \cdot 10^{-21}$ J) represents the thermal Brownian motion of a microorganism and was used as reference for cell adhesion, the interaction energy is commonly provided in k_bT scale (with k_b as Boltzmann constant and T as absolute temperature 293.15 K) (Ozkan, 2012). From the energetic point of view, all natural systems

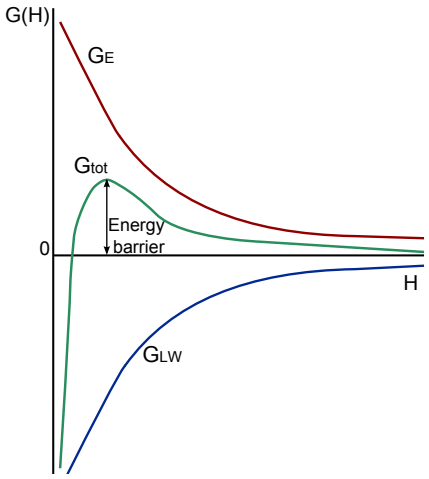

Figure 4.2: Schematic illustration of the total surface free energy G_{tot} according to the DLVO theory in a stable particle suspension. G_{tot} is the sum of repulsive electrostatic interactions G_E and attractive Lifshitz-Van der Waals interactions G_{LW} of a suspended particle in dependency of the separation distance H to another particle or surface.

aim for the achievement of a state of minimal free energy (Bos *et al.*, 1999). Therefore, a particle agglomeration is probable for negative values of G_{tot}. In contrast, positive values indicate a favored single cell suspension without cell adhesion (see Figure 4.2). Only the electrostatic interactions of particles can be influenced by e.g. the increase of the ionic strength or by the addition of flocculants to overcome the energy barrier illustrated in Figure 4.2. If the electrostatic interactions between particles decrease, a secondary energy minimum of G_{tot} arises where particle agglomeration becomes more probable. In biotechnology, the DLVO approach has been already proven to describe the microbial adhesive interaction in bio-film formation on several surfaces (Bos *et al.*, 1999; Ozkan, 2012), but it is also valid for the description of interactions between two microorganisms (Martienssen, 2001) and therefore applicable for the prediction of cell agglomeration.

4.2.3 Flocculation mechanisms

In general, the sedimentation velocity v_p (m s^{-1}) of a particle is driven by the density difference $\Delta\rho$ (kg m^{-3}) of the particle and the surrounding medium as well as by its gravity. This relation is approximately described by the Stokes's law (Liss *et al.*, 2005):

$$v_p = \frac{\Delta\rho}{18\eta_f} \cdot g \cdot d_p^2 \tag{4.5}$$

where η_f is the dynamic viscosity of the fluid in kg m^{-1} s^{-1}, g is the gravitational acceleration (9.81 m s^{-1}), and d_p is the diameter of the particle in m. For small particles with low densities such as microalgae, the Brownian motion dominates the gravity effect. The formation of bigger particle agglomerates influences d_p and $\Delta\rho$ and lead to

an enhanced effect of gravity (Brady *et al.*, 2014). Flocculation is one possible precon-

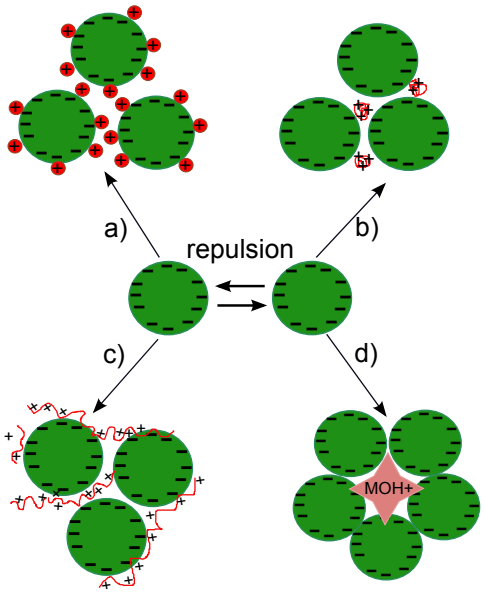

Figure 4.3: Principle of flocculation induced by a) charge neutralization, b) electrostatic patch mechanism, c) bridging and d) sweeping flocculation.

centration technique to overcome the obstacles of low cell density and small cell sizes by the agglomeration of single algal particles into bigger flocs. The approach derived from colloid process systems engineering is already exploited for a wide range of industrial applications (e.g. waste water treatment, paper industry, mining and brewery). There are basically four different mechanisms attributed to the flocculation of a single cell algae suspension. The simplest form of flocculation is induced by charge neutralization (Figure 4.3a). Positively charged ions or colloids stick to the algal surface and neutralize its negative charge. Repulsive electrostatic forces are reduced, leading to a higher probability of cell coagulation. The effect of an electrostatic patch occurs if positively charged polymers approach the algal surface and locally reverse its charge (Vandamme *et al.*, 2013). The thereby emerged patches can attach further particles or cells to form flocs (Figure 4.3b). In contrast, bridging represents a phenomenon where polymers or charged particles act as bridge between two or more particles by simultaneously binding to their surfaces (Figure 4.3c). Furthermore, sweeping flocculation is provoked by the precipitation of mineral medium compounds due to pH increase (Figure 4.3d). The precipitated minerals entrap cells or particles resulting in the formation of agglomerates.

4.2.4 Types of algal flocculation

The above described flocculation mechanisms are dependent on the used flocculants and come to pass alone or as a combination of each other. Generally, a distinction is

made into chemical, physical, biological and auto-flocculation. Chemical flocculation constitutes the mechanisms which are based on inorganic and organic poly-electrolytes or inorganic metal salts addition. This effective methodology is especially applied in water treatment to separate waste particles and phosphates. Due to the cationic effect of solved multivalent metal ions such as Al^{+3} or Fe^{+3} a charge neutralization of the algal surface occurs (see Figure 4.1b). The mechanism is well understood and effective for a wide range of microalgae (Eldridge *et al.*, 2012; Harun *et al.*, 2010a). However, the residual metal ions in the cell agglomerates can interfere with further downstream steps or negatively influence the product quality and acceptance on the food and feed market (Papazi *et al.*, 2010; Rwehumbiza *et al.*, 2012).

Flocculants in form of natural or synthetic cationic polymers such as the biodegradable cationic starch or chitosan are less harmful to remain in the biomass. Here, mechanisms of patching, bridging and charge neutralization are acting together to facilitate floc formation. The efficiency of biomass preconcentration of several charged polymers is significantly influenced by the pH value and the ionic strength of the suspension (Farid *et al.*, 2013). High salinity for example, lead to coiling and a shielding of the polymer charge, making it unsuitable for the harvesting of marine microalgae (Uduman *et al.*, 2010).

Another form of chemical flocculation is caused by a pH increase of the suspension above 9 (Vandamme *et al.*, 2012). In nature the so-called autoflocculation occurs spontaneously as a reaction of CO_2 depletion in the culture broth which is accompanied by an increased pH value. Here, the microalgal biomass is concentrated by sweeping flocculation as a consequence of the precipitation of Ca^{+2} or Mg^{+2} ions in the medium after pH increase (Vandamme *et al.*, 2012). In most natural water resources (lake or sea water) magnesium is highly abundant making this approach feasible for a wide range of algal production processes. Recently, this technique was successfully applied to *D. salina* in combination with air flotation by Besson & Guiraud (2013). But even for this methodology, a biomass contamination with less harmful magnesium or calcium precipitates is unavoidable.

Physical flocculation is induced by means of electrolysis, ultrasound or magnetic forces. During electrolysis the sacrificial electrode releases positively charged metal cations or hydroxide species (see Equations 4.6–4.7) which can attach to the counter-charged microalgal surfaces. Neutralization occurs and facilitates the formation of microalgae flocs (Uduman *et al.*, 2011). This can be supported by flotation (Gao *et al.*, 2010) due to the simultaneous oxidation of water at the anode (see Equation 4.8 with aluminum electrodes as example) or by sweeping flocculation, if insoluble aluminum hydroxide precipitates are generated. The latter effect was observed mainly in media with an alkaline pH value (Vandamme *et al.*, 2011). The flotation effect of electrolysis is further enhanced by the cathodic reduction of water into gaseous H_2 (see Equation 4.9).

The biomass pollution with metal ions is a negative side effect also of this process.

$$Al \longrightarrow Al^{3+} + 3e^- \tag{4.6}$$

$$mAl^{3+} + nOH^- \longrightarrow Al_m(OH)_n^{z+} \tag{4.7}$$

$$2H_2O \longrightarrow 4H^+ + O_2 + 4e^- \tag{4.8}$$

$$2H_2O + 2e^- \longrightarrow H_2 + 2OH^- \tag{4.9}$$

In contrast, ultrasound can be applied without causing undesired biomass contamination. Although the methodology was effectively approved for different microalgae in lab scale (Wan *et al.*, 2014), its implementation in large scales reveals diverse weaknesses so far (Vandamme *et al.*, 2013). Another concept of microalgae harvesting exploits the magnetic force. Here, magnetite nanoparticles (Fe_3O_4) are used to adsorb the algal cells prior to floc formation and separation by an magnetic field. The advantage of the method is the possibility to recycle the magnetite particles. Nevertheless, the technique is costly due to the special equipment required for particle regeneration and the expensive magnetite particles (Wan *et al.*, 2014).

In addition, bioflocculation is a recently explored flocculation approach which works without the addition of chemicals. In this case autoflocculating microorganisms such as bacteria, microalgae or fungi secrete biopolymers or carry positively charged hyphae which act as flocculants (Liu *et al.*, 2013; Vandamme *et al.*, 2013). So far, the underlying mechanisms are not completely understood and therefore more research efforts are required prior to its large scale application.

4.3 Materials and methods

4.3.1 Strain and cultivation conditions

D. salina CCAP 19/18 (delivered 2011 by the Culture Collection of Algae and Protozoa, Scotland) was grown photoautotrophically in a rotary shaking incubator (Multitron, Infors AG, Switzerland) at 3.5% CO_2 in air, a temperature of 26 °C and a shaking frequency of 100 rpm. The cultivations were carried out at a pH of 7.5 in 2 L shaking flasks filled with 1 L of the growth medium previously described by Lamers *et al.* (2010). To avoid inhibitory effects of NaFeEDTA, Na_2EDTA and HEPES on the flocculation performance, the medium was prepared without these ingredients. Due to the fact that iron is a crucial trace element for algal growth, NaFeEDTA was replaced by the addition of 5 μM $FeCl_3$ into the medium. Day/night cycles were simulated by the daily application of 16 h light at 75 μE m^{-2} s^{-1} and a dark phase of 8 h.
The induction of carotenogenesis in *D. salina* was done by applying abiotic stressors in form of continuous high light conditions at 1500 μE m^{-2} s^{-1} and nitrogen depletion.

For this purpose 1 L nitrate free culture medium was inoculated to reach approximately 1×10^6 cells mL^{-1} with a culture previously grown under control conditions as described above. This cultivation was carried out in a flat panel photobioreactor (FMT 150, PSI, Czech Republic) at a pH of 7.5, aerated with 400 mL min^{-1} of a synthetic air mixture containing 3.5% CO_2.
For the determination of algal growth and the harvesting efficiency η_H the optical density of the samples was measured at 735 nm using an UV/Vis spectrophotometer (Specord S600, Analytik Jena AG, Germany). Cell concentrations were determined by a cell counter (Cellometer Auto T4, Nexcelom Bioscience LLC., USA).

4.3.2 Measurement of the surface energy

The surface charge of *D. salina* was determined by means of electrophoretic mobility measurements of the cell suspension at room temperature. Therefore, *D. salina* cells were harvested by centrifugation, washed twice and resuspended in the previously mentioned medium, which was prepared with different ionic concentrations of NaCl (0.15-4.1 M) and adjusted to a final cell density of 1.1×10^6 mL. The electrophoretic mobilities of the cells were measured using a zetaziser (Zetasizer NanoZS, Malvern). The indices of refraction and the viscosities of the different medium variants were determined beforehand by a refractometer (RE40D, Mettler Toledo) and a rheometer (DVIII ultra, Brookfield). The index of refraction of the microalgae cells was set to 1.05, based on data presented by Kirk (1994). The dielectric constants of the NaCl rich media were adapted from Gavish & Promislow (2016). The ζ-potentials were derived from the electrophoretic mobility values using Smoluchowski's model. The surface potential was calculated based on the ζ-potential values according to the following equation Ozkan (2012):

$$\psi = \zeta \left(1 + \frac{\nu}{a}\right) \exp(\kappa\nu) \tag{4.10}$$

The parameter ν accounts for the hydration layer thickness surrounding the particle and was assumed to be $3x10^{-11}$ m in high ionic medium (adopted from Ozkan & Berberoglu (2013)). The parameter a is the radius of the particle in m.

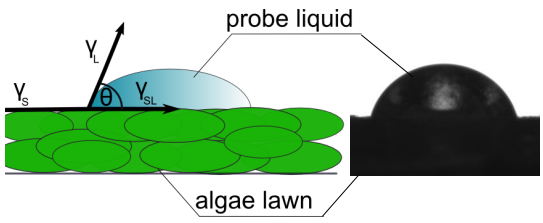

Figure 4.4: Contact angle of a probe liquid on algal surfaces using the measurement scenario with a diiodomethane droplet on *D. salina* lawn ($1.21x10^6$ cells μm^{-2} cellulose acetate filter) as an example.

The surface energy of *D. salina* was estimated based on contact angle measurements using the sessile drop method introduced by Busscher *et al.* (1984). First of all, cell lawns were prepared. Therefore, a *D. salina* culture was harvested by centrifugation (10 min, 1000xg), washed twice and resuspended in physiological saline solution (0.9% NaCl) to reach a final cell concentration of 54.5×10^6 mL^{-1}. After this, every cell lawn was generated with a final cell area density of 1.21x10^6 cells μm^{-2} by filtering a volume of 5 mL suspension through a cellulose-acetate filter (45 μm pore size, Ø 45 mm, Whatman). To keep the lawns moist until the measurements were started, all filters were placed on 1% agar plates containing 10% glycerol. Polar water, apolar diiodomethane and bipolar formamide were used as reference liquids with known physical properties. The contact angles were measured by a goniometer (OCA 1.5 Pro, DataPhysics) using the Young-Laplace method. Droplets of the probe liquids were placed on the lawns using a 0.5 mL syringe (Hamilton) as visible in Figure 4.4. The summarized results of the contact angle calculation in Table 4.1 account for the average values of at least 5 independent measurements.

Table 4.1: Contact angles θ of different probe liquids on *D. salina* cell lawn.

Probe liquid	θ $^\circ$
Water	26.7 ± 3.93
Formamide	26.82 ± 1.31
Diiodomethane	74.20 ± 3.96

Contact angles θ of lipid droplets on a surface or microbial cell lawn are related to the surface free energy. This relation is expressed by the Young equation:

$$cos\,\theta = -1 + \frac{2\left(\gamma_s^{LW}\gamma_l^{LW}\right)^{0.5}}{\gamma_l} + \frac{2\left(\gamma_s^{+}\gamma_l^{-}\right)^{0.5}}{\gamma_l} + \frac{2\left(\gamma_s^{-}\gamma_l^{+}\right)^{0.5}}{\gamma_l} \tag{4.11}$$

where γ_i^{LW} is the apolar surface energy component, γ^-, γ^+ are electron donor and acceptor parameters, respectively. The subscript s refers to the particle surface and l to the probe liquid. In the present study the known surface tension parameter γ_l^{LW}, γ_l^{AB}, γ_l^+ and γ_l^- for the different probe liquids published by Bos *et al.* (1999) were used to solve the equation system for γ_s^-, γ_s^+ and γ_s^{LW}. Furthermore, the results of γ_s^- and γ_s^+ were applied for the determination of the polar surface component γ_s^{AB} of the algae surface:

$$\gamma_s^{AB} = 2\sqrt{\gamma_s^-\gamma_s^+} \tag{4.12}$$

The effective Hamaker constant for two identical solid particle such as microalgae immersed in aqueous medium was determined as follows (Liu *et al.*, 2013):

$$A = 24\pi H_0^2 \left(\sqrt{\gamma_s^{LW}} - \sqrt{\gamma_l^{LW}}\right)^2 \tag{4.13}$$

where H_0 is the minimum separation distance in m. The result was used to solve the equation for G_{LW} according to DLVO theory expressed in Equation 4.2. Furthermore, the free energy of cohesion ΔG_{coh} was calculated based on the equation proposed by van Oss (1995) to get an impression of the hydrophobic properties of the *D. salina* cells:

$$\Delta G_{coh} = -2\left(\sqrt{\gamma_s^{LW}} - \sqrt{\gamma_l^{LW}}\right)^2 - 4\left(\sqrt{\gamma_s^+\gamma_s^-} + \sqrt{\gamma_l^+\gamma_l^-} - \sqrt{\gamma_s^+\gamma_l^-} - \sqrt{\gamma_s^-\gamma_l^+}\right) \tag{4.14}$$

4.3.3 Flocculation experiments with *D. salina*

Unless otherwise noted, all harvesting experiments were carried out for a sedimentation time of 30 min under lab scale conditions in duplicates of beaker glass vessels (jar tests) or electrolysis chambers. Therefore, *D. salina* cultures in a mid-logarithmic growth phase were adjusted to a pH of 7.5 and a culture density of approximately $OD_{735nm} = 1$ prior to flocculation. The applied culture density refers to approximately 0.3 g_{dw} L^{-1} biomass which is similar to the harvesting concentration of *D. salina* used in production scale (Curtain & Snook, 1983). The flocculation procedure was induced by chemical and physical techniques; namely the addition of metal ions via $Al_2(SO_4)_3{\times}16H_2O$ (alum), $AlCl_3$, $FeCl_3{\times}6H_2O$, $FeSO_4{\times}7H_2O$, $Fe_2(SO_4)_3{\times}6H_2O$ or electrolysis using aluminum electrodes as well as the pH increase by the addition of NaOH or $Ca(OH)_2$. Optimal flocculant doses c_F were identified by preliminary experiments. Therefore, the concentrations of the metal salts were varied between 0-1.2 mM. In the case of pH increase variations in the range of 0-25 mM $Ca(OH)_2$ or 0-50 mM NaOH were applied, respectively. In preparation of the flocculation experiments, each beaker glass vessel was filled with 100 mL culture suspension. The respective flocculants were added to the cultures under mixing at 250 rpm. Mixing was continued for 10 min followed by a sedimentation step of another 30 min. Samples of the suspension were taken at the measuring height h_m accounting for the middle of the suspension level h_1 in the beaker glass (see Figure 4.5). The harvesting efficiency η_H was calculated according to the following equation:

$$\eta_H = \frac{OD_{735nm}(t_0) - OD_{735nm}(t_{end})}{OD_{735nm}(t_0)} \cdot 100 \tag{4.15}$$

where $OD_{735nm}(t_0)$ is the absorbance of the algal suspension at 735 nm before and $OD_{735nm}(t_{end})$ after 30 min of flocculant addition. The concentration factor CF was determined as follows:

$$CF = \frac{h_1}{h_2} \tag{4.16}$$

with h_1 as fill level of the suspension at the beginning and h_2 as sedimented algal suspension height at the end of the harvesting experiment (see Figure 4.5). The flocculant doses for the electrolysis experiments were altered by applying different electrolysis durations in the range of 5-20 min or different current densities between 3.4-17 mA cm^{-2}

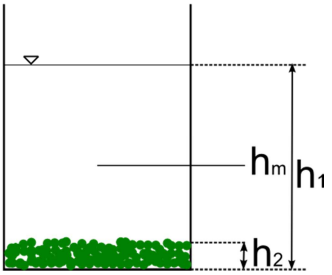

Figure 4.5: Scheme of the flocculation experiment illustrating the measurement height h_m, the fill level of the suspension h_1 and the height of sedimented algae h_2.

using a conventional power supplier (peqPOWER 250, Peqlab, Germany). For this purpose, glass chambers with a geometric dimension of 5.5×10.8×12 cm^3 were used and equipped with two aluminum electrodes keeping a distance of 4 cm, respectively. Each glass chamber was filled with 300 mL of the culture prepared as described above. During electrolysis an active area of 44 cm^2 sacrificial electrode was applied and the cultures were continuously mixed at 250 rpm. After electrolysis the electrodes were removed and the cultures were mixed for further 10 min. Samples were taken as described above to determine η_H and CF according to Equations 4.15-4.16. The energy consumption E_H in kWh kg_{dw}^{-1} was determined based on following equation:

$$E_H = \frac{UIt}{1000 m_{dw} \eta_H} \tag{4.17}$$

where U is the voltage in V, I the current in A, t the electrolysis duration in h and m_{dw} the used biomass. Furthermore, the mass of dissolved aluminum m_{Al} released during electrolysis was calculated according to Faraday's law:

$$m_{Al} = \frac{M_{Al} It}{zF} \tag{4.18}$$

with M_{Al} as molecular mass of aluminum, z as valence of the ions and F as Faraday constant (96485.33289 As mol^{-1}).

Centrifugation was used as comparative harvesting method as well as to further concentrate the flocculated *D. salina* cells prior to pigment extraction. For this purpose, cells were centrifuged for 30 min at 500xg in a laboratory centrifuge (6-16KS, Sigma Laborzentrifugen GmbH, Germany).

The diameters of single cells and flocs were estimated from their 2D projection using microscope images (Axio Imager A1, Carl Zeiss, Germany). The maximum diameters d_{max} and minimum diameters d_{min} of 30 single cells and 50 flocs of each flocculation

method were determined from these images to calculate the respective effective diameters d_e:

$$d_e = \sqrt{d_{max} d_{min}} \tag{4.19}$$

4.3.4 Reuse of the separated culture medium

The separated supernatants of the harvested cells were collected to investigate the recyclability of the cultivation medium after dewatering. The supernatants were readjusted to a pH of 7.5. $MgCl_2$ was added to the supernatants harvested via pH increase to regain the typical Mg concentration in the medium. In order to remove contamination from the medium, the recycled supernatants were filtered through polyethersulfone membrane filters (Filtermax, TPP, Switzerland) with a pore size of 0.22 μm prior to the second cultivation. To test on reusability, duplicates of 200 mL shaking flasks were filled with 100 mL recycled medium, respectively. Fresh medium was used for the control cultivation. All flasks were inoculated with *D. salina* cells to reach an initial optical density of approximately OD_{735nm}=0.1. The cultivation took place under control conditions as described in Section 4.3.1.

4.3.5 Elemental analysis of the separated culture medium

The contamination of supernatant and biomass with Al, Fe, Mg, P or Ca was investigated by analyzing the separated medium after the harvesting procedure via inductively coupled plasma optical emission spectrometry (ICP-OES, Currenta, Germany). The remaining flocculant load in the biomass m_F in % was estimated as follows:

$$m_F = \frac{m_F(t_0) - m_F(t_{end})}{m_{dw}} \cdot 100 \tag{4.20}$$

with $m_F(t_0)$ as the mass of the receptive flocculant added prior to flocculation and $m_F(t_{end})$ as the mass of the respective flocculant measured in the supernatant of the flocculated microalgae suspension.

4.3.6 Determination of the extraction efficiency in dependency of the used harvesting approach

To investigate the effect of the harvesting method on the subsequent pigment extraction, centrifuge-tubes were filled with 15 mL of a nitrogen-depleted *D. salina* cell culture, respectively. The flocculants NaOH, alum and $FeCl_3 \times 6H_2O$ were directly added to the tubes under continuous mixing at 250 rpm (ThermoMixer C, Eppendorf, Germany), followed by an additional mixing period of 10 min. Electrolysis was conducted as explained in Section 4.3.3. After 10 min mixing, 15 mL cell suspension samples were taken to fill the tubes. All samples were allowed to settle down for 2 h. Thereafter, samples were centrifuged (500xg, 30 min), supernatants were discarded and the pellets were freeze dried prior to the extraction step. All experiments were conducted in four replicates. As a control four 15 mL samples of *D. salina* were dewatered by sole centrifugation and subsequent freeze drying. Pigment extraction of the dried samples was

done according to the method of Lamers *et al.* (2010). The β-carotene content of the samples was quantified by high performance liquid chromatography (HPLC) (Agilent 1290, Agilent Technology, USA), using a reversed-phase C18 column (Zorbax Eclipse Plus, 1.8 μm pore size, 100 mm x 2.1 mm). An injection volume of 2 μL was used for analysis. The elution was performed by a linear gradient from 100 % solution A (84 % acetonitrile, 2 % methanol, 14 % Tris buffer (0.1 M, pH 8.0)) to 10 % solution A and 90 % solution B (68 % methanol, 32 % ethyl acetate) for 2 min followed by elution with 100 % solution B for 3 min at a flow rate of 0.5 mL min^{-1} (Polle *et al.*, 2001). For UV detection at 520 nm a photodiode-array detector (G1315D, Agilent Technology, USA) was applied. A standard curve with a β-carotene standard (Sigma Aldrich, USA) was prepared to quantify the carotenoid content.

4.3.7 Calculation of energy demand and economics

To assess the impact of the harvesting step on economics and energy demand, the overall process described in Section 3.2 was extended by a flocculation unit as illustrated in Figure 4.6.

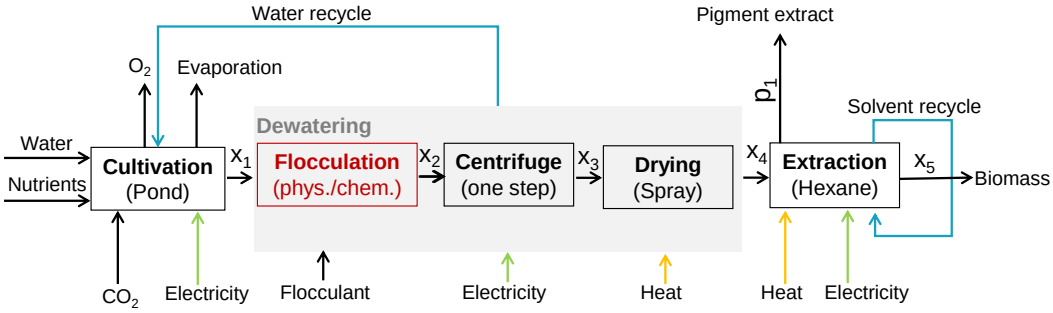

Figure 4.6: Process route of industrial β-carotene production by *D. salina*. The process is divided into three groups of process subunits; namely the biomass and product generation, the harvesting including a flocculation, a centrifugation and a drying step and the n-hexane extraction of the product. The red marked process indicates the modification compared to the reference scenario.

The flocculation methods (alum, $FeCl_3 \times 6H_2O$, NaOH and electrolysis) selected in Sections 4.4.2-4.4.4 were theoretically applied to preconcentrate the biomass in this step. Centrifugation without flocculation was used as a control method. Furthermore, the experimental data of the harvesting efficiencies η_H, the concentration factors CF, the extraction efficiencies η_E, the flocculant doses c_f and the recyclability analysis were directly incorporated in the process model. If centrifugation was used as first harvesting step, CF and η_H were quantified based on information provided by the company NBT Ltd. Eilat, Israel (personal communication with Prof. Ben-Amotz, 2014) using a centrifuge with 95 % efficiency and an output of 0.1 kg_{dw} L^{-1} biomass. The energy consumption of flocculation caused by metal salts or NaOH was assumed

to be 0.1 kWh m^{-3} (Weschler *et al.*, 2014). The energy demand and the mass of flocculant generated in-situ via electrolysis were quantified by the use of Equations 4.17-4.18. After flocculation, a 95% effective centrifugation was considered as a second dewatering step resulting in a final biomass concentration of 15% which is a typical level reported for industrial algae processes (Ben-Amotz, 2008; Molina Grima *et al.*, 2003). The implementation of the model and the consideration of uncertainties was done as outlined in Section 3.2.5.

4.4 Results and discussion

4.4.1 Physico-chemical properties of *D. salina*

The strongest impact of microalgal coagulation behavior is given by the typical species characteristic of size, morphology and surface charge (Chatsungnoen & Chisti, 2016). For this reason, the physico-chemical properties of *D. salina* were characterized prior to the flocculation experiments. The ζ-potential of suspended cells is strongly influenced by the ionic strength of the surrounding electrolyte solution. During cultivation of *D. salina* up to 4.1 M NaCl is present in the aqueous medium. An increase of the NaCl concentration from 0.1 M to 3 M provoked an incipient destabilization of the single cell suspension. This behavior was demonstrated by the rising ζ-potential from -23 mV to -10 mV as visible in Figure 4.7.

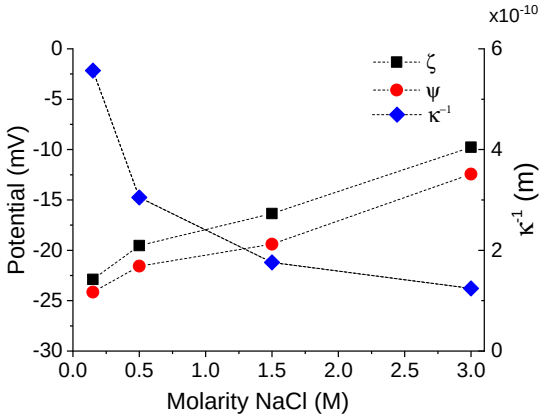

Figure 4.7: Effect of medium salt concentrations on the surface properties ζ-, ψ-potential and thickness of the electrostatic double layer κ^{-1} of *D. salina*.

Considering the fact, that coagulation of microalgae is effectively induced for a ζ-potential between -8 mV and +2 mV (Henderson *et al.*, 2006), the preconditions to flocculate *D. salina* cells seems to be optimal. The cells maintain their negative surface charge. Thus, they have the ability to bind cationic flocculants such as metal ions or positive charge polymers. This effect can be exploited to promote cell neutralization and induce flocculation. Due to technical constraints, a further increase of the ionic strength of the suspension up to 4.1 M NaCl was not feasible. The measurement of

electrophoretic mobility in high ionic cell suspensions leads to electrolysis of the measurement conductivity cell and with that to unreliable values of ζ. Nevertheless, the compression effect on the electrostatic double layer κ^{-1} of *D. salina* becomes clearly visible. Here, the increased NaCl concentration from 0.1 M to 3 M is accompanied by a more than 4-fold decrease of κ^{-1}. With that, the probability of homoaggregation of the cells is strongly enhanced (Ma *et al.*, 2015). In addition, the surface charge influences the required concentration of cationic flocculants. The lower the surface charge, the lower is also the needed dosage of flocculants. Consequently, a successful flocculation of *D. salina* with small amounts of flocculants is expectable.

The contributions of the Lifshitz-Van der Waals interactions G_{LW} and the electrostatic interactions G_E on the total surface free energy G_{tot} of*D. salina* in different medium compositions are presented in Figure 4.8.

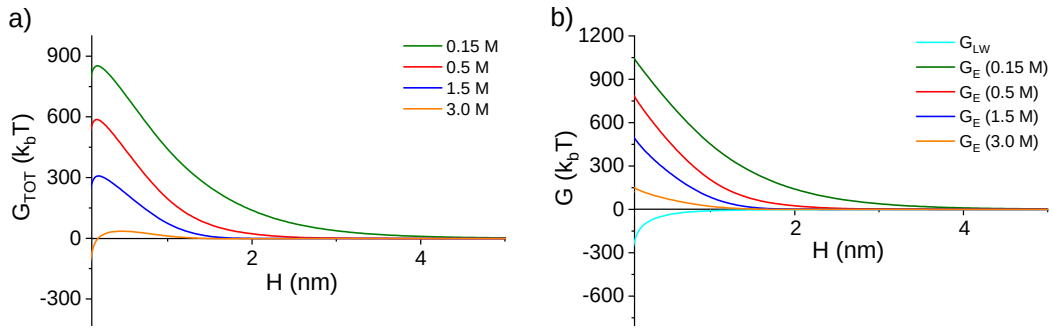

Figure 4.8: Effect of medium NaCl concentration on a) total surface free energy of interaction G_{tot} or b) on the divided interaction components Lifshitz-Van der Waals G_{LW} and electrostatic interactions G_E of *D. salina*.

Table 4.2: Physico-chemical surface properties of *D. salina* suspended in aqueous medium.

Property	Value	Unit
γ_s^{LW}	23.66	mJ m^{-2}
γ_s^{AB}	0[b]	mJ m^{-2}
γ_s^-	41.12	mJ m^{-2}
γ_s^+	-9.05[a]	mJ m^{-2}
γ_s	23.66	mJ m^{-2}
A	7.07×10^{-20}	mJ
ΔG_{coh}	27.45	mJ m^{-2}

[a] the negative value of γ_s^+ is explained by a surface composition where electron donors quantitatively predominate the electron acceptors (van Oss, 1995)
[b] γ_s^{AB} results in a negative square route and is therefore set to zero according to the results of other seawater species (Ozkan & Berberoglu, 2013)

As expected previously, G_{LW} is of attractive nature and independent from the ionic

strength of the surrounding medium (see Figure 4.8b). The repulsive force G_E visibly loses its strength with higher concentrations of NaCl in the suspension. Moreover, the electrostatic surface interactions are effective only for short separation distances, indicating optimal preconditions of cell agglomeration. G_{tot} as the sum of both forces according to classical DLVO theory (Equations 4.1-4.3) reveals a declining energy barrier for cell agglomeration with increased molarity of NaCl in the culture broth (see Figure 4.8a). Due to the fact, that β-carotene production is done at higher molarities of NaCl, the real energy barrier under these condition is possibly even lower. However, with A=7.07·10^{-23} J, the Hamaker constant demonstrates the relatively low contribution of the Lifshitz-Van der Waals interaction force to G_{tot}. Thus, an auto-flocculation of the cells is not expectable (Liu *et al.*, 2013). With regard to the free energy of cohesion G_{coh}=27.45 mJ m^{-2} (see Table 4.2), the weak hydrophilic surface character of *D. salina* is demonstrated. This finding supports the assumption that cell agglomeration is energetically unfavorable in the untreated cell suspension. Nevertheless, the results of the physico-chemical characterization of *D. salina* indicate a high probability of cell agglomeration by appropriate flocculation aids. Therefore, different flocculation methods are intensively investigated in the next sections.

4.4.2 Flocculation induced by the addition of metal salts

Solved cationic metal ions attach to the anionic algae surface and lead to charge neutralization. If the pH or flocculant concentration is increased up to a certain threshold value also sweeping flocculation occurs which is caused by a decreasing solubility of metal hydroxides (Duan & Gregory, 2003).

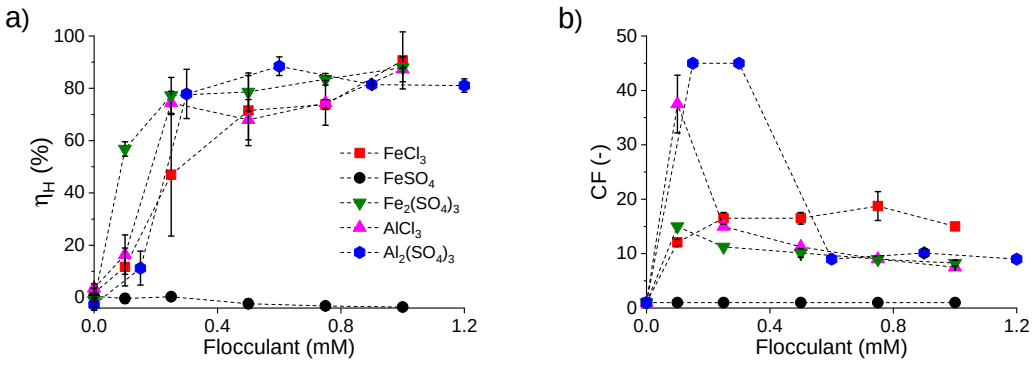

Figure 4.9: Flocculation a) efficiency η_H and b) concentration factor CF of *D. salina* determined 30 min after the addition of different concentrations of diverse aluminum and iron salts. Experiments were conducted in duplicates. Error bars represent the deviation of the measurements from the average value.

Figure 4.9 illustrates η_H and CF for *D. salina* cells provoked by the addition of $Fe_2(SO_4)_3$, $FeCl_3$, $FeSO_4$, $Al_2(SO_4)_3$ and $AlCl_3$. In all cases, except $FeSO_4$, flocculant concentrations of 0.5 mM resulted in an η_H of approximately 80 % which was further

increased to 90-97 % by applying flocculant concentrations up to 1 mM (see Figure 4.9a). Comparable tendencies were described for *Chlorella minutissima*, *Scenedesmus sp.* and the marine microalga *Dunaliella tertiolecta* using similar doses for Fe^{3+} and Al^{3+} (Chen *et al.*, 2013; Eldridge *et al.*, 2012; Papazi *et al.*, 2010). In contrast to the work of Papazi *et al.* (2010), all trivalent metal ions used in the present study reached comparable results regarding η_H, irrespective of whether chloride or sulfate were used as anion. In the aforementioned work, aluminum salts showed much faster coagulation times accompanied by higher efficiencies. Flocculation by divalent iron ions in form of $FeSO_4$ was inappropriate for *D. salina* since no flocculation effect was observed for all applied concentrations.
Considering the CF values reached for the different flocculants depicted in Figure 4.9b, it becomes obvious that the addition of aluminum salts is most effective to get a high dewatering effect of the biomass. In the case of ferric salts, $FeCl_3$ yields the best values regarding CF. Thus, 0.3 mM $Al_2(SO_4)_3$ and 1 mM $FeCl_3$ were chosen as promising flocculant doses for the subsequent analyses presented in Sections 4.4.5-4.4.9.

4.4.3 Flocculation via electrolysis

Generally, electrolysis is more appropriate for marine microalgae than for fresh water species (Vandamme *et al.*, 2013). Due to the high electric conductivity of sea water, the energy demand for electrolysis is reduced (Uduman *et al.*, 2011). Electrolysis of the saline microalga *D. salina* reveals a high potential for strong flocculation effects as the used culture medium in the present work contains 1.5 M NaCl. Another promoting effect for electro-flocculation is the already mentioned reduced thickness of the electrostatic double layer on the particle surface due to the high ionic culture medium (Duan & Gregory, 2003) as visible in Figure 4.7. The flocculation efficiencies η_H and

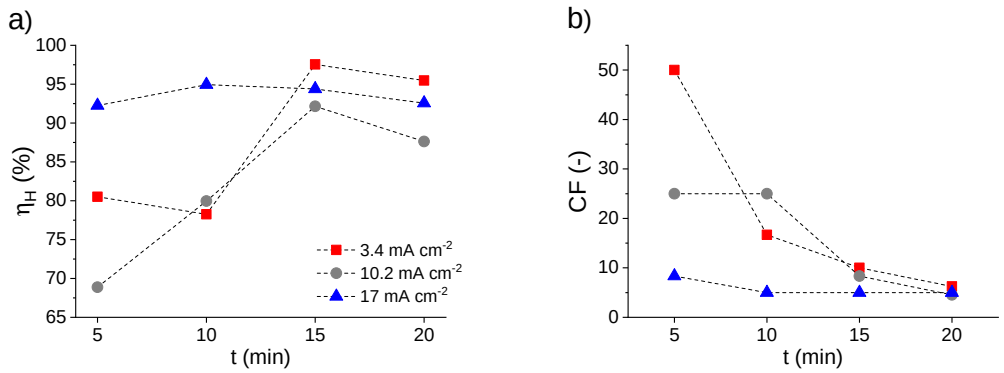

Figure 4.10: Flocculation a) efficiency η_H and b) concentration factor CF of *D. salina* determined 30 min after electrolysis with aluminum electrodes. Flocculant load was varied by applying current densities of 3.4 mA cm^{-2}, 10.2 mA cm^{-2} and 17 mA cm^{-2} for 5, 10, 15 and 20 min, respectively.

concentration factors CF for *D. salina* cells are summarized in Figure 4.10. Here, cur-

rent densities of 3.4-17 mA cm^{-2} were applied for 5, 10, 15 and 20 min, respectively using aluminum electrodes. Figure 4.10a demonstrates that increasing flocculant loads provoke enhanced flocculation efficiencies η_H. Using a current density of 17 mA cm^{-2}, best algae recovery results were achieved for an electrolysis duration of 5 or 10 min. In these experiments, η_H values of more than 95 % were reached, being comparable to literature data of e.g. Gao *et al.* (2010) or Uduman *et al.* (2011). The current densities needed to initiate coagulation of *D. salina* are higher compared to the 0.6-3 mA cm^{-2} used for the marine microalga *Phaeodactylum tricornutum* in the work of Vandamme *et al.* (2011). However, in other studies dealing with electrolysis of *Dunaliella* or other marine microalgae comparable or even 2-3 fold higher current densities were applied to gain similar η_H values (Uduman *et al.*, 2011; Zenouzi *et al.*, 2013).

Table 4.3: Final pH, calculated mass of solved aluminum $m_{Al^{3+}}$ and energy demand E_H of electrolysis in dependence of the applied electrolysis time using current densities of 3.4 mA cm^{-2}, 10.2 mA cm^{-2} and 17 mA cm^{-2}.

	$\mathbf{pH}_{end}$ (-)			$\mathbf{m}_{Al^{3+}}$ (g kg_{dw}^{-1})			$\mathbf{E}_H$ (kWh kg_{dw}^{-1})		
mA cm^{-2}	3.4	10.2	17	3.4	10.2	17	3.4	10.2	17
5 min	7.61	7.61	7.80	84.0	277.86	275.71	0.2	0.68	1.15
10 min	7.66	7.64	7.92	144.72	500.06	535.84	0.36	1.49	2.07
15 min	7.75	7.72	8.12	188.33	564.27	808.46	0.45	1.68	3.25
20 min	7.76	7.95	8.22	264.09	819.87	845.7	0.65	2.44	4.25

The most significant dewatering effect was observed for 3.4 mA cm^{-2} and 5 min. Nevertheless, Figure 4.10b reveals that an increase of the flocculant load directly caused a decline in the CF values. For industrial production lower CF would directly imply a higher energy consumption in subsequent dewatering steps. The origin of this phenomenon is given by the suspension pH. An optimal pH for electrolysis is below pH 7 (Gao *et al.*, 2010), where the predominant flocculation mechanism is charge neutralization by monomeric or cationic hydrolyzed forms of Al ions. At higher pH values, the solubility of aluminum hydroxides decreases (Duan & Gregory, 2003), precipitation occurs and leads to an embedding of algal particle. This effect seems to be less efficient for the electrolysis (Vandamme *et al.*, 2011). In the present study, the suspension pH was 7.5 according to the real production conditions. Therefore, sweeping flocculation was the predominant mechanism visible by the formation of white insoluble aluminum hydroxide (data not shown) and by the increase of the pH value from 7.5 to 7.6-8.2 during electrolysis (see Table 4.3). The generated flocs are bigger (see Table 4.4) compared to that of charge neutralization causing an enlarged sedimentation sludge volume.

With respect to the economic feasibility of the harvesting procedure due to energy and material costs, a current density of 3.4 mA cm^{-2} and a duration of 5 min was found to be appropriate for the following studies discussed in Sections 6.4.4-4.4.9. With this setting, the lowest investigated flocculant load and energy demand per kg harvested

biomass were required (see Table 4.3) going along with the best harvesting performance regarding the CF value. With 84 g_{Al} kg_{dw}^{-1} the theoretical flocculant demand of the electrolysis (according to Equation 4.18) is higher compared to the 68.5 g_{Al} kg_{dw}^{-1} needed for the flocculation by 0.3 mM $Al_2(SO_4)_3$.

4.4.4 Flocculation by pH increase

The harvesting efficiency η_H, the concentration factor CF and the pH values of a *D. salina* suspension after flocculation by NaOH or $Ca(OH)_2$ are shown in Figure 4.11. The increase of both flocculant concentrations was accompanied by an expected increase of the pH and by an improved harvesting efficiency η_H. In both cases, a pH value above 12 produced the highest η_H values. Comparable observation were recently done by Chen *et al.* (2013) and García-Pérez *et al.* (2014). In the latter work *Chlorella vulgaris* was flocculated most efficiently at a suspension pH of 12. Nevertheless, it has to be emphasized, that η_H is not only a function of the pH but also of the cell concentration as well as the Mg concentration in the suspension (García-Pérez *et al.*, 2014; Wu *et al.*, 2012). On the other hand, in the work of Besson & Guiraud (2013) the pH was observed to be less important than the base dosage for optimal NaOH flocculation-flotation of *D. salina*. In the present work, η_H is nearly constant after reaching a pH of 12. Accordingly, instead of the flocculant dose, the pH seems to be decisively for an effective flocculation of *D. salina* cells under the given conditions.

High pH flocculation is considered as an indirect flocculation mechanism, since the

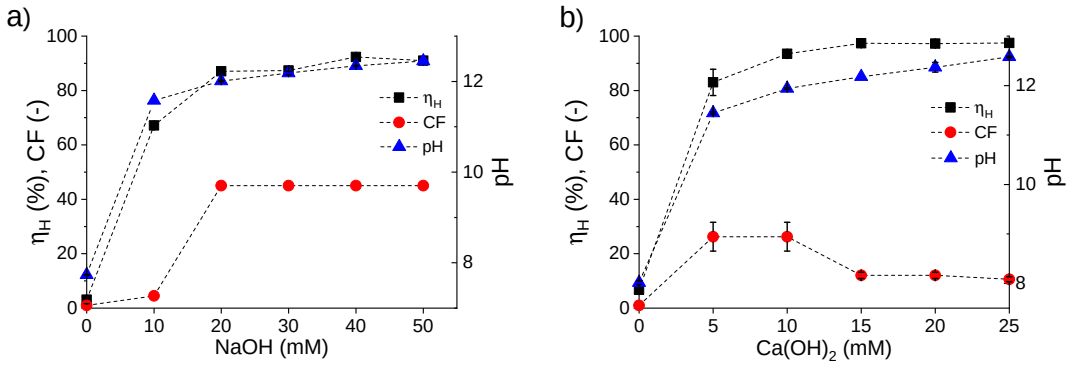

Figure 4.11: Flocculation efficiency η_H, concentration factor CF and pH of a *D. salina* suspension determined 30 min after addition of a) NaOH or b) $Ca(OH)_2$. Experiments were conducted in duplicates. Error bars represent the deviation of the measurements from the average value.

added NaOH or $Ca(OH)_2$ is not the flocculant itself. In fact, the increase of the pH destabilizes the algae suspension by sweeping flocculation due to Mg or Ca precipitation or by charge neutralization of charged hydroxides (Vandamme *et al.*, 2013). By considering only the η_H values, the addition of $Ca(OH)_2$ seems more preferable than the addition of NaOH. For *D. salina* a η_H value of 97 % is reached with 15 mM of

$Ca(OH)_2$, whereas 40 mM of NaOH causes an efficiency of 93 % after 30 min settling. Similar findings were presented by Castrillo *et al.* (2013) and Schlesinger *et al.* (2012) for the flocculation of various other microalgal species. Consequently, $Ca(OH)_2$ reveals a slightly higher flocculation strength than NaOH. Furthermore, it represents an attractive harvesting agent as it is inexpensive and widely available, if it is prepared from limestone as raw material. In addition, the biomass flocculated by $Ca(OH)_2$ is accepted for animal feed application (Schlesinger *et al.*, 2012).

However, the dewatering effect of NaOH addition clearly exceeded that of $Ca(OH)_2$ which becomes obvious by the comparison of the CF values (see Figure 4.11a, b). The flocs generated by NaOH addition are morphologically more dense than that generated by $Ca(OH)_2$ (see Supplementary material Figure A.2g and h), resulting in a lower algae sludge volume. High pH flocculation obviously tend to decreased CF values for pH values above 11 (Besson & Guiraud, 2013; García-Pérez *et al.*, 2014; Horiuchi *et al.*, 2003). The higher the pH, the higher is also the amount of precipitated $Mg(OH)_2$ in the biomass. Brady *et al.* (2014) predicted an exponential increase of $Mg(OH)_2$ precipitates in the medium for a pH above 10.5. This is accompanied by a reduction of functional algal surface groups which are bound via Mg^+ sorption. Furthermore, a co-precipitation of other compounds in the suspension is conceivable. Solved Ca in the medium can precipitates into insoluble $CaCO_3$ if the pH exceeds the value 11 (Şirin *et al.*, 2013), which would further enlarge the algal sludge volume. Due to the fact that an addition of 20 mM NaOH entailed an extraordinary high CF value of 50, this flocculant concentration was chosen to be further investigated in Sections 6.4.4-4.4.9.

4.4.5 Cell and floc size

The size of a particle is one of the most significant parameter affecting the sedimentation velocity which is explainable by the Equation 4.5 proposed by Stokes. The floc diameters of *D. salina* induced by flocculation with the selected methods are summarized in Table 4.4.

Table 4.4: Effective diameter d_e of single cells and flocs of *D. salina*. Flocculation was induced by electrolysis for 5 min at 3.4 mA cm^{-2} or the addition of 0.3 mM $Al_2(SO_4)_3$, 1 mM $FeCl_3$ or 20 mM NaOH.

Flocculant	$\mathbf{d}_e$ μm
Control (Single cell)	5.30 ± 0.47
Electrolysis	116.87 ± 37.53
NaOH	151.17 ± 58.65
$Al_2(SO_4)_3$	44.09 ± 18.02
$FeCl_3$	68.14 ± 22.91

Obviously, all flocculants led to a significant magnification of the particle size of 5.3 μm up to 151 μm. Flocs arose from sweeping flocculation by pH increase or elec-

trolysis are at least two or three times larger in size than those arose from charge neutralization by multivalent metal cations. Consequently, the sedimentation duration of cells flocculated by sweeping flocculation is shorter than that harvested by charge neutralization (Duan & Gregory, 2003). The duration is highly relevant for industrial application of *D. salina* as the main product of the alga is unstable. Thus, a fast downstream processing is essential.

4.4.6 Reuse of the separated culture medium

From the economic point of view, a recycling of nutrients and water from the separated medium after dewatering can be beneficial. Furthermore, for some microalgae the recycling could even positively impact the algal biomass production and the product yields (Farooq *et al.*, 2015). Therefore, this issue was investigated in detail in the present work. Figure 4.12 depicts the growth of *D. salina* on recycled medium after centrifugation or flocculation induced by 0.3 mM $Al_2(SO_4)_3$, 1 mM $FeCl_3$, 3.4 mA cm^{-2} electrolysis for 5 min and 20 mM NaOH. Fresh medium was used for the control cultivation. As clearly visible, the alga was able to grow in the recycled medium after flocculation by $Al_2(SO_4)_3$, $FeCl_3$ or electrolysis. Here, *D. salina* reached a growth rate comparable to that of fresh medium or culture medium separated by centrifugation (see Figure 4.12a, b). This observation was expected, since the separated media contained only traces of the possibly growth inhibitory flocculants Fe or Al (see Table 4.5) and all other major growth nutrients were found to be present in adequate concentration (for more details, see Pirwitz *et al.* (2015a)).

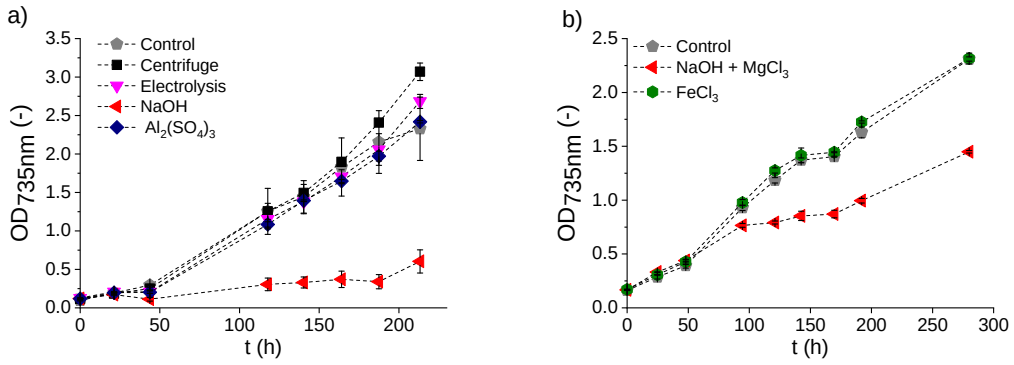

Figure 4.12: Growth of *D. salina* on separated medium after flocculation indicated as OD_{735nm}. Cultivation was carried out in recycled medium after a) centrifugation for 30 min and 500xg, electrolysis for 5 min at 3.4 mA cm^{-2}, the addition of 0.3 mM $Al_2(SO_4)_3$ or the addition of 20 mM NaOH and b) the addition of 20 mM NaOH with readjusted $MgCl_3$ concentration or the addition of 1 mM $FeCl_3$. Control cultivations were conducted in fresh medium. The experiments were carried out in duplicates. Error bars represent the deviation of the measurements from the average value.

Since Mg is an essential trace element for the growth of marine microalgae (Ho *et al.*, 2003), it is not surprising that the medium separated from flocculation via pH increase was not applicable for recycling without readjusting the Mg concentration (Figure 4.12a). Almost all Mg ions were precipitated in the medium (see Table 4.5) after pH increase. However, it must be noted that the used cultivation medium contains a relatively low Mg concentration (7.3 mg L^{-1}) compared to natural salt water resources. It is therefore not to be expected that the addition of NaOH would cause Mg limitation in natural sea water which is used for industrial cultivation of *D. salina*. For this reason, the concentration of Mg was readjusted to its typical level in a further experiment. But also in the readjusted medium, algal growth appeared strongly inhibited in comparison to the control culture (Figure 4.12b). These observations suggest that further effects along the precipitation of Mg and Ca influencing algal growth on the recycled medium after high pH flocculation. Triggered by these high pH values above 12, it is conceivable that a co-precipitation of additional medium ingredients occurred. For example, the work of Castrillo *et al.* (2013) demonstrates that a readjustment of NO_3^- and PO_4^{-3} ions to their original level lead to comparable algal biomass yields of control cultures and cultures grown on recycled medium after NaOH flocculation. Moreover, a study of Sukenik & Shelef (1984) indicates that high pH flocculation also induces orthophosphate and calcium phosphate precipitation. However, the analysis of the initial and residual Ca and P concentrations in the presently used medium of *D. salina* after NaOH addition, shows no significant decreases in these concentrations (see Table 4.5). In consequence, the reuse of supernatant of NaOH flocculation for *D. salina* cultivation was excluded in the later process analysis. In all other cases, the reusability of the medium after flocculation was assumed.

4.4.7 Contamination of *D. salina* biomass with flocculants

The biomass contamination caused by the respective flocculant was determined indirectly by quantifying their concentrations in the separated culture medium after flocculation of *D. salina*. The results are presented in Table 4.5. Each flocculant was found to be almost completely in the concentrated biomass. Accordingly, the complete applied flocculants were consumed during flocculation, indicating that optimal flocculant dosages were identified beforehand. With 205.84 $mg_{Fe}\ g_{dw}^{-1}$, the highest flocculant concentration was observed in the biomass harvested by $FeCl_3$. In comparison, the lowest flocculant load was found to be 26.96 $mg_{Mg}\ g_{dw}^{-1}$ provoked by NaOH flocculation. In this case, the already mentioned accompanied contamination with co-precipitates of P or Ca is negligible (see Sections 4.4.4) since the elements were found only in traces or were even not detectable. Flocculants in the concentrated biomass can interfere with subsequent downstream processing steps and possibly lower the product quality (Borges *et al.*, 2016; Uduman *et al.*, 2010). In contrast, the work of Rwehumbiza *et al.* (2012) demonstrates a decreasing flocculant concentration with every downstream processing step for polyaluminum flocculated *Nannochloropsis salina*. Here, the flocculant did not affect the final product composition. In some cases, remaining flocculants in the biomass can even promote the downstream processing. For instance it is possible to integrate

the flocculant as a potential reactant in downstream processes like the extraction or transesterification (Seo *et al.*, 2015). Moreover, an elimination of the flocculant contamination by further biomass treatments e.g. pH decrease and/or washing steps can be efficiently used to recover the product quality (Farooq *et al.*, 2015; Vandamme *et al.*, 2014). Consequently, the biomass contamination caused by flocculation is not necessarily a disadvantage. For example, the work of Ben-Amotz & Mori (2014) demonstrates an enhanced pigment yield after pH increase of the carotenogenic culture sludge of *D. salina*. Thus, the application of high pH flocculation could even be favorable in the β-carotene production process.

Table 4.5: Initial and residual flocculant in the culture medium and flocculant load in the biomass after flocculation of *D. salina* by electrolysis (5 min, 3.4 mA cm^{-2}), the addition of 0.3 mM $Al_2(SO_4)_3$, 1 mM $FeCl_3$ or 20 mM NaOH.

Method	**Flocculant**	**Initial Flocculant** mg L^{-1}	**Residual Flocculant** mg L^{-1} (%[a])	**Flocculant load biomass** mg g_{dw}^{-1}
Electrolysis	Al	11	0.13 (1.18)	56.17
$Al_2(SO_4)_3$	Al	16.19	0.1 (0.62)	62.19
$FeCl_3$	Fe	55.85	0.05 (0.27)	205.84
NaOH	Mg	7.3	0.25 (3.42)	26.96
	P	27	27 (100)	–
	Ca	0.72	0.65 (90.27)	0.27

[a] percentage of the initial applied flocculant in the separated culture medium after flocculation

4.4.8 Influence of the harvesting method on the extraction efficiency

As the last section clearly demonstrates, flocculant molecules physically interact with the algal particles and remain in the concentrated biomass after dewatering. Thus, an impact on the product yield or quality after extraction of *D. salina* is conceivable. To identify possible differences of the extraction efficiency η_E caused by the harvesting step, β-carotene concentrations were determined as described in 4.3.6. Samples harvested by centrifugation were used as reference. As visible in Table 4.6 extraction efficiencies η_E were comparable for samples harvested via centrifugation and those flocculated by the addition of metal ions via electrolysis, alum or ferric chloride. Consequently, metal ions in the biomass do not hamper the extraction yields. These findings are in line with the observations of Anthony *et al.* (2013) comparing transesterification yields for lipids from algae harvested via centrifugation or alum-induced flocculation. In addition, Rwehumbiza *et al.* (2012) found that the aluminum content of extracted lipids from *Nannochloropsis salina* was 2–3-fold lower after alum-induced flocculation than that of the harvested biomass. Accordingly, aluminum does not tend to significantly dissolve in the extraction solvent which is desirable to achieve an adequate product quality.

Table 4.6: Extraction efficiencies η_E in dependence on the used harvesting method.

Method	η_E %
Centrifugation	$100^a \pm 5.72$
Electrolysis	97.25 ± 2.01
$Al_2(SO_4)_3$	97.45 ± 0.23
$FeCl_3$	97.49 ± 0.86
NaOH	85.52 ± 1.48

[a] η_E reached after single centrifugation was set to 100%

In the present study, the extraction of *D. salina* samples harvested by NaOH flocculation was only 85.5 % efficient compared to the control samples. These results are contradicting to the already mentioned observations of Ben-Amotz & Mori (2014), who reported enhanced pigment extraction yields after pH increase of the biomass to 9.5 or higher. The NaOH addition to *D. salina* suspension comes along with an pH increase up to 12. This value is far from the pH optimum of *D. salina* which is located at pH 7.5 (Chidambara Murthy, 2005). Accordingly, the algal cells are exposed to additional abiotic stress during flocculation. This implies a possibly reduced stability of the cells during subsequent centrifugation leading to facilitated cell breakage and loss of β-carotene prior to extraction. An indication of this theory is given by the reduced cell vitality and the disturbed photo-chemical activity of *D. salina* cells after NaOH flocculation (see Supplementary material Table A.1).

4.4.9 Energy and operating costs analysis of the competing harvesting methods

For the evaluation of the diverse flocculation techniques the experimental data for η_H, CF, η_E, c_F and the recyclability analysis were incorporated in the process model introduced in Sections 3.2 and 4.3.7. The cumulative energy demand and net operating costs (without considering manpower and tax) of all applied harvesting scenarios of the *D. salina* process are depicted in Figure 4.13. Single centrifugation without preconcentration was used as reference method, since it is currently industrially applied for the dewatering of *D. salina* biomass (Ben-Amotz, 2008; Sun *et al.*, 2011). The energy demand needed for cultivation is almost the same in all cases (referred to as growth in Figure 4.13 a). Also the energy demands of biomass flocculation reveal no significant differences in all applied methods. However, as expected beforehand, centrifugation is the most energy intensive dewatering method. The observation is in great accordance with the common literature opinion (Davis *et al.*, 2011; Molina Grima *et al.*, 2003; Pittman *et al.*, 2011). Due to the fact that flocculation provoked a preconcentration of the biomass, higher biomass concentrations were achieved in the second harvesting step compared to sole centrifugation. With that energy was saved in the subsequent biomass drying step. These results are in line with the model calculations reported by Weschler *et al.* (2014) for the downstream processing of microalgal biomass. Nevertheless, the

energy demand of the process is only one factor contributing to the overall process costs. Therefore, it is necessary to take into account other factors that influence the operating costs, such as the demand of raw materials, flocculants, CO_2 or water treatment. Figure 4.13b illustrates the significant effect of the missing medium recycling after NaOH addition on the overall costs for biomass generation. The higher cultivation expense increases the overall costs from 138 to 246 USD kg^{-1} β-carotene and thereby lead to the highest process costs per kg product. In all other cases, the recycling of culture medium caused a reduced demand of nutrients and sea water preparation.

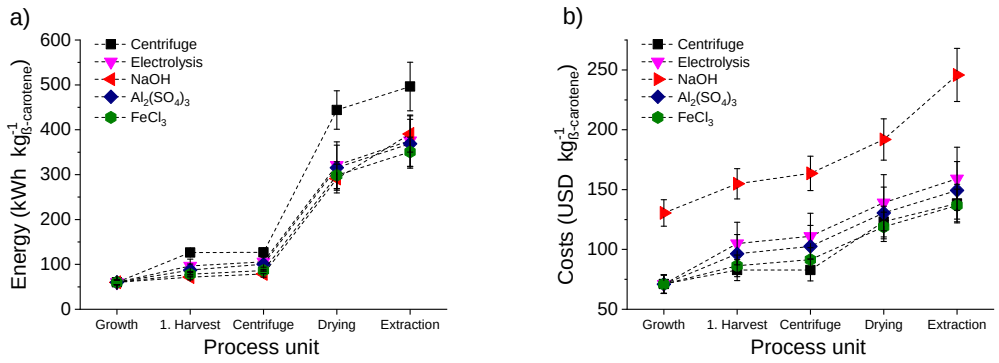

Figure 4.13: Cumulative a) energy demand and b) net operating costs for the production of β-carotene by *D. salina* harvested by different methods, namely centrifugation, electrolysis, the addition of NaOH, $Al_2(SO4)_3$ or $FeCl_3$. Error bars account for one standard deviation from the estimated average value based on Monte Carlo simulation.

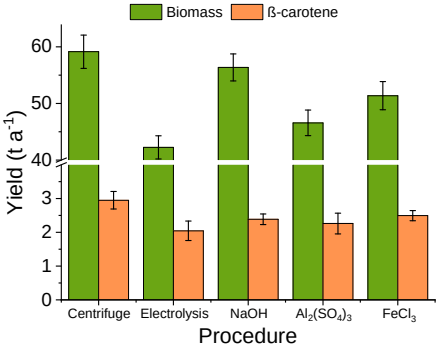

Figure 4.14: Annual yields of biomass and β-carotene by *D. salina* in dependence on the applied harvesting method (centrifugation, electrolysis, addition NaOH or $Al_2(SO4)_3$ or $FeCl_3$). Error bars account for one standard deviation from the estimated average value based on Monte Carlo simulation.

One advantage of centrifugation is that it works without additional chemicals such

as flocculants. This is expressed in the slightly lower operating costs for centrifugation compared to that of the flocculation techniques. Among these methods, the addition of aluminum ions by electrolysis or aluminum sulfate caused higher costs than that of single centrifugation or the addition of ferric chloride. However, the cumulative costs of the competing harvesting methods, except NaOH flocculation, are almost the same. To fairly assess these methods additional information needs to be considered. Therefore, the annual yields of biomass and β-carotene were calculated based on the underlying process model (see Figure 4.14). In terms of product yield, centrifugation is the most appropriate method in our study. Here, 59 t a^{-1} biomass and nearly 3 t a^{-1} pigment can be obtained. At the first sight, flocculation of *D. salina* by pH increase seems a promising method as well, since the output of biomass is 56 t a^{-1}. Nevertheless, the extraction efficiency η_e was visibly reduced after NaOH treatment of the algal suspension (see Table 4.6) which consequently decreases the β-carotene yield. The preconcentration of *D. salina* by the addition of aluminum or iron ions led to lower product yields compared to that reached after centrifugation or pH increase. Among these metal cations, the addition of ferric chloride turned out as the most promising one by achieving a production of 2.5 t a^{-1} β-carotene and 51 t a^{-1} biomass.

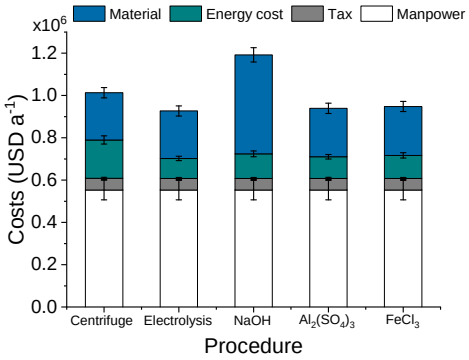

Figure 4.15: Annual operating costs for the production of β-carotene by *D. salina* harvested via single centrifugation, electrolysis, NaOH, $Al_2(SO4)_3$ or $FeCl_3$ addition. Costs are composed of operating costs for energy, raw materials, manpower and tax. Error bars account for one standard deviation from the estimated average value based on Monte Carlo simulation.

The total annual process costs divided in cost of energy, materials, tax and manpower are shown in Figure 4.15 and Table 4.7. The highest annual energy costs were calculated for the process scenario using sole centrifugation without flocculation (see Figure 4.15). Here, 181,603 $\pm$ 19,330 USD a^{-1} were estimated using the developed process model. These result is almost the amount of 180,000 USD a^{-1} reported from the real industrial *D. salina* production site in Israel (Sun *et al.*, 2011). Accordingly, the here proposed process and cost models seem to deliver reliable energy consumption estimates for the considered microalgae production process. The highest overall pro-

cess costs were calculated using NaOH flocculation for preconcentration of *D. salina* biomass. In this case, the costs arose by the raw materials for water treatment and nutrient supply are obviously of a considerable degree. All process scenarios with flocculation by metal ions result in similar values regarding the overall annual operating costs.

With regard to the theoretical annual process cost per kg product (see Table 4.7), it become obvious that the centrifugation based process caused lowest costs for both; β-carotene and biomass generation. Here, the biomass production costs were calculated to be 17.13 ± 1.59 USD kg_{dw}^{-1} biomass which is similar to value of 17 USD kg_{dw}^{-1} biomass, published for the industrial *D. salina* production in Israel (Ben-Amotz, 2008). If $FeCl_3$ was used as flocculation agent, the second-best result was reached regarding product costs. Compared to the net cost calculation depicted in Figure 4.13, a slightly discrepancy is visible since the production of β-carotene was calculated to be less expensive after biomass preconcentration by $FeCl_3$ than that harvested by sole centrifugation. In this case, the fixed production costs are compensated by the higher product yields reached in the process scenario based on single centrifugation.

Table 4.7: Estimated operating costs referred to one kg product in dependence on the individual harvesting method of choice, namely sole centrifugation, electrolysis, NaOH, $Al_2(SO4)_3$ or $FeCl_3$ flocculation. Cost for manpower and tax are considered in the calculation. Errors account for one standard deviation from the estimated average value based on Monte Carlo simulation.

Method	**Cost of biomass** USD kg_{dw}^{-1}	**Cost of β-carotene** USD kg_{dw}^{-1}
Centrifuge	17.13 ± 1.59	343.54 ± 31.93
Electrolysis	21.95 ± 2.01	453.25 ± 41.45
NaOH	21.15 ± 1.74	499.59 ± 41.08
$Al_2(SO4)_3$	20.17 ± 1.84	415.66 ± 37.92
$FeCl_3$	18.45 ± 1.69	380.08 ± 34.89

Taking together all findings of the here discussed process analysis, it was clearly demonstrated that centrifugation is the most cost effective harvesting method for *D. salina* among all investigated techniques in the present work. The use of flocculants enabled a higher preconcentration of the biomass and thereby significantly decreased the energy cost for drying. Nevertheless, centrifugation saved material cost since it can be conducted without the addition of flocculants. Furthermore, this method reached a high dewatering efficiency of 95% for *D. salina* biomass which was not achieved in all investigated flocculation strategies.

4.5 Conclusion

In the present chapter, flocculation was investigated as possible preconcentration approach in the downstream route of *D. salina* production. By the physico-chemical characterization, the low surface potential and the weak hydrophobic character of the microalga were identified. These properties reveal optimal preconditions to reach high flocculation efficiencies. Therefore, different types of chemical and physical flocculation were applied in an experimental study, namely the flocculation via metal salts, pH increase and electrolysis. Optimal flocculant concentration were determined based on the harvesting efficiency η_H and the dewatering factor CF. Further experimental efforts were done, devoted to the reusability of separated culture medium, the extractability of β-carotene and the biomass contamination in dependence on the applied harvesting scenario. The results of the NaOH flocculation reveal the importance of such interlinkage studies. In this example it was not sufficient to consider exclusively the experimentally determined factors η_H and CF to evaluate a harvesting method. At first glance, the flocculation strategy seems very favorable since both performances factors are high and the flocculant is not harmful compared to metal salts. However, the harvesting procedure directly affects interlinked process steps, namely the medium recycling and the extraction efficiency. This effect becomes even more evident after applying the experimental data in a process analysis to calculate process energy and operating costs for the individual harvesting methods. It turned out that centrifugation, which is the actual industrially applied technology in the underlying process, is the most cost efficient one for *D. salina* compared to the other investigated approaches. NaOH flocculation causes the highest production cost due to the lack of medium recycle and the reduced extraction efficiency caused by the flocculant.
Nevertheless, microalgae harvesting is intensively investigated in research and new innovative methods are arising, e.g. the use of hollow fiber filtration (Mixson *et al.*, 2014) or magnetophoretic harvesting (Seo *et al.*, 2015). The presently developed evaluation concept can be easily applied for the evaluation of such upcoming harvesting methods.

5

Extraction strategies of β-carotene from *D. salina* biomass

In the present chapter the extraction of β-carotene from *D. salina* biomass is investigated. For this purpose, supercritical carbon dioxide extraction is compared with conventional organic solvent extraction. To fairly evaluate the potential of both techniques, the first envisaged target of the study is to optimize conventional solvent extraction for the used biomass. Secondly, the potential of supercritical fluid extraction is assessed comparative to the conventional way by means of experimental work as well as the calculation of the energy footprint and the economics of the innovative technique in the β-carotene production process.

5.1 Motivation

Products derived from natural resources are used for a diverse variety of applications and extend the market of the chemical and pharmaceutical industry. However, every product asks for an individual downstream processing concept to ensure product quality and quantity. In particular, the extraction of natural products is challenging since they are composed of various components with different physical and chemical properties.

The solvent of choice is selected by different specification criteria. On the one hand, the solvent type is determined by the product solubility in the solvent. Furthermore, every industrial process prefers the use of an inexpensive solvent to keep extraction cost low. On the other hand also the application of the product possibly is accompanied by some restrictions. For example, products purchased in the food and nutrition sector are permitted to be extracted by CO_2, propane, butane, ethyl acetate, ethanol, acetone and nitrous oxide (Parliament, 2009). For some solvents, particular restrictions need to be considered. The commonly used solvent n-hexane, for instance, which is important for the extraction of lipids and pigments, needs to be removed from the final product with a maximal solvent residue of 1 mg kg^{-1} product (Parliament, 2009).

β-carotene is a non-polar and lipid-soluble pigment, which is used as a colorant, anti-oxidant and immunostimulator in the nutrition, cosmetic and pharmaceutical industry (Dias Ribeiro *et al.*, 2011; Kyriakopoulou *et al.*, 2015). The precursor of vitamin A belongs to the chemical class of isoprenoids (terpenoids) and can be found in microorganisms (fungi or algae) or higher plants (Del Campo *et al.*, 2007; Talisic *et al.*, 2012). The extraction of lipophilic compounds such as β-carotene from renewable raw materials is normally conducted by organic solvents (Molina Grima *et al.*, 2003). However, the risk of product contamination or loss of quality due to organic solvent residuals in the extracts leads to a rising need of innovative extraction methods. Moreover, the demand for green processes increases constantly. Therefore, it is important to investigate sustainable extraction methods and identify effective alternatives of the conventional ones. One potential approach in this direction is the supercritical fluid extraction (SCFE) which makes use of the improved solvent power of fluids or gases which are heated and pressurized above their critical points p_c and T_c. This methodology has the advantage of a complete solvent recovery from the extracts without the need of harsh evaporation steps.

SCFE is presently not applied for the extraction of β-carotene from *D. salina* in industrial application (Mäki-Arvela *et al.*, 2014). Accordingly, little information is available on the ideal operating parameter set-up or the efficiency of the SFCE extraction. To evaluate the potential of supercritical fluids as alternative to conventional solvent extraction of *D. salina* biomass, a detailed analysis was performed in this work.

5.2 Theoretical background

5.2.1 Principles of solid-liquid extractions

In general, extraction is the mass transfer of at least one chemical component from one phase into another. Extraction processes of natural products are mainly solid-liquid extraction aiming for high product yields and purity as well as high selectivity (Palma *et al.*, 2013). Figure 5.1 demonstrates the simplified solid-liquid extraction by the example of β-carotene extraction from a *D. salina* cell. The liquid solvent enters the biological matter represented by the algal cell via molecular diffusion and solubilizes the solute e.g. the carotenoid globuli. The solute can be present as an adsorbed or dissolved component in the organic matter. Thus, the solvation into the solvent can be accompanied by the cleavage of chemical bounds or the desorption of the solute from a surface (Rizvi, 2010). Afterwards, the dissolved solute diffuses into the external solvent solution and can be separated by further downstream processes.

Since the process is based on molecular diffusion, extraction can be described by Fick's law

$$\frac{\dot{M}_i}{A_T} = -D_{is}\frac{\mathrm{d}C_i}{\mathrm{d}z} \tag{5.1}$$

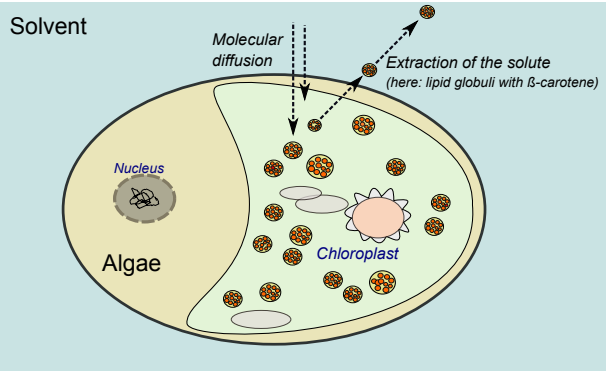

Figure 5.1: Simplified illustration of solid-liquid extraction by the example of β-carotene extraction from *D. salina*.

where $\dot{M}_i$ is the rate of mass transfer of the solute i in mol s^{-1}, A_T is the surface area of mass transfer (solid-fluid interface) in m^2, D_{is} is the diffusion coefficient of the solute i into the solid phase s in m^2 s^{-1}, C_i is the solute concentration in mol m^{-3} and z is the extraction distance in m (Palma *et al.*, 2013).

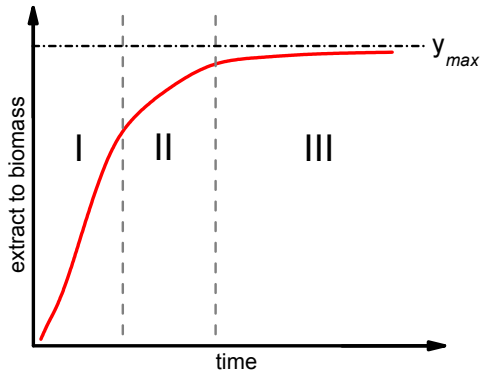

Figure 5.2: Schematic diagram of solid-liquid extraction. In phase I the solute is extracted by a constant rate (CER) from the solvent-solute-interface. Afterwards, the induced solvent molecule diffusion into the solute decreases the extraction rate (phase II). Phase III is characterized by high mass transfer resistance of the solvent molecules into deeper layers of the solute matrix hampering that the maximum extraction yield y_{max} is reached.

Theoretically, nearly all solid-liquid extractions reveal a kinetics similar to the diagram shown in Figure 5.2. In the first phase, also considered as wash-out phase, the extraction occurs linearly at the interface of the solute and the solvent with a constant extraction rate (CER) (Stahl *et al.*, 1987). In the following two phases II+III the mass transfer resistance of diffusion is higher leading to lower extraction rates (Brunner, 1994). After linear extraction, the kinetics is determined by the diffusion of the solvent

into the biomass matrix causing reduced extraction yields over time (see phase II). The deeper the solvent needs to diffuse into the solute matrix, the higher is also the mass transfer limitation to reach the maximum extraction yield y_{max}. With increasing mass transfer limitation or extraction distance z, the extraction starts to stagnate (phase III).

5.2.2 Conventional organic solvent extraction

Organic solvents are widely applied to recover metabolites like pigments and fatty acids from algal biomass (Molina Grima *et al.*, 2003). For this purpose, different techniques are used in industry, namely soaking and Soxhlet extraction. In the soaking process the biomass is maintained for a certain incubation time in a simple extraction vessel filled with the respective solvent (Palma *et al.*, 2013). To enhance the mass transfer of the solute and the solvent, agitation, temperature increase and multi-stage processing can be applied. The Soxhlet procedure is done in a characteristic extraction vessel with a spatial separation of the extraction material and the solvent. This technology, which is based on the distillation of extract and solvent, enables a repeated extraction of the biomass. Compared to soaking, the yield of the extracted solute is increased in line with a reduced solvent consumption. However, to reach high product yields, a biomass pretreatment in form of drying is reasonable to enhance the percolation of the solvent (Williams & Laurens, 2010).

Carotenoids such as astaxanthin, lutein and β-carotene are compounds of lower polarity. Thus, they are soluble in low polar solvents i.e. n-hexane or ethyl ether (Lin *et al.*, 2015; Mezzomo & Ferreira, 2016). To enhance the carotenoid yield and save processing time, innovative technologies based on conventional solvents are applied, namely accelerated fluid extraction, ultrasound-assisted extraction or microwave-assisted extraction (Casas Cardoso *et al.*, 2012; Denery *et al.*, 2004; Kyriakopoulou *et al.*, 2015). Extractions with short incubation times and moderate temperatures are favorable for carotenoids due to their critical properties regarding auto-oxidation and isomerization (Arvayo-Enriquez *et al.*, 2013; Herrero *et al.*, 2006). The solvent selection of carotenoid extraction is mainly done by the criteria of price, toxicity and solubility of the pigments in the respective solvent (Mäki-Arvela *et al.*, 2014).

5.2.3 Sub- and supercritical fluid extraction

Supercritical and near-critical fluids are used for a wide range of application including the extraction of biochemical compounds, drying or cleaning processes and also for analytical purposes (Kiran *et al.*, 2000; Martínez, 2008). Therefore, the physical properties of liquids or gases are influenced by increasing their pressure or temperature near or above their critical points T_c and p_c as highlighted in Figure 5.3. From the physical point of view, a clear differentiation into gas or fluid is not possible. The density of the substance is comparable to liquids whereas the viscosity is similar to that of gases. This physical behavior enhances the heat and mass transfer from the solvent into the solute.

Consequently, the diffusivity of the solvent is higher than that of conventional liquids resulting in an improved solvent power (Martínez, 2008; Meullemiestre *et al.*, 2015). Furthermore, the selectivity and solvency of a supercritical fluid can be influenced by altering the pressure and the temperature within the supercritical area, allowing a more precise extraction of specific products (Brunner, 2005).

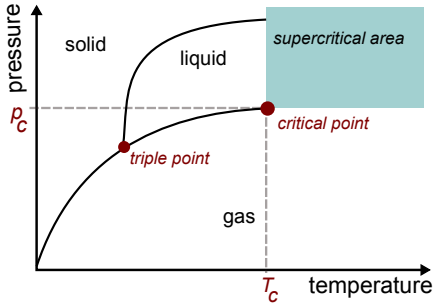

Figure 5.3: p-T diagram of a pure substance.

Most frequently, supercritical carbon dioxide ($scCO_2$) is used as the solvent of choice since the gas is low in cost and toxicity aside with high purity and uncomplicated handling. It is already industrially applied for decaffeination, deoiling, fractionation and refining of vegetable oil as well as the extraction of herbal flavorings and fragrances (Brunner, 2005; Feroiu *et al.*, 2013; Mukhopadhyay, 2009). However, an industrial application for the extraction of β-carotene from algal biomass is still missing. In principle, the solvent character of $scCO_2$ is comparable to that of a non-polar solvent like n-hexane. However, the gas is generally regarded as safe (GRAS) which is import for the use of solvents in the food and pharmaceutical industry (Mukhopadhyay, 2009). Further benefits in using $scCO_2$ are given by the relatively mild process conditions which are needed to reach the supercritical stage (see Table 5.1) as well as the volatile character of the gas at atmospheric pressure, leading to complete solvent removal from the extract. For the extraction of thermolabile natural products such as pigments or flavorings it is favorable, that the critical temperature T_c of $scCO_2$ is low. The addition of polar co-solvents e.g. ethanol or water can increase the extraction yield especially for hydrophilic compounds (Chemat & Abert Vian, 2014). However, one of the main disadvantages of the extraction by $scCO_2$ is its miscibility with water leading to reduced extraction yields. Thus, the extraction of wet biomass is not feasible with this solvent (Seibert, 2012).

Besides CO_2, also other solvents like ethane, ethylene, propane, methane, ammonia and water can be applied as super- or subcritical fluids (Illés *et al.*, 1999; Mäki-Arvela *et al.*, 2014). Typical values for the critical parameter temperature T_c or pressure p_c of selected solvents are listed in Table 5.1.

Table 5.1: Critical values T_c and p_c of selected solvents.

Solvent	$\boldsymbol{T_c}$ K	$\boldsymbol{p_c}$ bar
Carbon dioxide	304.1	73.7
Propane	369.8	42.5
Water	647.1	220.6
Ethane	305.3	48.7
Ethylene	282.2	50.4
Methane	190.6	45.9

One promising gas for subcritical fluid extraction in algal biomass application is propane since it is feasible also for the extraction of wet biomass (Dierkes *et al.*, 2011). The gas is regarded as a green solvent which is seen as a sustainable alternative for conventional organic solvent extraction (Knez Hrnčič *et al.*, 2012). Furthermore, it is completely miscible with vegetable oil leading to improved extraction yields, which is the most important advantage compared to $scCO_2$. Since β-carotene is located within the lipid globuli of *D. salina* (Ben-Amotz & Avron, 1983), it can be extracted in the same way as vegetable oil. Consequently, the extraction efficiency of the pigment might be improved as well, when using propane instead of $scCO_2$. The use of co-solvents like ethanol has proven advantageous regarding solubility and selectivity also for subcritical propane extraction (Baumgardt *et al.*, 2016). However, due to its high flammability, the handling of sub- and supercritical propane reveals a challenging issue. Accordingly, the use of $scCO_2$ is preferable from the safety point of view.

SCFE of pigments from algal biomass is rarely used in industrial processes. However, there are a numerous research studies investigating the possibility to use sub- and supercritical fluids as green alternative to conventional solvent extraction (overview in Macías-Sánchez *et al.* (2007); Yen *et al.* (2015)). Generally, the solubility of most pigments in $scCO_2$ seems to be low whereas other solvents like supercritical ethane and ethylene or subcritical propane possess a high solvent power to extract pigments (Illés *et al.*, 1999; Talisic *et al.*, 2012)).

5.3 Materials and methods

5.3.1 Determination of β-carotene concentrations in the extracts

In the present study tetrahydrofuran (THF), acetone, n-hexane, ethanol (96% and 99%), ethyl acetate and chloroform/methanol (2:2.5) were investigated regarding their extractability of β-carotene from *D. salina* biomass. Standard curves of β-carotene absorption were prepared in the respective solvent to determine the pigment concentration in the extracts according to the protocol of Craft & Soares (1992). In short, a stock solution containing 3 mg mL^{-1} of a β-carotene standard (Sigma-Aldrich Chemie

GmbH, Germany) was prepared in THF supplemented with 0.1% (v/v) of the antioxidant butylated hydroxytoluene (BHT). The stock was diluted 1000-fold with the respective organic solvent (referred to as stock solution 2). In the next step, the wavelength of the individual absorbance maximum was determined for each solvent stock solution 2 by analyzing the complete spectrum of β-carotene from 200 to 700 nm (see Table 5.2). The individual wavelength λ_{max} at this absorption maximum was used to spectrophotometrically measure the absorbance of further dilutions of the pigment in the respective solvent. With the data, linear regression models relating absorbance and β-carotene concentration were derived and used to calculate the β-carotene concentrations in the samples.

Table 5.2: Individual wavelength of the absorption maximum of β-carotene in selected solvents.

Solvent	$\boldsymbol{\lambda_{max}}$ nm
THF	456
Acetone	455
Hexane	456
Ethanol (96%, 99%)	455
Ethyl acetate	452
Chloroform/Methanol	456

5.3.2 Extraction of β-carotene by organic solvents

The extraction experiments were conducted in triplicates of sealed 100 mL shaking flasks filled with 25 mL of the respective solvent and 100 mg β-carotene-containing *D. salina* biomass (Denk Ingredients GmbH, Germany, Art. no: 967996). The solvent to biomass ratio was defined according to the experimental determined solubility values of β-carotene (Craft & Soares, 1992). The incubation took place in the dark using a rotary shaking incubator with a shaking frequency of 100 rpm. Incubation times of 30, 60, 90, 120 and 180 min were applied at room temperature to examine its effect on the extraction efficiency. Furthermore, the β-carotene extraction efficiency after 30 min incubation time was analyzed at different incubation temperatures, namely room temperature, 40 and 60 °C. To study the impact of water on the extraction results, a biomass slurry with a water content of 85% was prepared, similar to the content reached in industry after centrifugation (personal communication, Prof. Ami Ben-Amotz, *Dunaliella* plant NBT Ltd., Eilat, Israel). The extraction was carried out at room temperature and 30 min extraction time.

The success of the extraction was examined by absorbance measurements of the samples. Therefore, duplicates of samples were taken from each shaking flask after extraction, transferred into non-transparent, brown tubes and centrifuged at 5000 rpm for

5 min to separate biomass and solvent. The supernatant was analyzed by spectrophotometric measurements at the previously determined wavelengths λ_{max} summarized in Table 5.2. Pigment concentrations were calculated by the linear regression models obtained from the standard curves (see Section 5.3.1).

5.3.3 Extraction of β-carotene by scCO$_2$

The theoretical solubility of β-carotene in scCO$_2$ can be estimated based on the knowledge of the molecular structure of the solute (Dean *et al.*, 1995). Therefore, the solubility parameter δ in cal$^{0.5}$ cm$^{-1.5}$ was determined as relation between the energy of vaporization ΔE_v in cal mol^{-1} and the molar volume ν in cm^3 mol^{-1} by following equation:

$$\delta = \sqrt{\frac{\Delta E_v}{\nu}} \tag{5.2}$$

The parameter was calculated by considering the sum of contributions of functional groups to the vaporization energy and molecular volume of the β-carotene molecule. For this reason, standard sources tables by Fedors (1974) were used to collect the data.

The extraction experiments with supercritical CO$_2$ were carried out in pilot scale in cooperation with the Fraunhofer Center for Chemical-Biotechnological Processes (CBP, Leuna, Germany). Figure 5.4 illustrates the schematic design of the underlying plant. For each run 100 g *D. salina* biomass was placed into a 2 L extractor vessel and mixed with approximately 1300 g stainless steel cylindrical packing material (5x5x0.3 mm, Raschig GmbH, Germany). The extractor was sealed with sintered metal plates on both sides. The plates were covered by cellulose filter paper (2.5 μM, Cat. no.: 1005320, Whatman, UK) to avoid a biomass transport within the solvent stream through the plates into further plant units. CO$_2$ was delivered from a feed tank operated at 62 bar previously filled by an external CO$_2$ pressure cylinder. The feed was further pressurized by a compressor to generate a liquid solvent. The temperature was maintained by a heat exchanger.

The co-solvent ethanol (96%) was added to the CO$_2$ stream by a further feed tank prior to the extractor vessel inlet with a final mass fraction of 10%. Temperature and pressure were adjusted similar to the CO$_2$ stream by a compressor and a heat exchanger. During the experiments, extraction temperatures of 50, 60 and 70 °C were applied. Furthermore, the extraction pressure in the extractor was varied from 300 to 500 bar. After passing the extractor the solvent-extract mixture was transferred into a separation vessel operated at 50 °C and 62 bar. Here, CO$_2$ and the ethanol-extract mixture was realized by expansion and a feedback stream into the CO$_2$ tank. For sampling, an outlet valve was used allowing the complete draining of the separator vessel into preweighted brown glass flasks. A mass flow meter was used to observe the total mass flow during the extraction which was approximately 4-5 kg h^{-1}. The influence of the co-solvent was analyzed by decreasing the ethanol mass fraction in the solvent stream to 4% and 0%.

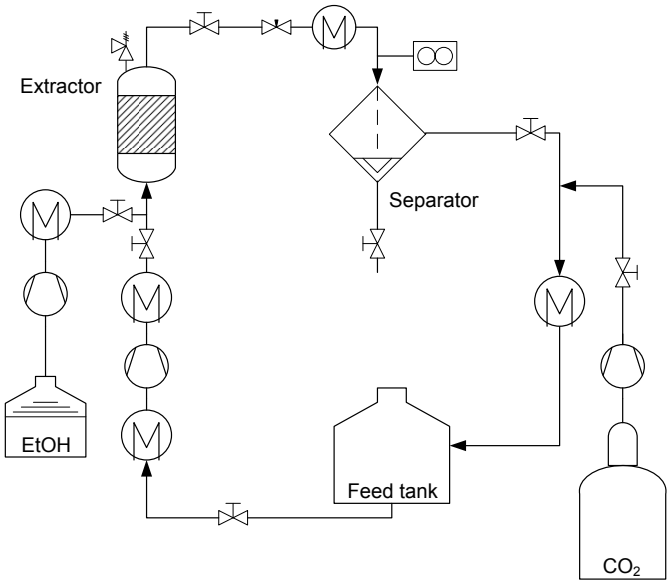

Figure 5.4: Scheme of the pilot scale plant for supercritical CO_2 extraction operated at the Fraunhofer CBP.

In the experiment without co-solvent, 500 mL ethanol was filled in the separator before extraction to facilitate the collection of separated β-carotene.

The samples taken during the experiments were analyzed by spectrophotometric measurements (Spectrophotometer, Type 7310, Jenway, UK) at the specific wavelength determined as described in Section 5.3.1. A standard curve of β-carotene in 96% ethanol was used to calculate the pigment concentration in the samples. To determine the yield of β-carotene, an additional analysis was done by comparing the β-carotene content of the used *D. salina* biomass before and after supercritical CO_2 extraction (see Section 5.3.4).

5.3.4 Determination of $scCO_2$ extraction efficiency and β-carotene solubility

The extraction of β-carotene in acetone based on the protocol of Lichtenthaler (2001) was used as a control method to determine the efficiency of the extraction experiments with supercritical fluids. For this purpose, biomass samples were taken prior to and after every $scCO_2$ extraction experiment and stored until processing in non-transparent, brown tubes at -20 °C. To evaporate residual traces of the co-solvent ethanol, all samples were dried in the dark at 40 °C for 1 h. Afterwards, the samples were weighted into aluminum foil covered 15 mL tubes (n=3-4) in portions of 0.5-1.2 mg. 5-12 mL acetone was added respectively, in dependence of the weight of the used biomass. Samples were mixed and incubated in the dark at 20 °C for 1 h. After extraction the tubes were centrifuged to separate the biomass from the solvent and solvent samples were measured

at 455 nm. The β-carotene concentration of the individual samples was quantified using a standard curve (see Section 5.3.1). The extraction efficiency was determined based on the following equation:

$$\eta_E = \frac{c_{t_0} - c_{t_{end}}}{c_{t_0}}, \tag{5.3}$$

where η_E is the extraction efficiency, c_{t_0} and $c_{t_{end}}$ are the measured β-carotene concentrations in the biomass before and after extraction in mg g_{dw}^{-1}. An analog procedure was applied for hexane-extracted biomass to determine the extraction efficiency of conventional hexane extraction.
The solubility S_e of β-carotene in $scCO_2$ in mg $g_{CO_2}^{-1}$ was calculated according to the method of Danielski *et al.* (2007) as the slope of the linear phase CRE of the extraction curves (see Figure 5.2).

5.3.5 Energy and operating cost analysis of $scCO_2$ extraction

To quantify the additional energy demand and operating costs for the $scCO_2$ extraction, the process model described in Section 3.2 was modified as illustrated in Figure 5.5.

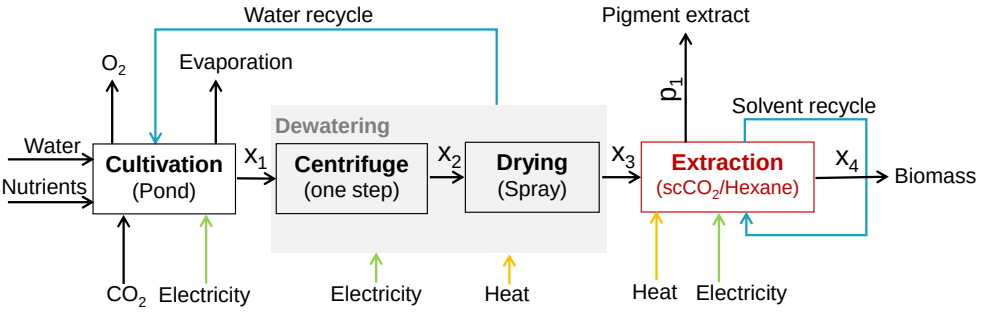

Figure 5.5: Process route of industrial β-carotene production by *D. salina*. The process is divided into three groups of process subunits; namely the biomass and product generation, the dewatering including a centrifugation and a drying step as well as the $scCO_2$ or n-hexane extraction of the product.

The energy consumption of extraction comprises the energy required for solvent pumping as well as for compression, heating and refrigeration. Extraction conditions of 500 bar and 70 °C were chosen according to the most promising experimental results. Compression work of CO_2 and EtOH was calculated based on the methods described by Attard *et al.* (2015). Therefore, the specific enthalpies h_i of 320.97 kJ $kg_{CO_2}^{-1}$ and 854.79 kJ kg_{EtOH}^{-1} were used to calculate the electrical power P_{E_i} in kJ h^{-1} (NIST, 2016; VDI, 2013):

$$P_{E_i} = \frac{h_i \cdot m_{s_i}}{t_E} \tag{5.4}$$

The extraction with $scCO_2$ and 10% EtOH was assumed to be operated in a continuous mode using an isolated reactor with a working volume of 400 L and a bed density of

0.5 kg_{dw} L^{-1}. The assumption was derived from the $scCO_2$ extraction of ginger powder by Rosa & Meireles (2005). The mass flows of the solvents were 2.12 kg_{CO_2} L^{-1} h^{-1} and 0.24 kg_{EtOH} L^{-1} h^{-1} as well as the time of extraction t_E was 3 h, adapted from the experimental set-up, respectively. Accordingly, the mass of the solvents m_{s_i} was calculated to be 2550 kg_{CO_2} and 288 kg_{EtOH}. The reactor was simulated to be heated by a conventional heat exchanger with an efficiency η_{ex} of 80% (Delrue *et al.*, 2013). The energy required for heating was estimated by:

$$Q_{h_i} = \frac{c_{p_i} \cdot \Delta T \cdot m_i}{\eta_{ex}} \tag{5.5}$$

where Q_{h_i} is the required heat energy in kJ, c_{p_i} is the heat capacity of the component i in kJ kg^{-1} K^{-1}, ΔT is the temperature change in K and m_i is the mass of species i in kg. For the algal biomass a heat capacity of 1.25 kJ kg^{-1} K^{-1} was assumed (Orosz & Forney, 2008). The heat capacities of EtOH and CO_2 were set as 2.50 and 0.83 kJ kg^{-1} K, respectively (VDI, 2013). After extraction, the mixture consisting of CO_2, EtOH and β-carotene was separated in a separation vessel at 62 bar and 50 °C. Therefore, a refrigeration of the solvent stream was provided by a cooling unit operated with cooling water. The cooling energy Q_{c_i} was quantified under consideration of a coefficient of performance COP of 1.875 using Equation 5.6 (Attard *et al.*, 2015). At the given temperature the heat capacities of EtOH and CO_2 were 3.10 and 0.87 kJ kg^{-1} K, respectively (VDI, 2013).

$$Q_{c_i} = c_{p_i} \cdot \Delta T \cdot m_i \cdot COP \tag{5.6}$$

The evaporation process was simulated with an efficiency η_v of 70% to compensate heat transfer limitation and boiling point elevation due to impurities in the EtOH extract solution. To calculate the heat of evaporation $Q_{v_{EtOH}}$ for the co-solvent EtOH, an evaporation enthalpy $h_{v_{EtOH}}$ of 841 kJ kg^{-1} (boiling point T_b=78.37 °C) was assumed (NIST, 2016).

$$Q_{v_{EtOH}} = \frac{h_{v_{EtOH}} \cdot m_{EtOH}}{\eta_v} \tag{5.7}$$

To consider solvent losses during recycling, a solvent recovery efficiency of 99% was applied.

The determination of the energy consumption of the conventional hexane extraction method was done based on the parameters and assumptions already explained in Section 3.2. However, the efficiency of extraction η_E was adjusted to the value 86.4%, based on the performance of hexane illustrated in Section 5.3.4. In the analysis the residual β-carotene content of hexane-extracted *D. salina* biomass was quantified. Thus, a more reliable comparison of $scCO_2$ and hexane extraction was possible. Furthermore, the initial amounts CO_2, EtOH and hexane were considered in the operation costs calculation by splitting them into their daily portion on the 330 production days of the year.

5.4 Results and discussion

5.4.1 Organic solvent extraction of β-carotene from *D. salina*

The extraction of β-carotene and other carotenoids requires mild conditions regarding temperature, light exposure and time to reduce the negative side effects of autoxidation and isomerization (Arvayo-Enriquez *et al.*, 2013; Herrero *et al.*, 2006). Currently, the pigment is industrially extracted by conventional solvents such as n-hexane or hot vegetable oil (Potts, 1987; Ruane, 1974). Therefore, the present study aims for the investigation of different process parameters influencing the extraction results of β-carotene from *D. salina* biomass in order to identify an optimal organic solvent extraction set-up which is usable as reference to reliably compare to supercritical fluid extraction.

5.4.1.1 Selection of appropriate organic solvents

A selection of organic solvents to extract the hydrophilic β-carotene from *D. salina* was done according to the relative and the experimental determined solubilities of β-carotene in the respective substance. For this reason, a theoretical prediction by the quantum chemistry based equilibrium thermodynamics method COSMO-RS (Klamt, 1995), implemented in the commercial software package COSMOtherm (conducted by Dr. Kevin McBride) and experimental data according to Craft & Soares (1992) were used for assistance. Figure 5.6 depicts a comparison of both data sets. In most of the cases the theoretical solubility predictions are in accordance with the experimental determined ones. Tetrahydrofuran (THF) was identified as the solvent with the highest solvent power for pure β-carotene. Since the pigment was unstable in benzene, cyclohexane, dichloromethane and ethyl ether (Craft & Soares, 1992); these substances were not used in the extraction experiments with *D. salina* biomass. Due to the low solubility of β-carotene in acetonitrile, the solvent was not further considered. A mixture of chloroform and methanol is frequently used in literature to extract carotenoids (e.g. Lamers *et al.* (2010); Mezzomo & Ferreira (2016)). Therefore, a chloroform/methanol mixture of 2:2.5 was applied for extraction instead of using the single solvents. Ethanol was applied in form of a 99% and 96% solution since the presence of low amounts of water in ethanol has proven to be beneficial for the extraction results (Seibert, 2012).

In addition, the COSMO-RS method identified isobutyraldehyde as a promising and innovative green solvent for β-carotene. After preparing the stock solutions described in Section 5.3.1, the absorbance of β-carotene declined within minutes (data not shown), indicating a low stability of the pigment in this solvent. Accordingly, the solvent was not used in the further investigations. In general, the results of the solubility analysis are not expected to be completely identical to the real extraction results of the pigment. There are further impact factors, e.g. the efficiency of molecular diffusion of the solvent into the biomass or the solubility of the solvents for other biomass components, which might cause differences of the expected and the real solvent properties. Nevertheless,

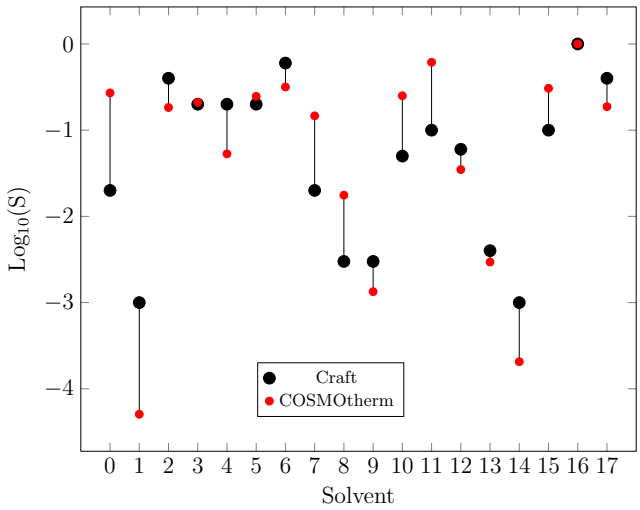

Figure 5.6: Relative solubility of β-carotene in selected organic solvents based on theoretical predication by the COSMO-RS method (kindly provided by Dr. Kevin McBride) or experimental data according to Craft & Soares (1992). 0: acetone, 1: acetonitrile, 2: benzene, 3: chloroform, 4: cyclohexane, 5: cyclohexanone, 6: dichloromethane, 7: dimethylformamide (DMF), 8: dimethyl sulfoxide (DMSO), 9: ethanol (EtOH), 10: ethyl acetate, 11: ethyl ether, 12: hexane, 13: 2-propanol, 14: methanol (MeOH), 15: methyl tert-butyl ether (MTBE), 16: tetrahydrofuran (THF), 17: toluene.

the solubility analysis allows a preliminary indication of the theoretical potential of the solvents to extract β-carotene.
In the following subsections, conventional solvent extraction experiments were conducted using a solvent selection of THF, acetone, n-hexane, ethanol (96% and 99%), ethyl acetate and chloroform/MeOH (2:2.5).

5.4.1.2 Influence of extraction temperature and time on β-carotene yield

The stability of pigments is sensitively influenced by temperature, light and the selected solvent (Tang & Chen, 2000). Therefore, it is important to choose an environment with adequate conditions. To address this challenge, detailed investigations were done to identify the optimal time and temperature for lab scale β-carotene extraction. Figure 5.7 illustrates the effects of time on extracted β-carotene reached at room temperature. It is clearly seen, that the best solvents under these conditions are acetone, THF, ethyl acetate or the chloroform/MeOH mixture. Ethanol and hexane demonstrate insufficient β-carotene extraction yields which are roughly half as much as the results of the other solvents. These results are contradicting to the study of Taungbodhitham *et al.* (1998), showing optimal carotenoid extraction results from different matrices for both solvents. Except for ethyl acetate, there is no clear effect visible which is caused by the variation of the extraction time. The same conclusion was drawn for β-carotene extraction from tomato or carrot powder using different organic solvents by Ishida & Chapman (2009)

as well as for lutein extraction of marigold biomass by Surendranath *et al.* (2016). In the present work, the typical kinetics of extraction as described in Figure 5.2 is not visible in the results, leading to the assumption that the linear phase of extraction was already reached within the first 30 min. For ethyl acetate the pigment yield even decreased over extraction time which might indicate instability of the pigment in the solvent. As a consequence of these observations, the shortest investigated extraction time of 30 min was applied as fixed parameter in the following extraction experiments.

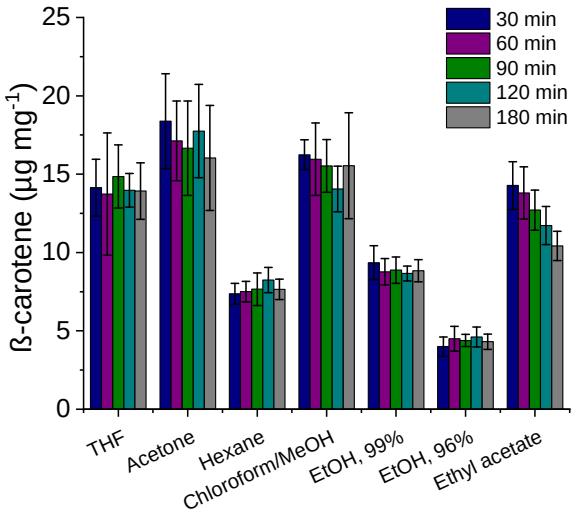

Figure 5.7: Influence of the time of organic solvent extraction on the extracted β-carotene yield from *D. salina* biomass. Experiments were conducted in duplicates at room temperature. Error bars represent the deviation of the measurements from the average value.

Apart from the time, also the temperature affects the extraction yield by altering the properties of the solute and the solvent. On the one hand the solubility and the diffusivity of the solute are influenced; on the other hand physical properties of the liquid solvent like the viscosity are changed (Palma *et al.*, 2013). Figure 5.8 depicts the influence of the extraction temperature on β-carotene yield in the present study. Here, it becomes obvious that the temperature optimum for extraction strongly depends on the applied solvent. For the extractions via THF, acetone, chloroform/MeOH and ethyl acetate a decrease of β-carotene yield can be noted if the temperature was raised. This phenomenon can be attributed to the thermolability of the pigment at higher temperatures which is also influenced by the surrounding solvent (Craft & Soares, 1992). In contrast, the extraction success of EtOH is improved for an increased temperature. The solubility of the pigments seems to be increased in line with the temperature due to the enhanced diffusivity of the solvent. For the extraction of β-carotene by hexane, there is no significant effect of the temperature visible. Since the pigment is generally less stable at higher temperatures (Ishida & Chapman, 2009) and nearly all investigated

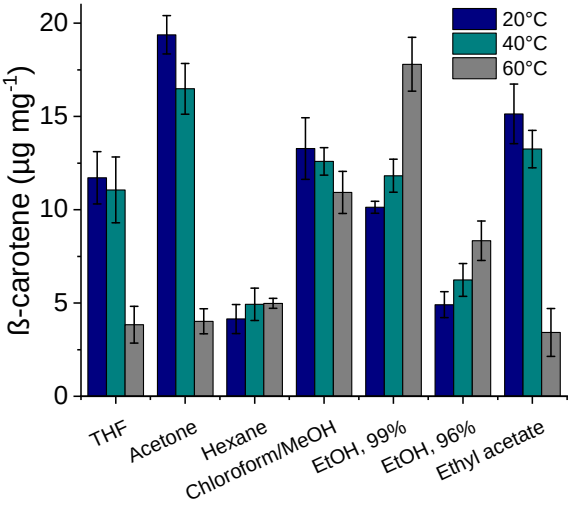

Figure 5.8: Influence of the temperature of organic solvent extraction on the extracted β-carotene yield from *D. salina* biomass. Experiments were conducted in duplicates with an extraction time of 30 min. Error bars represent the deviation of the measurements from the average value.

solvents are little affected by the temperature increase, further experiments were done at room temperature.

5.4.1.3 Influence of the water content on the yield of β-carotene

In algal based production processes the drying step is energy intensive since the biomass concentration after centrifugation is only between 2-22% (Molina Grima *et al.*, 2003). However, the extraction of wet biomass is a challenging issue (Sathish *et al.*, 2015). Currently, the extraction of β-carotene and other carotenoids requires the use of dry biomass to achieve high pigment yields and qualities (Mäki-Arvela *et al.*, 2014). Figure 5.9 illustrates the impact of the water content on the extraction of β-carotene from *D. salina*. After drying the biomass had a concentration of approximately 99% dry weight. The biomass slurry obtained after centrifugation revealed a dry weight content of 15% (personal communication, Prof. Ami Ben-Amotz, *Dunaliella* plant NBT Ltd., Eilat, Israel). For nearly all solvents a clear decrease of the extracted β-carotene concentration is visible in the presence of water. For the extraction via hexane and 96% EtOH no influence of water is identifiable. However, it needs to be emphasized that both solvents lead to the lowest extraction results independently of the water content. β-carotene is a lipophilic molecule. Thus, the presence of high amounts of polar water decreases the solubility of the solute in the solvent and thereby also the extraction efficiency.

Due to the negative effect of water, the drying step before pigment extraction was maintained unchanged in the protocol.

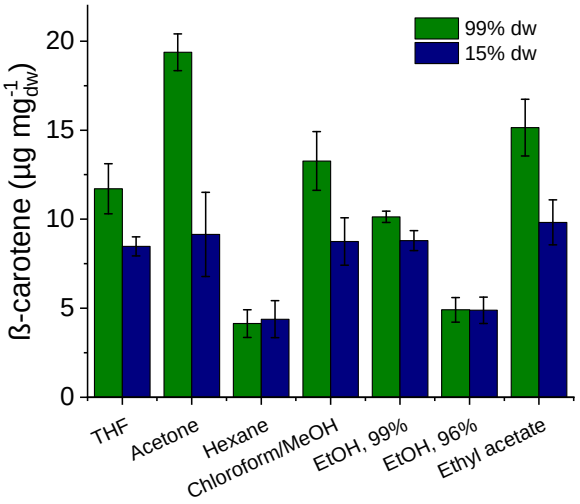

Figure 5.9: Influence of water in the biomass on the extraction results of β-carotene from *D. salina* biomass. Experiments were conducted in duplicates at room temperature and a extraction time of 30 min. Error bars represent the deviation of the measurements from the average value.

5.4.1.4 Definition of an optimal organic solvent extraction set-up

The aim of the previous experiments was to investigate the impact of different parameters on the extraction results and thus to identify an optimal parameter set-up for β-carotene extraction by conventional organic solvents. Surprisingly, the extraction efficiency of the industrially used β-carotene extraction solvent hexane was low in the above discussed experiments. In all experimental trials acetone achieved the best extraction yields, even at room temperature and a short extraction time of 30 min. The solvent is highly efficient also for the analytical determination of β-carotene (Lichtenthaler, 2001) as explained in Section 5.3.4. In consequence, acetone was used as a reference solvent to reliably compare to supercritical fluid extraction.

5.4.2 $scCO_2$ extraction of β-carotene from *D. salina*

Due to its manifold beneficial characteristics (see Section 5.2.3), $scCO_2$ is one of the most frequently applied supercritical fluids in industry (Brunner, 2005; Feroiu *et al.*, 2013; Mukhopadhyay, 2009). However, so far its industrial implementation for β-carotene extraction is still missing. Therefore, the feasibility to use the solvent for this purpose is intensively discussed in the following sections.

5.4.2.1 Solubility of β-carotene in $scCO_2$

It is known that $scCO_2$ extracts hydrocarbons and lipophilic compounds but that the extraction is hampered by polar functional groups or hydroxyl and carboxyl groups

(Stahl *et al.*, 1987) which are however not present in β-carotene (see Table 5.3).

Table 5.3: Atomic or group contributions to the vaporization energy Δe_{v_i} and the molecular volume ν_{v_i} of β-carotene ($C_{40}H_{56}$) at 25 °C.

Atom or group	**Number**	$\sum \boldsymbol{\Delta e_{v_i}}$ cal mol^{-1}	$\sum \boldsymbol{\nu_i}$ cm^3 mol^{-1}
CH_2	6	7080	96.6
CH_3	10	11250	335
C	2	700	-38.4
=C	8	8240	-44
=CH-	14	14420	189
Ring closure 5 or more atoms	2	500	32
$\sum$		42190	570.2
$\boldsymbol{\delta}$		**8.6**	**cal$^{0.5}$ cm$^{-1.5}$**

To have a first indication whether $scCO_2$ is appropriate to extract the pigment, a theoretical solubility analysis was conducted according to the method of group contributions proposed by Fedors (1974) as explained in Section 5.3.3. Table 5.3 summarizes the contributions of the functional groups in β-carotene to the vaporization energy Δe_{v_i} and the molecular volume ν_i. The solubility parameter δ was calculated using Equation 5.2 and can serve for the qualitative determination of the solubility of compounds in $scCO_2$. Dean *et al.* (1995) defined a classification of the parameter values on the basis of a theoretical and experimental solubility analysis of steroids in $scCO_2$. Accordingly, steroids with a solubility parameter higher than 13.8 cal$^{0.5}$ cm$^{-1.5}$ are considered as insoluble in $scCO_2$. A value in the range of 12-13.8 cal$^{0.5}$ cm$^{-1.5}$ indicates a medium solubility of the compound in the solvent. For molecules with solubility parameter values lower than 12, a good solubility in this supercritical fluid is expected. β-carotene reveals a δ value of 8.6 suggesting a high solubility of the pure substance in $scCO_2$. With that, the theoretical preconditions to use $scCO_2$ as alternative β-carotene extraction solvent seem to be promising. Thus, further experiments were done to find an optimal parameter set-up for β-carotene extraction by $scCO_2$ from *D. salina* biomass.

5.4.2.2 Influence of the co-solvent concentration

CO_2 is non-polar and by nature highly selective for the lipophilic pigment β-carotene (Casas Cardoso *et al.*, 2012). Nevertheless, the use of polar co-solvents has proven to be advantageous for $scCO_2$ extraction (Chemat & Abert Vian, 2014). In principle, there are two main effects causing an improved mass transfer of the solvent within the cells. On the one hand, the use of polar entrainer increases cell permeability (Panesar *et al.*, 2007). On the other hand, the co-solvent can lead to cells rupture or swelling (Mäki-Arvela *et al.*, 2014).

To analyze its effect on the β-carotene yield in the present study, different EtOH ratios were added to the CO_2 feed. The experiments presented in Section 5.4.1 iden-

Table 5.4: Effect of the EtOH fraction in $scCO_2$ (300 bar, 50 °C, 180 min) on the extraction efficiency η_E of β-carotene from *D. salina*.

EtOH %	**CO_2** g g_{dw}^{-1}	**η_E** (-)
0	127	0.04 ± 0.02
4	127	0.12 ± 0.02
10	127	0.25 ± 0.02

tified EtOH as not appropriate in conventional solvent extraction of β-carotene from *D. salina*. Nevertheless, the work of Yen *et al.* (2012) pointed out that a solvent with weak performance in conventional solvent extraction can serve as an effective entrainer. Table 5.4 summarizes the results of the present investigation. In all cases, the biomass was extracted for 180 min at 50 °C and 300 bar, respectively. In the experimental run without EtOH only 4.3% of the entire β-carotene was extracted. By adding 4 wt% EtOH to the CO_2 stream, a 3-fold improvement of the extraction yield was achieved. Further increase of the EtOH fraction to 10% led to an additional enhancement of the extraction efficiency to 25%. Comparable co-solvent-caused effects were reported for the extraction of different carotenoids from *Nannochloropsis gaditana*, *Synechococcus sp.*, *Scenedesmus sp.* and *Haematococcus pluvialis*, respectively (Casas Cardoso *et al.*, 2012; Machmudah *et al.*, 2006; Macías-Sánchez *et al.*, 2009b; Nobre *et al.*, 2006; Yen *et al.*, 2012). However, too high EtOH concentrations in $scCO_2$ lead to a decrease of solvent density and thereby to a decrease of solvent power (Brunner, 1983). This theory was also confirmed for the extraction of carotenoids from different algal biomass matrices (Machmudah *et al.*, 2006; Yen *et al.*, 2012). Furthermore, the use of high amounts of co-solvent would additionally raise purification cost due to solvent evaporation. Consequently, concentrations above 10% EtOH were not considered in the present analysis.

5.4.2.3 Influence of the pressure and temperature

The results of Section 5.4.2.2 indicate that in spite of co-solvent addition, only a partial recovery of β-carotene can be achieved. It is therefore crucial to find an optimal set-up for the most important parameters of supercritical fluid extraction; namely the pressure and the temperature. Both process parameters are directly correlated to the density of the solvent. A pressure increase is accompanied by the increase of the solvent density which improves the solvent power of the supercritical fluid. In contrast, high temperatures cause an increase in diffusivity but lower the solvent density and the solubility of the solute. In some research works, the negative effect of increased temperatures on carotenoid extraction was observed, especially at low operating pressures (Bustamante *et al.*, 2011; Ruen-ngam *et al.*, 2012). This effect was not visible in the results of the present study as depicted in Figure 5.10. Here, the use of higher temperatures led to higher final β-carotene yields. The same impact was observed by Macías-Sánchez *et al.* (2009a,b) for the carotenoid extraction of *D. salina* by $scCO_2$ with or without EtOH as

co-solvent.
However, in the present work an increase from 50 to 60 °C only slightly increased the amount of extracted β-carotene, although the solubility of the pigment in $scCO_2$ is even lower for 60 °C than for 50 °C (see Figure 5.12). This can be explained by the aforementioned combined effects of the enhanced diffusivity, which improves the extraction rate and at the same time the decreased solvent density, which lowers the extraction yields of the pigment. The overlap of these physical impacts was also visible for $scCO_2$ extraction of lutein from *C. vulgaris* for 60 and 70 °C at 300 bar (Kitada *et al.*, 2009). In this study same pigment yields were obtained for both temperatures.

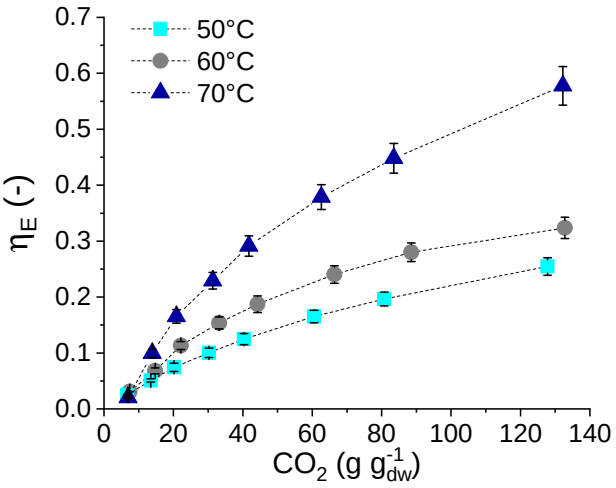

Figure 5.10: Influence of temperature on $scCO_2$ extraction of β-carotene from *D. salina* biomass. Experiments were conducted at a constant pressure of 300 bar using 10% EtOH as co-solvent. The mass flow rate of $scCO_2$ was between 69-74 g min^{-1}. Error bars indicate one standard deviation of the average measurement value (n=6).

At the highest investigated temperature of 80 °C (see Figure 5.10) the positive effect of enhanced diffusivity strongly outweighed the negative influence of decreased density. Comparable results are reported for the temperature increase during lutein extraction from *Scenedesmus* and *C. vulgaris* as well as the astaxanthin extraction from *H. pluvialis* (Kitada *et al.*, 2009; Machmudah *et al.*, 2006; Yen *et al.*, 2012). Although the increase of temperature strongly enhanced the final β-carotene yield of *D. salina* from 25 to 60%, further improvement is expected by the variation of the pressure as additional control parameter.

Figure 5.11 illustrates the effect of pressure variation on β-carotene extraction using a constant temperature of 70 °C. Theoretically, the solubility of the carotenoid increases with increased pressure (Mendes *et al.*, 1995). This observation is also confirmed by the

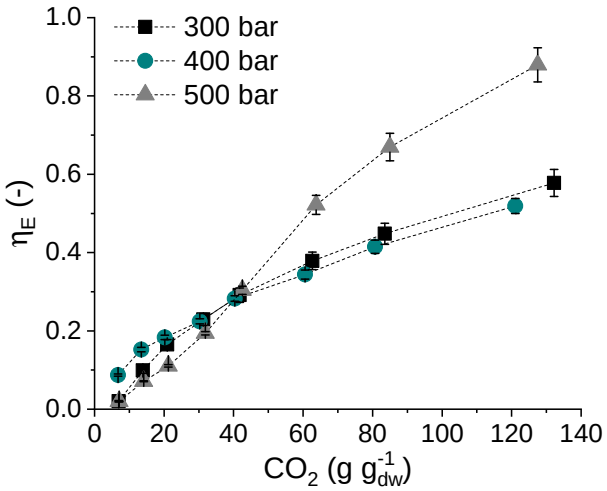

Figure 5.11: Influence of pressure on $scCO_2$ extraction of β-carotene from *D. salina* biomass. Experiments were conducted at a constant temperature of 70 °C using 10% EtOH as co-solvent. The flow rate of $scCO_2$ was between 67-71 g min^{-1}. Error bars indicate one standard deviation of the average measurement value (n=6).

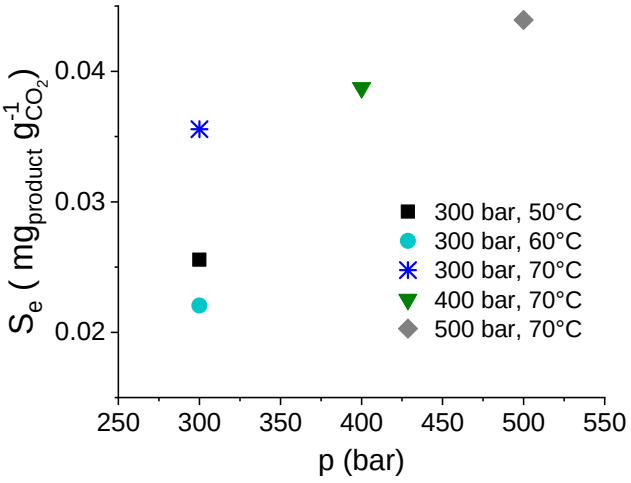

Figure 5.12: Solubility of β-carotene from *D. salina* biomass in $scCO_2$ as a function of the pressure p. The solubility values account for the slope of the linear phase CRE of the extraction curves.

results of the solubility analysis in Figure 5.12. Nevertheless, the reached extraction efficiencies of approximately 60% are comparable for the extractions at 300 and 400 bar (see Figure 5.11). This was provoked by the already mentioned inhibitory effect of high temperature application at low pressure and seems to be relevant especially for the mass transfer controlled phases of extraction kinetics (see Figure 5.2 phases II, III). At this point, most of the pigments are already solved from the solid-liquid interface (Macías-Sánchez *et al.*, 2009b). The solubility values were calculated from the slope of the initial phase of constant extraction. Here, the diffusion limitation plays only a minor role. The mass transfer inhibition can be overcome by further increase of the pressure, where the temperature impact is less pronounced (Brunner, 2005). Thus, the application of 500 bar led to the highest extraction yield as well as solubility value in the present study. With that set-up nearly 90% of the entire pigment were extracted.

All in all, it was demonstrated that the combined effect of high pressure and high temperature (500 bar, 70 °C) resulted in the most effective extraction of β-carotene.

5.4.3 Energy and cost assessment of the extraction strategies

The parameters and results of the experimental extraction studies (e.g. η_E, Q_E, Q_{E2},...) were integrated into the process model of *D. salina* based β-carotene production (see Sections 3.2 and 6.3.5) to compare conventional solvent extraction and $scCO_2$ extraction regarding their costs and energy demand.

In principle, conventional hexane extraction occurs in two main energy consuming steps: 1. the heating of the solvent up to the wished extraction temperature and 2. the recovery of the solvent by evaporation. In contrast, $scCO_2$ extraction additionally requires compression energy to achieve the critical process pressure as well as a cooling step for the separation of $scCO_2$ and the solute. Furthermore, evaporation energy needs to be provided if a co-solvent is used. Thus, a higher energy consumption is expected for the supercritical solvent extraction at the first glace.

Figure 5.13 illustrates the estimated contributions of extraction energy in the case of β-carotene extraction from *D. salina* for a production plant with a production area of 10 ha and 200 kg biomass yield per day (for more details see Section 3.2). Obviously, with 63% the compression of both solvents (scCO2 and EtOH) consumes the highest energy amount in the extraction process. This seems to be characteristic for $scCO_2$ extraction (Shariaty-Niassar *et al.*, 2009). Another considerable energy input is needed for the evaporation of the co-solvent EtOH. According to the results of the extraction energy and cost estimation listed in Table 5.5, conventional hexane extraction has a lower energy demand compared to that of supercritical fluid extraction. With 57.42 kWh kg^{-1} β-carotene, the extraction by $scCO_2$ consumes twice as much energy as the hexane extraction.

However, the solvent-to-biomass ratios are significantly lower for $scCO_2$ extraction. Consequently, the cost of solvents is even lower in this case. Considering all operation

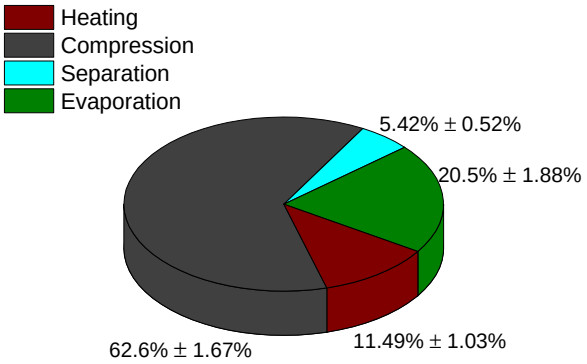

Figure 5.13: Estimated energy contribution of the extraction unit in industrial scale $scCO_2$ extraction of β-carotene from *D. salina* biomass using 10% EtOH as co-solvent. Errors represent one standard deviation from the estimated average values based on Monte Carlo simulation.

Table 5.5: Comparison of characteristic energy and cost data for the extraction of β-carotene from *D. salina* biomass by conventional hexane extraction or $scCO_2$ (+10% EtOH) extraction. Errors account for one standard deviation from the estimated average values based on Monte Carlo simulation.

Property	**Unit**	**$scCO_2$**	**Hexane**
Annual β-carotene	t/a	2.73 ± 0.19	2.68 ± 0.18
Annual production cost	MUSD/a	0.402 ± 0.031	0.409 ± 0.031
Annual selling value	MUSD/a	1.64 ± 0.18	1.61 ± 0.17
Extraction cost	USD/kg[a]	7.70 ± 0.83	10.38 ± 0.99
Extraction energy	kWh/kg[a]	57.42 ± 4.31	28.88 ± 2.79
$\sum$ production cost	USD/kg[a]	147.98 ± 15.27	153.08 ± 15.34
$\sum$ production energy	kWh/kg[a]	562.41 ± 50.76	542.57 ± 48.92

[a] calculated per kg of the product β-carotene

costs for the solvents including first fill and make-up as well as the expended energy, hexane extraction was estimated to be more expensive than $scCO_2$. Here, extraction costs of 10.38 ± 0.99 USD kg^{-1} β-carotene were calculated, whereas the $scCO_2$ extraction only needs 7.7 ± 0.83 USD kg^{-1} β-carotene. Regarding the yield of the pigment, no considerable differences are visible in the simulation results. Both technologies are expected to achieve an annual production of approximately 2.7 t β-carotene. With 1.6 MUSD, also the annual selling price is comparable. Nevertheless, $scCO_2$ extraction has the advantage to save approximately 5 USD kg^{-1} β-carotene which is visible in the cumulative production cost. However, the annual production costs which consider the costs of all production steps differ only slightly for both scenarios. Here, values of 409 ± 31 kUSD a^{-1} and 402 ± 31 kUSD a^{-1} were calculated for the hexane or $scCO_2$ extraction.

Nonetheless, it is important to take into account the environmental aspect of product extraction. In recent years, the demand for more sustainable products and goods has been risen constantly. Green products such as β-carotene should be extracted also with green solvents, especially if they are used in cosmetic, pharmaceutical or food industry. The toxicity of solvent residues in the final product after hexane extraction is always a critical issue and controlled by quality constraints (Parliament, 2009). Due to the green character of $scCO_2$ as well as its co-solvent EtOH, the solvent is more appropriate for environmental-friendly and sustainable pigment extraction than hexane. Furthermore, $scCO_2$ has a volatile character at atmospheric pressure, leading to complete solvent removal from the extract which is important for the quality of the product (Chemat & Abert Vian, 2014).

5.5 Conclusion

Supercritical fluid extraction is an already exploited methodology for a wide range of applications. So far, it is not used for industrial scale β-carotene extraction from algal biomass. The present chapter aims for the comparison of conventional and supercritical fluid extraction by using the example of β-carotene extraction from *D. salina* biomass. To find optimal conditions of conventional solvent extraction, different parameters, namely pigment solubility, time and temperature as well as the influence of water were investigated by theoretical or experimental efforts. The effects of the different parameters are strongly dependent on the individual solvent of choice. Interestingly, hexane the commonly used solvent for β-carotene extraction from algae in industrial scale did not achieved optimal extraction results. In all experiments the performance of acetone led to the best extraction yields, also at low temperatures and short extraction times (room temperature, 30 min). Accordingly, acetone was chosen as reference extraction method to evaluate the extraction efficiency of $scCO_2$ extraction.

To assess the feasibility of supercritical fluids as environmental friendly extraction method for β-carotene, pilot scale experiments were done in cooperation with the Fraun-

hofer IGB Leuna, Germany. Theoretical considerations demonstrated a good solubility of the hydrophilic pigment in $scCO_2$. Therefore, the pilot scale experiments were used to find an optimal parameter set-up to extract β-carotene under consideration of the technical constraints. 10% EtOH was found to be an optimal co-solvent ratio to increase extraction yields. In addition, the extraction conditions of 500 bar and 70 °C led to the most effective extraction of approximately 90% β-carotene.

With the help of energy and operating cost analyses, a final assessment of conventional solvents and supercritical fluid extraction was done. It turned out, that $scCO_2$ extraction consumes nearly 2-times more energy than hexane extraction which is mainly attributed to the high compression work needed to achieve the critical pressure. However, the lower solvent to biomass ratio during $scCO_2$ extraction lowers the extraction costs compared to hexane. With that, the economic viability of $scCO_2$ extraction in industrial microalgal β-carotene extraction was demonstrated for the first time. Furthermore, from today's perspective, the green solvent character of $scCO_2$ and its co-solvent EtOH is more consistent with the rising pursuit of sustainable production processes. Based on the results of the present study, the use of $scCO_2$ in industrial β-carotene extraction is highly recommended.

6

Valorization of *D. salina* remnant biomass by mild hydrothermal treatment

A maximum and effective exploitation of the whole biomass as a multi-product is required to create more sustainable bio-processes. In the case of *D. salina*, up to 90% of biomass remains unused after extraction of the main product β-carotene. This remnant is an attractive source of by-product generation. In the present chapter the potential of mild hydrothermal liquefaction (HTL) as an innovative green methodology to release by-products after β-carotene production is assessed. Therefore, the theoretical background of thermochemical processes is summarized. In addition, possible by-products are discussed by considering the biochemical and the elemental composition of the biomass remnant. Optimal process conditions are found experimentally by applying different HTL reaction times and temperatures. A potential by-product is identified and possible applications are proposed. Finally, an energy consumption and operating costs calculation is done to evaluate the feasibility of hydrothermal by-product generation in the β-carotene process. The chapter incorporates methods and results published in Pirwitz *et al.* (2016).

6.1 Motivation

The cultivation of algal biomass has become an important alternative to generate valuable products as well as second-generation biofuels. Nonetheless, the valorization of the complete biomass is still a crucial challenge in microalgal production processes and not yet feasible (t Lam *et al.*, 2018). In most cases, considerable quantities of up to 90% of the biomass are unused after the extraction of the main product. The residuals can provide additional products or feedstocks to satisfy further industrial needs and increase the process economy and competitiveness of the overall process. But which options are conceivable to realize a beneficial use of the remnant?

After the algal production of biofuels or other hydrophilic compounds (e.g. functional lipids, pigments,...), the remnant biomass consists of carbohydrates, proteins, residual lipids and further organic or inorganic molecules. One possibility is to apply these fractions for aquaculture and animal feed (Mata *et al.*, 2010). Here, proteins and carbohydrates are essential key molecule to promote the animal growth during cultivation. This strategy is supported by the fact that the biomass can be used directly as by-product without the need of further pretreatment. However, a biomass contamination with organic solvent due to main product extraction could hinder this opportunity by inhibitory effects and regulatory restrictions (Parliament, 2009). Furthermore, the economic revenue achieved by this application is considered small.

With respect to the carbohydrate fraction of the residual biomass also microbial fermentation or anaerobic digestion could reveal an alternative pathway of remnant valorization to produce ethanol or biogas (Harun *et al.*, 2010a; Zhu, 2014). To get high conversion yields, an additional pretreatment of the biomass by enzymes, chemicals or physical methods is usually needed to make the carbohydrates accessible (Jeevan Kumar *et al.*, 2017). This is a big drawback especially with respect to the processing cost and time (Kwon *et al.*, 2016).

Another approach to valorize the remnants of microalgae production processes is the use of thermochemical conversion processes. Currently, these methods are investigated for the extraction of bio-crude as well as the generation of biofuels from high-lipid containing algal biomass (e.g. Chen *et al.* (2015); Khoo *et al.* (2013); López Barreiro *et al.* (2013); Orosz & Forney (2008)). Notwithstanding, first studies demonstrate promising results of thermochemically converted microalgal remnant (Kim *et al.*, 2015; Rihko-Struckmann *et al.*, 2017). The conversion can be done in one step which is easily implementable as a unit extension of an existing production plant. Next to bio-crude, also other combustible (e.g. gas or char) or valuable compounds can be derived from thermochemical processes. Consequently, thermochemical conversion is a potential strategy to fully exploit the complete biomass in the *D. salina* process (see Figure 6.4) and worthy of detailed investigations.

6.2 Theoretical background

6.2.1 Types of thermochemical biomass conversion

In principle, thermochemical processes are strongly determined by the water content of the algal biomass. For dry biomass gasification, pyrolysis and torrefaction can be applied, whereas wet biomass can be converted by hydrothermal liquefaction or hydrothermal gasification. Figure 6.1 summarizes the key technologies of thermochemical conversion processes which were already investigated for microalgal biomass. In contrast to conventional lipid extraction for biofuel generation, all methods share the benefit to

use a single-step conversion of the whole biomass.

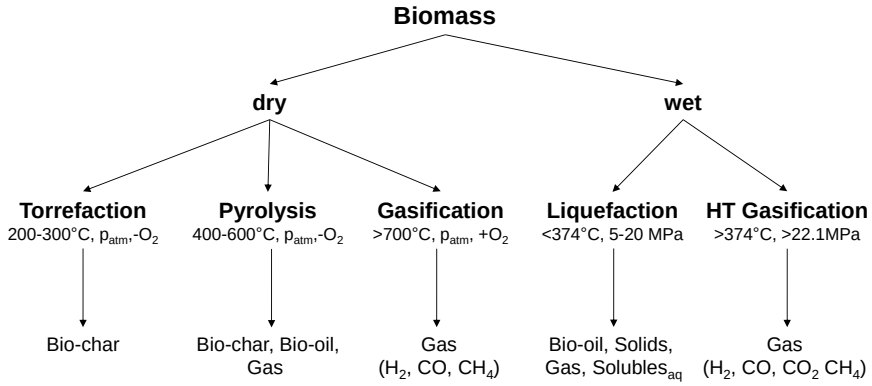

Figure 6.1: Types of thermochemical conversion processes of algal biomass.

Torrefaction is operated at mild temperatures under 300 °C at atmospheric pressure and inert conditions with the aim to increase the low heating value of dry microalgae biomass (Chen *et al.*, 2015). The main product of this process is a combustible solid. Pyrolysis is characterized by the biomass treatment under exclusion of oxygen operated at atmospheric pressure and temperatures between 400-600 °C (López Barreiro *et al.*, 2013). The main products of this kind of dry microalgae biomass conversion are bio-oil, char and gas in different ratios which are strongly influenced by the used strain and operating parameters (Gong *et al.*, 2014; Marcilla *et al.*, 2013). In general, there are four types of pyrolysis: slow, moderate and fast pyrolysis depending on the operating temperature and heating rate, as well as the microwave-assisted pyrolysis (Chen *et al.*, 2015; Hognon *et al.*, 2015). Gasification leads to the partial oxidation of dry carbonaceous microalgal biomass into H_2, CO and CH_4 at temperatures above 700 °C and atmospheric pressure (López Barreiro *et al.*, 2013). The produced gas mixture can be used as fuel itself (Khoo *et al.*, 2013).

Unlike the aforementioned technologies, hydrothermal liquefaction converts wet biomass into bio-crude, gas, aqueous phase and solid residuals (Orosz & Forney, 2008). Therefore, temperatures under the critical point 374 °C and elevated pressures of 5-20 MPa are applied. The fractions obtained by the hydrothermal treatment are strongly dependent on the biochemical composition (lipids, proteins, carbohydrates and ash) of the applied biomass (Biller & Ross, 2011; Shakya *et al.*, 2017). If the operating temperature reaches a value above the critical one of the reaction solvent water (< 374 °C, 22.1 MPa), the thermochemical conversion process is called hydrothermal gasification or supercritical water gasification (López Barreiro *et al.*, 2013). Hydrothermal gasification products are mainly composed of gas, in particular CO_2, CO, CH_4 and H_2, whereas the major product fraction of liquefaction is in fluid form.

To find the optimal conversion technique for algal remnant, different aspects must

be considered. Accordingly, the energy consumption, costs and feasibility of the thermochemical conversion as well as the added value of the by-product are essential assessment criteria. As the raw material in the present work is biomass remnant, a method with low energy input is required. Here, torrefaction and liquefaction are the most promising techniques, since they can be operated at lower temperatures and pressures compared to the other methods. Regarding the reaction products, hydrothermal liquefaction seems to offer a more versatile product profile to generate high valuable by-products (see Figure 6.1). In consequence, its potential to valorize *D. salina* remnant is analyzed in the following sections.

6.2.2 Hydrothermal liquefaction as potential technique of microalgae biomass conversion

In recent years, hydrothermal liquefaction has become an attractive subject of research, especially in the area of microalgal biofuel generation (Orfield *et al.*, 2014). During pyrolysis, torrefaction and conventional gasification water act as strong inhibitor of the reaction yield. As water is the chemical reactant in the HTL approach, wet algal biomass is applicable without an energy consuming drying step (Yang *et al.*, 2004). In microalgae production processes biomass dewatering is one of the most cost-intensive production steps. Thus, product extraction technologies which operate efficiently with wet biomass are in great demand. In addition, the bio-oil yield under typical HTL conditions is significantly higher compared to that of conventional extraction because carbohydrates and proteins are partly converted into organic solubles as well (Delrue *et al.*, 2013; Frank *et al.*, 2013). The reaction is originally operated at high temperatures of 300-350 °C and pressures of 5-20 MPa (Chen *et al.*, 2015), derived from its use for lignocellulose containing raw materials. However, various studies using microalgal biomass demonstrating significant product yields even under milder conditions (e.g. Gai *et al.* (2015a); Minowa *et al.* (1995)).

The bio-oil yield is strongly determined by the biochemical composition of the used algae strain (Biller & Ross, 2011). Consequently, the highest bio-oil quantities are reached for biomass with high lipid contents. Considering the residual biomass of the β-carotene process, a low-lipid content can be expected since lipophilic compounds are extracted with the main products (pigments, triglycerides,...). For this reason, liquefaction seems to be inappropriate to effectively valorize the algal remnant of β-carotene production. However, the work of Yu *et al.* (2011) indicates, that even low-lipid biomass can be highly attractive for bio-oil production by liquefaction. Moreover, there are a various other interesting molecules (see Figure 6.2) next to bio-oil which can be found in the product fractions e.g. nutrients, organic acids, alkanes, alkenes, cyclic ketones and phenols and nitrogenous organic compounds (Biller & Ross, 2011; Brown *et al.*, 2010; Pham *et al.*, 2013). In addition, the aqueous phase obtained after liquefaction can be used as nutrient source for microalgae cultivation (Biller *et al.*, 2012; Hognon *et al.*, 2015; López Barreiro *et al.*, 2015) or as recycled liquefaction medium to improve bio-crude yields (Hu *et al.*, 2017).

In the case of β-carotene extraction up to 90% of the *D. salina* biomass remains unexploited in the production process. As the alga has no rigid cell wall, cell constituents are easily accessible and due to the small cell size a rapid heat transfer during liquefaction is possible. This could facilitate the release of other valuable products from the remnant biomass at moderate temperatures. Taking all facts together, the HTL technique seems to have the potential to beneficially convert process waste into valuable products.

6.2.3 Reaction pathways during HTL

To get an idea of the products derived from HTL, the reaction pathways in the process must be understood. In principle, liquefaction is characterized by two main reactions; the initial depolymerization of macromolecules by hydrolysis into monomers and their repolymerization into new molecules at a later stage (Garcia Alba *et al.*, 2012). The main pathways of proteins, carbohydrates and lipids in dependency of the reaction temperature are illustrated in Figure 6.2.

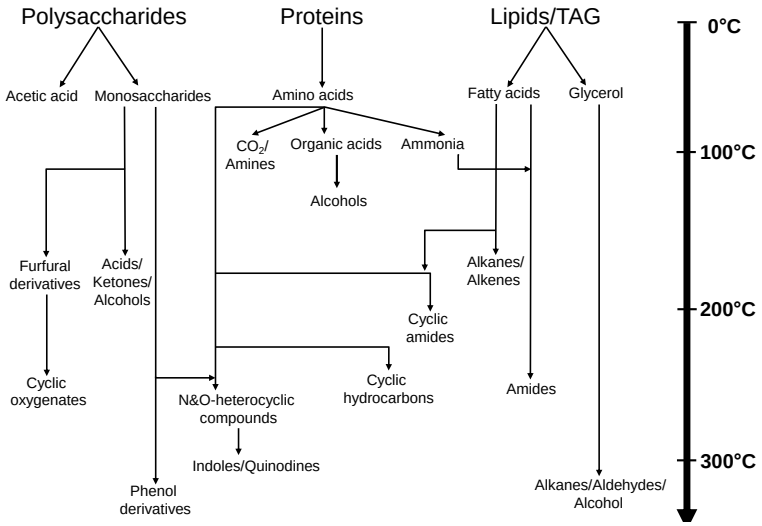

Figure 6.2: Reaction pathways of liquefaction for polysaccharides, proteins and lipids from microalgae biomass adapted from Chen *et al.* (2014) and Gai *et al.* (2015b).

As in the most biological systems, also algal lipids are mainly composed of triacylglycerols (TAGs) which are miscible in water under subcritical condition. In the initial phase of HTL the lipid polymers are hydrolyzed to generate glycerol and free fatty acids without the need of catalysts (Gai *et al.*, 2015a). Fatty acids are stable under subcritical conditions. They are further converted into long-chain hydrocarbons ($\geq C_{16}$) e.g. alkanes and alkenes which can be recovered from the bio-oil product fraction (Watanabe *et al.*, 2006). The production of short-chain hydrocarbons is suppressed

under these conditions. At temperatures around 250 °C amides are formed as a product of the cyclization reaction of the hydroxyl group in long-chained fatty acids and the ammonia derived from deamination of amino acids (Gai *et al.*, 2015b). Glycerol is a product which is present in the aqueous phase at low temperatures (Guo *et al.*, 2015). The molecule is decomposed in alcohols, light alkanes and aldehydes at temperatures above 310°C (Buehler *et al.*, 2002; Qadariyah *et al.*, 2011).

The depolymerization of polysaccharides is initiated at relatively mild conditions and results in monosaccharides like glucose, maltose, fructose and acetic acid (Chen *et al.*, 2014). Acetic acid is next to glycerol one of the most abundant products in the aqueous phase of HTL (Zhou *et al.*, 2010). The monosaccharides are further decomposed in C_1-C_3 intermediates (acids, ketones, alcohols, etc.) or dehydrated in furfural derivatives which undergo polymerization in cyclic oxygenates at temperatures above 200 °C (Chen *et al.*, 2015, 2014; López Barreiro *et al.*, 2013). Furfural derivatives as 5-hydroxylmethylfurfural (5-HMF) are rated as innovative building block chemicals for bio-based products in industry (Peterson *et al.*, 2008). The pathways of monosaccharides and amino acids from protein hydrolysis can interact by the Maillard reaction to form polycyclic nitrogenous compounds (Toor *et al.*, 2011). These chemical species are known to potentially inhibit the bio-oil yield (Yang *et al.*, 2015). At high temperatures, polysaccharides are hydrolyzed to produce phenol (Gai *et al.*, 2015b).

The initial hydrolysis of proteins results in amino acids which are either broken down into alcohols, amines, carbonic acids and CO_2 by decarboxylation or in ammonia and organic acids by deamination at intermediate temperatures between 100 and 200 °C (López Barreiro *et al.*, 2013). The CO_2 generated during degradation is one main product of the gas phase. A repolymerization of the molecules in cyclic hydrocarbons as well as cyclic amides starts at temperatures above 200 °C.

6.3 Materials and methods

6.3.1 Biomass pretreatment and analysis of its biochemical composition

D. salina biomass was purchased as a carotenoid-containing dried powder from Denk Ingredients GmbH, Germany (Art. no: 967996). Prior to hydrothermal treatment, pigments were extracted to get a remnant biomass comparable to that obtained in the β-carotene production (see Figure 6.3b). The extraction was carried out for 5 h using a Soxhlet extractor and n-hexane as extraction solvent. After the solvent has been evaporated in a rotary evaporator, the concentrated extract as well as the extracted biomass was dried overnight, respectively. The lipid content of the raw biomass was estimated from the weight of the dried, solvent free extract. The fraction of carotenoids in the biomass was measured spectroscopically using the protocol of Lichtenthaler (2001).
Contents of carbon, hydrogen, nitrogen and sulfur (CHNS) in the remnant biomass were

analyzed by elemental analysis (Currenta, Germany). The heating value HHV_{Boie} of the extracted biomass was calculated according to the Boie equation (Boie, 1953) in MJ kg^{-1}:

$$HHV_{Boie} = 0.3516C + 1.16225H - 0.1109O + 0.0628N \tag{6.1}$$

The moisture and ash contents of the extracted *D. salina* powder were determined by weight difference of samples prior and after overnight drying at 100 °C and 450 °C, respectively. The carbohydrate concentration was quantified by an enzymatic assay kit based on the determination of glucose (R-Biopharm AG, Germany). For the determination of the protein content the method of Lowry was used (Lowry *et al.*, 1951). The residual lipid content in the remnant biomass was calculated as difference of all other biochemical components from 100%.

6.3.2 Hydrothermal treatment of remnant biomass

A 200 mL stainless steel batch reactor (Picoclave 3, Büchi Labortechnik GmbH, Germany; recording software: Büchi log'n see bls2, Büchi Labortechnik GmbH) was used to hydrothermally liquefy the *D. salina* biomass (see Figure 6.3a). Therefore, the reactor

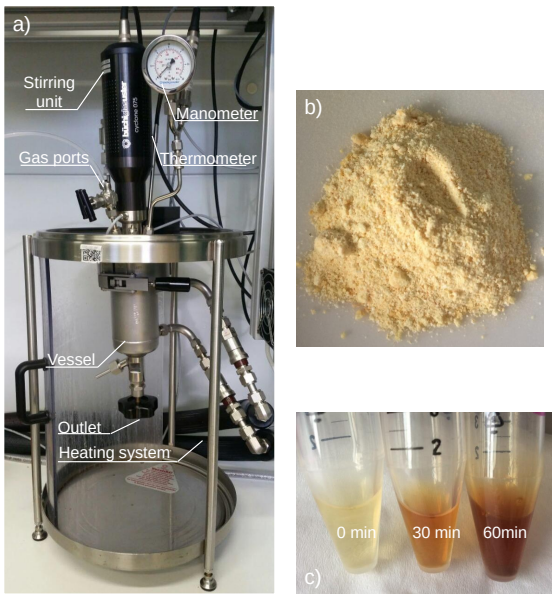

Figure 6.3: a) Hydrothermal liquefaction reactor, b) used biomass remnant and c) aqueous phase of three experiments using 180 °C and 0-60 min.

was filled with a slurry containing 6 g of the extracted biomass mixed with 100 mL bidistilled water. After sealing the reactor, the headspace was purged by nitrogen for 5 min to remove air. The reactor was operated under constant mixing with a frequency of 1800 rpm at temperatures and reaction times between 100-200 °C and 0-60 min,

respectively. The reaction time started running from the moment the set point of temperature was reached. After cooling down, the reactor content was transferred through a preweighted filter into a separation funnel. To collect any remaining lipophilic products, the reactor and stirrer were rinsed with 60 mL n-hexane. Afterwards, the n-hexane mixture was passed through another preweighted filter into the separation funnel containing the aqueous phase. Filters were dried and oil residuals in the filter and on the solid surface were recovered by applying 30 min Soxhlet extraction using 60 mL n-hexane. Thereafter, filters were dried again and weighted to determine the yield of the solid phase. The immiscible water-hexane fraction in the separation funnel was intensively mixed to extract all bio-oil products into the hydrophobic phase. After that, the biphasic mixture was allowed to separate into an aqueous and a hydrophobic n-hexane phase. To recover the bio-crude, the n-hexane phase was mixed with that obtained by Soxhlet extraction and evaporated at 40 °C and reduced pressure. For the quantification of the bio-crude fraction the remaining lipophilic substances were dried overnight. The yields of all product fractions were calculated based on the dry weight of the used biomass. The yield of the aqueous phase was determined by weighting two overnight-dried 6 mL samples of the aqueous phase. The yield of the gas phase was calculated as subtraction of all other products yields from 100%.

6.3.3 Analysis of the aqueous phase

Concentrations of glucose, fructose, sucrose, galactose and glycerol were determined in duplicates or triplicates using substrate specific enzymatic test kits (R-Biopharm AG, Germany) based on absorbance measurements at 340 nm. Nutrient concentrations were determined by ion chromatography (930 compact IC flex, Metrom, Switzerland). Concentrations of anions were measured using a Metrosep A Supp 5 column at 35 °C, an eluent containing 3.2 mM Na_2CO_3 and 1 mM $NaHCO_3$ and a flow rate of 0.7 mL min^{-1}. Cations concentrations were measured using a Metrosep C6 column at 45 °C, an eluent containing 1.7 mM HNO_3 and 1.7 mM $C_7H_5NO_4$ and a flow rate of 0.9 mL min^{-1}.

6.3.4 Cultivation experiments using glucose from the aqueous phase as carbon source

Chlorella vulgaris SAG 211.12, *Escherichia coli* MG1655 and *Saccharomyces cerevisiae* Y187 were used as model organisms to test the glucose recovered from the HTL experiments as carbon source for microbial growth. In all cultivation trials media were applied with a glucose concentrations commonly used for the individual microorganism. The respective glucose concentration in the individual control medium was adjusted by the addition of purchased glucose (Sigma-Aldrich, USA). The glucose concentration in the individual test medium was adjusted by adding appropriate volumes of the glucose-rich aqueous phase (∼48 g L^{-1} glucose) obtained by mild HTL at 100 °C to reach concentration equal to the corresponding control medium. The aqueous phase (approx. 10 mL/100 mL LB, 10 mL/100 mL BG11, 42 mL/100 mL YPD) was added to the medium before the water and pH adjustment was done. All other media ingredients

were identical in source and concentration to the described control media recipes. The pH in the control and test media was adjusted to the same value.

C. vulgaris was grown mixotrophically at a pH of 7.1 in 300 mL shaking flasks containing 100 mL BG11 medium (Stanier *et al.*, 1971) with 0.5% glucose. The cultivations were carried out in a rotary shaking incubator as previously described in (Pirwitz *et al.*, 2015b). *E. coli* was cultivated aerobically in 500 mL shaking flasks filled with 75 mL LB medium (tryptone 1%, yeast extract 0.5%, sodium chloride 0.5%, glucose 0.5%) adjusted to a pH of 7. The cultivation occurred at 37 °C and a mixing frequency of 200 rpm. Growth experiments with *S. cerevisiae* were carried out under aerobic condition using 500 mL shaking flasks filled with 100 mL YPD medium (tryptone 2%, yeast extract 1%, glucose 2%). The cultures were incubated at 30 °C and 200 rpm.
The growth of all microorganisms was followed by absorbance measurements of the cultures at 735 nm for *C. vulgaris* or 600 nm for *E. coli* and *S. cerevisiae*, respectively. The glucose consumption of the individual cultures was determined from filtrated samples of the supernatants by the previously mentioned enzymatic assay kit (see Section 6.3.3).

6.3.5 Energy and operating cost analysis of mild HTL

To calculate the additional energy demand and the operating costs for the glucose generation from the remnant biomass, the process model described by Pirwitz *et al.* (2015a) was extended by a process unit of liquefaction as illustrated in Figure 6.4. The energy consumption of liquefaction comprises the energy required for water and slurry pumping, for mixing as well as for heating. Pumping and mixing work were calculated according to the assumptions made in the process model already described in 3.2. The energy required for the heating of the algal slurry containing 6% dry weight biomass was estimated by the heat capacity equation (see Equation 5.5).

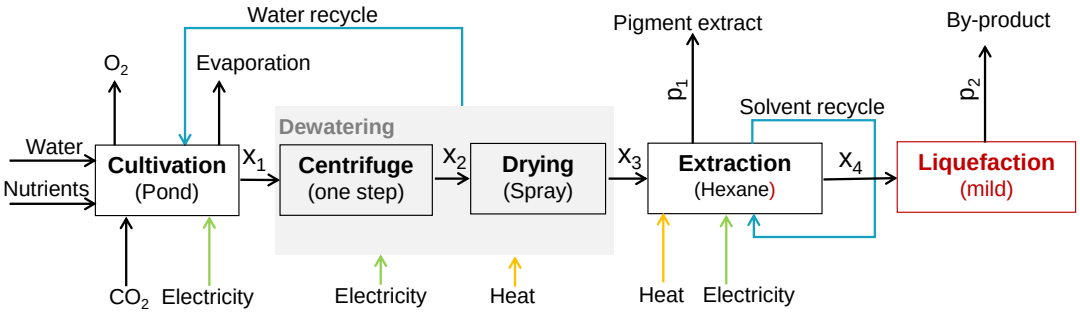

Figure 6.4: Process scheme of industrial β-carotene production by *D. salina* divided in four main subunits: cultivation of the algae for biomass generation, harvesting and dewatering of the biomass, β-carotene extraction and utilization of the residual biomass.

Liquefaction was assumed to be operated in a continuous-working isolated reactor with a working volume of 400 L. The reactor was simulated to be heated from 20 °C

to 100 °C by a conventional boiler in combination with a heat exchanger with an efficiency of 80% (Delrue *et al.*, 2013). The heat capacity of algal biomass was set to the value 1.25 kJ kg^{-1} K^{-1} (Orosz & Forney, 2008). After liquefaction the reaction mixture was separated in a separation unit. The biomass concentration as well as the biomass conversion and the yield of glucose were adopted from the results of the mild HTL experiment at 100 °C presented in this study. The total revenue of glucose was estimated considering the recent commodity price of 747.55 USD t^{-1} published by the United States Department of Agriculture (USDA, 2016).

For the consideration of uncertainties in the parameter values used in the process model, Monte Carlo simulations were applied in Matlab (MathWorks) using 5×10^5 independent normally distributed samples. The variances were defined in dependence of the used parameters as explained in Section 3.2.5.

6.4 Results and discussion

6.4.1 Potential products of the remnant biomass

The feedstock composition is one of the most influential factors on the product yields reached in HTL (Biller & Ross, 2011). For this reason, the used *D. salina* remnant was analyzed regarding its biochemical and elemental compositions prior to hydrothermal treatment. The results presented in Figure 6.5 and Table 6.1 were used to shortly discuss some potential applications of the remnant.

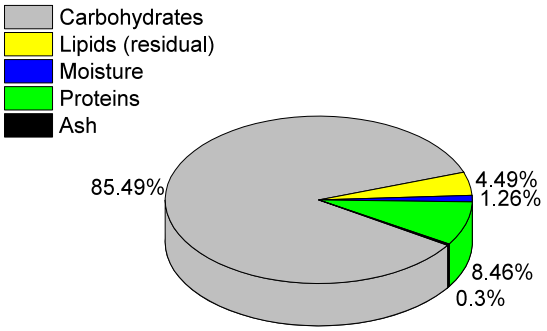

Figure 6.5: Biochemical composition of the used *D. salina* remnant.

Apart from 4.5% all hydrophilic compounds in form of lipids and carotenoids were removed from the biomass by the initial solvent extraction. Thus, the remnant biomass seems to be unattractive as a source of lipid-based fuels or unsaturated fatty acid at first sight. However, the works of Shakya *et al.* (2017) and Yu *et al.* (2011) indicate, that the liquefaction of low-lipid containing biomass can also lead to efficient bio-oil production since the source of bio-oil in the biomass is not only the lipid fraction but

Table 6.1: Elemental composition of the used *D. salina* remnant.

Element	Value wt%
C	42.5 ± 0.15
H	6.85 ± 0.5
N	<0.2
O[a]	50.34
S	<0.01

[a] calculated by difference

also the protein and the carbohydrate fraction (Biller & Ross, 2011). Thus, it seems to be possible to obtain adequate bio-oil yields even with the extracted biomass which contains less than 5% lipids.

The biomass possesses a low nitrogen content of less than 0.2%, which is also expressed by the low protein content of 8.5%. The low values are caused by the required nitrogen deprivation during β-carotene production in *D. salina*. Hence, the remnant is not a potential protein source for human nutrition or animal feed. Another approach is the recycling of nutrients recovered from the aqueous phase after liquefaction into the cultivation unit (Hognon *et al.*, 2015; López Barreiro *et al.*, 2015). However, in the present work the ash content, and thereby also the mineral salt content in the biomass is negligible. Consequently, a nutrient recycling within the *D. salina* process is not recommendable.

Generally, microalgae have a higher water content than lignocellulosic biomass, making direct combustion inefficient. However, in the present study the biomass has a low moisture content of approximately 1%. Thus, direct combustion could be an interesting alternative to utilize the remnant. The heating value of the extracted biomass was calculated according to the Boie equation (see Equation 6.1) to evaluate this approach. With a value of 17.32 MJ kg^{-1} it is low compared to lignocellulosic biomass or coal, but similar to other algal feedstocks (Chen *et al.*, 2015; Daneshvar *et al.*, 2012). Accordingly, direct combustion of the biomass comparable to lignocellulose containing feedstocks does not seem to be promising.

Interestingly, the carbohydrate content of the used *D. salina* remnant is with of 85.6% remarkably high which once again can be explained by the nitrogen deprivation under production conditions. In this state, proteins in the biomass are decomposed and lipids as well as carbohydrates serve as storage molecules for cell maintenance. As the major fraction of the storage lipids was removed by extraction, the remnant biomass mainly consists of carbohydrates (Ben-Amotz *et al.*, 2009). This macromolecule class can serve as precursor of fine chemicals and fuels (Hara *et al.*, 2014).
All in all, two potential approaches to valorize the residual biomass need to be further

investigated. On the one hand, there is the possibility to achieve satisfactory biofuel yields comparable to the above mentioned low-lipid biomass. On the other hand, the extraordinary high carbohydrate content of the biomass seems to be exploitable as most promising by-product in the overall process.

6.4.2 Influence of the reaction parameter time and temperature on HTL yields

To examine the impact of the reaction time on the yields of the gas, solid, bio-crude and aqueous fractions, liquefaction experiments were carried out for 0, 30 and 60 min at 160, 180 and 200 °C, respectively. The results of the examination are shown in Figure 6.6.

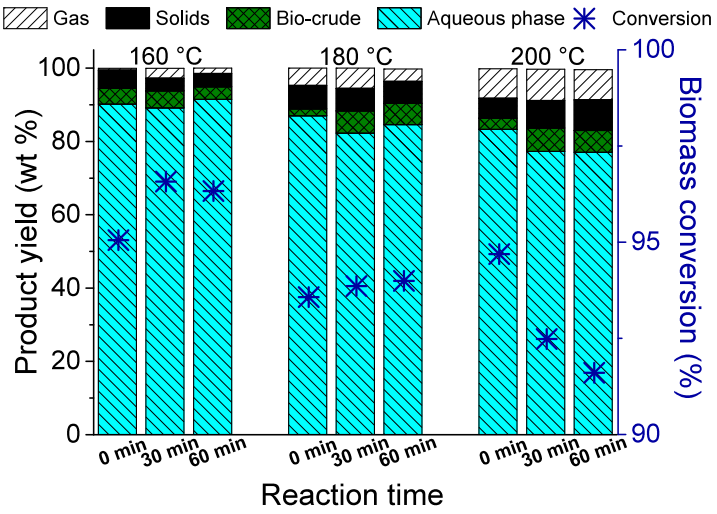

Figure 6.6: Product fractions and biomass conversion of lipid extracted *D. salina* biomass after the application of mild hydrothermal liquefaction for 0 min, 30 min and 60 min at 160, 180 and 200 °C, respectively.

There is no clear correlation between the reaction time and the product yield. After liquefaction at 180 °C as well as 200 °C, a slight increase of the bio-crude phase was visible accompanied by the decline of the aqueous phase yield. A similar behavior was described by Yu *et al.* (2011) for the low-lipid alga *Chlorella pyrenoidosa*. In addition, the liquefaction experiment at 200 °C resulted in a decreased biomass conversion with prolonged reaction times. Here, the initiation of repolymerization is indicated. At longer reaction times, the repolymerization reactions of the previously depolymerized molecules lead to higher yields of bio-crude and solid residues (Gai *et al.*, 2015a). The latter product provokes a reduced biomass conversion. For all investigated reaction times, the main part of the biomass was converted into aqueous phase components. With increasing temperature and time, the color of the aqueous phase turned from light yellow into deep brown (see Figure 6.3c). In parallel, the solid yield slightly increased to a maximum of up to 8%. These observations could be a first indication of a high

sugar content of this phase as sugars tend to visibly oxidize at higher temperatures. For comparison, in the study of Biller & Ross (2011) a solid yield of up to 20% was attained after HTL of the model compounds glucose and starch, demonstrating that carbohydrates are partly converted into solids during HTL.

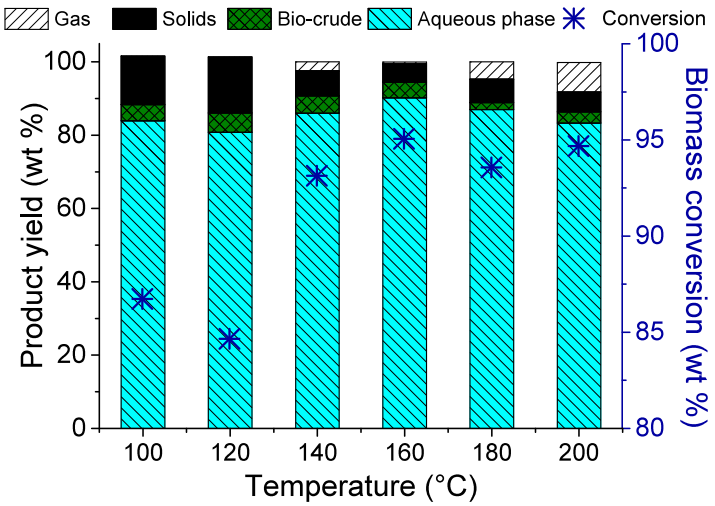

Figure 6.7: Product fractions for the biomass conversion of lipid extracted *D. salina* biomass by mild hydrothermal liquefaction at 100, 120, 140, 160, 180 and 200 °C, respectively.

Considering the pathway of liquefaction depicted in Figure 6.2, the impact of the reaction temperature on product species and yields becomes obvious. It was observed also for low-lipid-containing algae, that temperature increase leads to significantly enhanced bio-oil yields (e.g. Shakya *et al.* (2017)). The influence of this process parameter on the HTL product yields for the *D. salina* remnant is illustrated in Figure 6.7. Here, the temperature was varied from 100 to 200 °C in 20 °C steps whereas the reaction time was constantly fixed at 0 min. That means that the heating process was directly stopped after reaching the set reaction temperature. 2-6% of the extracted biomass was converted into bio-crude by mild HTL which is not sufficient for the purpose of biofuels. This phenomenon can be attributed to the previously mentioned degradation of macromolecules like proteins or carbohydrates during hydrothermal treatment (Biller & Ross, 2011). For example, Yang *et al.* (2015) demonstrated a conversion of up to 5% of pure polysaccharides into bio-oil during liquefaction which is comparable to the results achieved in our study by liquefying the carbohydrate-rich biomass.
Obviously, the yield of the solid phase declined from 15% to 5% with increasing temperature. In contrast, the gas fraction increased in line with the temperature which can be explained by the more intensive hydrothermal gasification at higher temperatures (Gai *et al.*, 2015a). Both observations are characteristic for hydrothermal liquefaction of microalgal biomass (Jena *et al.*, 2011a; López Barreiro *et al.*, 2014; Yu *et al.*, 2011).

Nevertheless, in all experiments, the yield of the gas fraction was relatively low and can be neglected as potential product source. The yield of the aqueous phase was constantly in the range of 80-90%. Thus, it represents the main product fraction of hydrothermal treatment of the residual *D. salina* biomass.

The reaction temperatures investigated in the present study are below the commonly used HTL temperatures ranges of 200 to 400 °C (Chen *et al.*, 2015; Hognon *et al.*, 2015; Toor *et al.*, 2013). In the case of *D. salina*, cell disruption as well as biomass decomposition requires less energy input than that of other microalgae species, due to the lack of a rigid cell wall. Even at a reaction temperature of 100 °C a biomass conversion level of 87% was achieved (see Figure 6.7). For higher temperatures the conversion was further improved by 10%. These results are contradicting to the low HTL conversion of 49% reached for a lipid-rich *D. salina* at 200 °C (Yang *et al.*, 2011). Accordingly, the previously done lipid extraction used in the present work seems to improve the efficiency of mild liquefaction for *D. salina* biomass.

6.4.3 Products in the aqueous phase

Taking into account the results presented in Section 6.4.2, an efficient recovery of valuable compounds from the aqueous phase of remnant biomass seems to be possible. Even at low temperatures, high amounts of solubles were released into the aqueous phase. However, the products of interest and their value need to be identified and quantified to assess the economic feasibility of the approach.

Table 6.2: Anion concentrations in the aqueous phase of HTL treated *D. salina*.

T	**t**	**Na^+**	**NH_4^+**	**K^+**	**Ca^{2+}**	**Mg^{2+}**
°C	min	mg g_{dw}^{-1}	mg g_{dw}^{-1}	mg g_{dw}^{-1}	mg g_{dw}^{-1}	mg g_{dw}^{-1}
100	0	0.16	0.01	0.18	0.41	0.13
120	0	0.14	0.01	0.15	0.35	0.11
140	0	0.15	0.01	0.14	0.32	0.15
160	0	0.39	0.01	0.20	0.61	0.18
	30	0.32	0.01	0.30	1.00	0.22
	60	0.15	0.02	0.22	1.08	0.21
180	0	0.15	0.01	0.25	0.86	0.21
	30	0.13	0.01	0.21	0.73	0.18
	60	0.24	0.02	0.16	0.62	0.15
200	0	0.17	0.01	0.22	0.84	0.22
	30	0.28	0.03	0.29	1.06	0.26
	60	0.31	0.02	0.33	1.04	0.24

Therefore, the nutrient content of the aqueous phase was analyzed by ion chromatography. The results of these analyzes are illustrated in Tables 6.2 and 6.3. Anion as well

Table 6.3: Cation concentrations in the aqueous phase of HTL treated *D. salina*.

T	t	Acetate	Formate	Cl^-	NO_2^-	NO_3^-	PO_4^{3-}	SO_4^{2-}
°C	min	mg g_{dw}^{-1}	mg g_{dw}^{-1}	mg g_{dw}^{-1}	mg g_{dw}^{-1}	mg g_{dw}^{-1}	mg g_{dw}^{-1}	mg g_{dw}^{-1}
100	0	0.70	2.24	0.42	0.04	0.45	0.52	0.52
120	0	0.60	1.92	0.36	0.03	0.39	0.45	0.45
140	0	0.86	3.23	0.35	0.03	0.36	0.57	0.47
160	0	1.12	1.96	1.04	0.05	0.68	0.83	0.74
	30	2.95	4.86	0.80	0.05	0.67	0.75	0.77
	60	2.79	4.50	0.56	0.06	0.67	0.76	0.73
180	0	5.30	15.97	0.63	0.06	0.74	0.88	0.82
	30	4.48	13.50	0.53	0.05	0.63	0.74	0.69
	60	4.01	10.42	0.54	0.05	0.57	0.67	0.86
200	0	1.49	2.30	0.41	0.04	0.51	0.59	0.54
	30	3.67	9.95	0.73	0.06	0.74	0.88	0.92
	60	3.82	12.13	0.71	0.06	0.79	0.96	0.90

as cation concentrations were detectable only in traces and significantly lower than the results obtained with other microalgal species (Biller *et al.*, 2012; López Barreiro *et al.*, 2015). The low nitrogen content of the biomass was reflected in the negligible concentrations of NH_4^+, NO_2^- and NO_3^-. Thus, the unfeasible use of the aqueous phase as protein source was once again confirmed. The crucial nutrients of the culture medium, namely, Na^+, K^+, Ca^{2+}, Mg^{2+}, SO_4^{2-}, Cl^- and PO_4^{3-} were detected in concentrations not higher than 0.1 wt% of the investigated biomass. Consequently, the recycling of the aqueous phase in the *D. salina* cultivation unit seems to be unreasonable. Interestingly, in all samples small amounts of organic acids identified as acetate and formate were detected with increasing tendency in line with temperature and reaction time (see Table 6.2). They are intermediates in the HTL pathway of polysaccharides and proteins especially for operating temperatures above 200 °C (see Figure 6.2). Green microalgae can potentially use these metabolites as carbon sources for mixotrophic growth (Biller *et al.*, 2012).

One expected product in the aqueous phase was the polar molecule glycerol (Guo *et al.*, 2015), which is a degradation product of triglycerides and a by-product in the β-carotene production located in the cytoplasm of *D. salina* (Avron, 1980). However, no detectable concentrations were measured in the samples (data not shown).
Table 6.4 summarizes the analyzed carbohydrates in the aqueous phase of HTL. Due to the lack of a rigid cell wall, cellulose as well as hemicellulose were not expected to be present in the *D. salina* samples and thus not investigated. Galactose, fructose and saccharose were present only in small portions or not detectable in the aqueous phase samples of the present study.

In contrast, glucose concentrations were remarkably high. Even at the lowest tem-

Table 6.4: Carbohydrate yields in the aqueous phase of hydrothermally treated *D. salina*.

T	t	Galactose	Fructose	Saccharose	Glucose
°C	min	wt%	wt%	wt%	wt%
100	0	n.d.	n.d.	n.d.	77.01 ± 0.39
120	0	n.d.	n.d.	n.d.	66.47 ± 5.82
140	0	n.d.	n.d.	n.d.	79.54 ± 1.18
160	0	n.d.	n.d.	2.93 ± 0.01	68.40 ± 4.43
	30	1.32 ± 0.00	n.d.	1.02 ± 0.17	62.49 ± 0.74
	60	1.60 ± 0.66	n.d.	n.d.	68.73 ± 1.12
180	0	1.60 ± 0.18	0.37 ± 0.12	n.d.	59.44 ± 1.35
	30	2.41 ± 0.04	n.d.	n.d.	65.68 ± 3.14
	60	0.38 ± 0.03	0.47 ± 0.24	n.d.	52.67 ± 0.37
200	0	2.70 ± 0.05	n.d.	1.00 ± 0.46	69.63 ± 1.39
	30	5.50 ± 0.37	n.d.	5.30 ± 2.09	69.08 ± 0.60
	60	3.66 ± 0.25	n.d.	3.73 ± 1.21	66.54 ± 0.50

perature a glucose yield of 77 wt% was reached. The glucose seems to be easily recoverable from the biomass by mild hydrothermal treatment which could be attributed to the lack of the rigid cell wall of the alga. The cell constituents such as mono- and polysaccharides are easily accessible. A rapid heat transfer during liquefaction, triggered by the small cell size, leads to high conversion yields at moderate temperatures. Hydrolysis of polysaccharides is the predominant reaction at the low reaction temperatures applied in the present work (see Figure 6.2) provoking the formation of monosaccharides such as glucose. The high glucose concentrations can be explained by the role of glucose as primary product of photosynthesis and depolymerization product of the storage molecule starch. In the present work, no clear tendency of the glucose yield with the increase of the reaction temperature or time was identified. Nevertheless, it is expected, that a further increase of the temperature above 200 °C would lead to the repolymerization of glucose into other molecules, especially 5-HMF (Peterson *et al.*, 2008; Srokol *et al.*, 2004). Similar findings were made in the work of Masarin *et al.* (2016) using *Kappaphycus alvarezii* remnant for efficient production of glucose after carrageenan extraction. However, in this study, glucose was released after the application of an enzymatic hydrolysis for 72 h. This approach is slow compared to the applied chemical hydrolysis at 100 °C in the present work. Furthermore, the need of enzymes further increase material cost in the process.

As glucose is a valuable feedstock and carbon source for chemical and biotechnological applications, it was selected as promising by-product of the β-carotene production process. Due to the fact that the high product yield of the liquefaction at 100 °C is accompanied a relatively low energy input, this scenario was used as a base of further investigations.

6.4.4 Glucose from the aqueous phase as microbial carbon source

Glucose is a commonly used organic carbon source for a wide range of microorganisms. Consequently, diverse biotechnological products can be derived from the monosaccharide. However, the extensive applicability also carries a high risk of undesired contamination for open pond cultivations using glucose as substrate. The molecule is therefore more feasible for closed bioreactor cultivations. In the following, the glucose-rich aqueous phase was applied as carbon source in the growth media of three different biotechnologically well-established production organisms, namely *E. coli*, *C. vulagaris* and *S. cerevisiae*.

In the first investigation, the bacterium *E. coli* was applied as one of the most important production organism in biotechnology. It is currently used for the production of recombinant proteins in pharmaceutical industry and for biomolecular products like amino acids and primary as well as secondary metabolites (Choi *et al.*, 2006). Due to the fact that glucose is one of the main substrates in *E. coli* fermentation, its ability to convert the liquefaction-derived glucose was investigated. For this reason, the glucose concentration in the modified cultivation medium was adjusted by addition of the aqueous phase. All other ingredients were added with identical concentrations to the control medium (see Section 6.3.4). As demonstrated in the growth curves in Figure 6.8a the bacterium was able to grow on the HTL-derived glucose with a similar behavior to the growth on control medium. In both cases, the glucose consumptions of the bacteria cultures were comparable. Accordingly, there is no inhibitory effect of the aqueous phase components aside glucose which would hamper the growth of *E. coli*. A similar conclusion was drawn for the use of the aqueous phase from HTL of *Nannochloropsis oculata* in *E. coli* as well as *Pseudomonas putida* cultivations (Nelson *et al.*, 2013). Both microorganisms revealed an improved final biomass density in the medium mixed with up to 30% of the aqueous phase which contained approximately 20 g L^{-1} organic carbon (e.g. in form of glycerol and acetate). In the case of *P. putida* even an increase in growth rate was reached for cultivation in the mixed medium compared to the control medium. In addition, a recently published life cycle analysis of algal liquefaction also demonstrated a clear beneficial effect of the use of the aqueous phase for *E. coli* cultivation on the overall process economics (Orfield *et al.*, 2014).

In the next cultivation *C. vulgaris* was chosen as a microorganism with high biotechnologically relevance. The green microalga is intensively used for biomass cultivation especially for nutritional purpose. One important product derived from *C. vulgaris* is β-1,3-glucan, which serves as immunostimulator (Richmond, 2007). Furthermore, the alga is cultivated for the production of lipid-rich flour as well as protein-rich powder applied in functional, dietary nutrition (Piechocki *et al.*, 2011). Besides photoautotrophic cultivation with CO_2, *C. vulgaris* is cultivated mixotrophically and heterotrophically by utilizing carbon sources like glucose (Richmond, 2007). Figure 6.8b illustrates that *C. vulgaris* was able to mixotrophically convert the liquefaction-derived glucose comparable to the glucose in the control medium. Both cultures grow to similar densities.

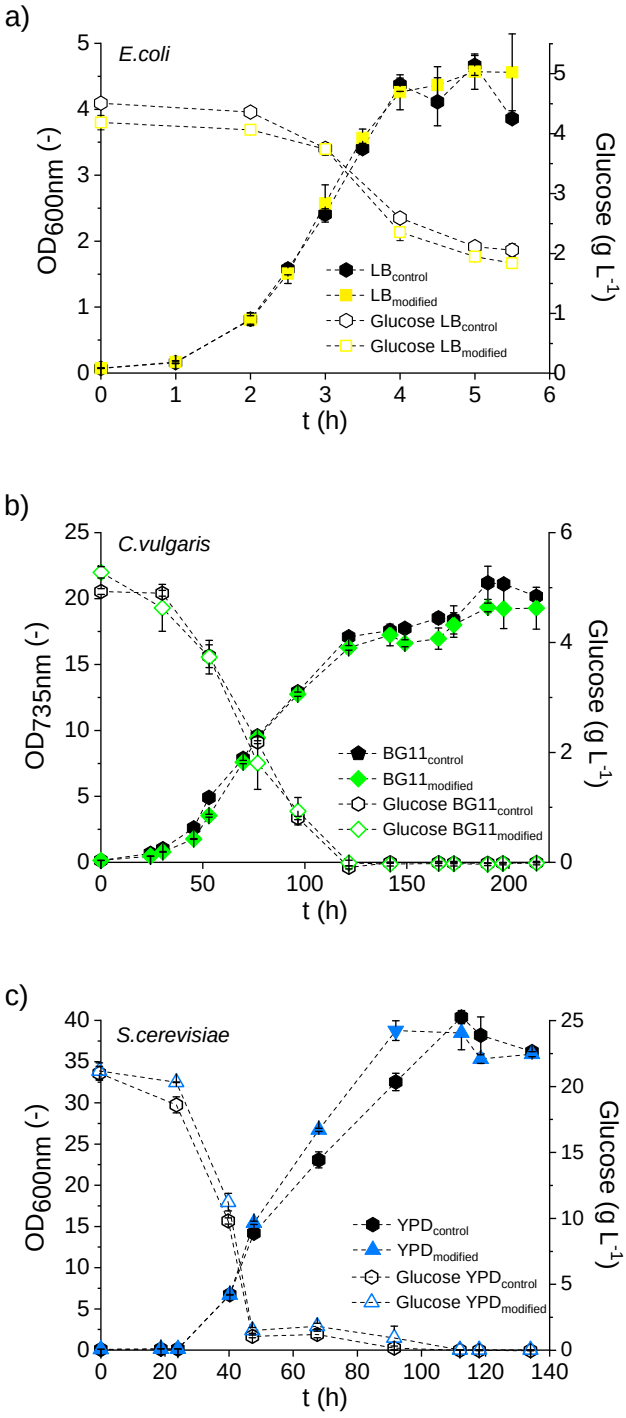

Figure 6.8: Growth and glucose consumption of a) *E. coli*, b) *C. vulgaris* and c) *S. cerevisiae* on standard culture medium and medium where the glucose concentration was adjusted by addition of the aqueous phase of liquefied *D. salina* (100 °C, 0 min). Cultivations were carried out in duplicates of shaking flasks. Error bars represent the deviation of the measurements from the average value.

Comparable results were reported by Biller *et al.* (2012), who cultivated *C. vulgaris* phototrophically on diluted aqueous phases after liquefaction to recycle nutrients and carbon sources. The alga was able to use the recycled nutrients in a 200-fold diluted aqueous phase comparable to the culture in the standard medium. However, a less diluted aqueous phase resulted in an inhibitory effect of algal growth; a phenomenon also observed in other studies (Godwin *et al.*, 2017; Jena *et al.*, 2011b). In the present work, an initial glucose concentration of 5 g L^{-1} was applied which requires an approximate 10-fold dilution of the aqueous phase. In spite of its high concentration, there was no visible inhibitory effect on mixotrophic growth caused by other substances in the aqueous phase. A possible explanation for the observation of Biller *et al.* (2012) is the presence of toxic compounds in the aqueous phase of HTL (Gai *et al.*, 2015a). Pham *et al.* (2013) revealed the correlation between cytotoxicity of the aqueous phase from HTL of *Spirulina patensis* and the presence of nitrogenous organic compounds. These compounds are generally derived from the degradation and repolymerization of carbohydrates and proteins (see Figure 6.2) during HTL at temperatures above 200 °C (Gai *et al.*, 2015a). However, the aqueous phase used in the present study was generated by hydrothermal treatment at 100 °C of low-protein biomass. Accordingly, no inhibitory effects on algal growth by nitrogenous organic compounds are expectable.

In the last cultivation experiment, the utilization potential of liquefaction-derived glucose was investigated for *S. cerevisiae*. The microorganism is currently the most frequently used yeast strain to produce a wide range of commercial platform chemicals (overview in Li & Borodina (2015)). The growth curves in Figure 6.8c indicate a comparable biomass generation and glucose consumption of cultures growing on standard medium and those growing on the modified medium. In contrast to the above mentioned work of Nelson *et al.* (2013), the growth of the yeast was not inhibited by the aqueous phase. The aqueous phase applied by Nelson *et al.* (2013) consisted of a variety of different organic carbon sources which partly inhibited the growth of *S. cerevisiae* growth. The aqueous phase derived from mild HTL of *D. salina* mainly consists of glucose (see Tables 6.2-6.4), which seems to be the preferred carbon source of the yeast. With respect to product generation, Pervez *et al.* (2014) reported an ethanol yield of 84% using *S. cerevisiae* fermentation with glucose originating from cassava starch by saccharification and liquefaction. Ethanol is one possible product derived from glucose which is largely used as secondary biofuel (Kim *et al.*, 2015).

The cultivation experiments clearly demonstrate the high potential of glucose-rich aqueous phase from HTL of *D. salina* remnant. The co-product of β-carotene production seems to be successfully applicable as carbon source for biotechnological purpose.

6.4.5 Energy and operating cost assessment of glucose production

One of the main disadvantages of HTL is the considerable energy consumption due to the high operation temperatures and pressures used in the process. To finally evaluate the results of the present work, the energy consumption and operating costs of the applied

liquefaction condition of *D. salina* were calculated. For this reason, the experimentally determined biomass concentration, biomass conversion and glucose yields of the HTL treatment of *D. salina* remnant at 100 °C were incorporated in the extended process model proposed in Sections 3.2 and 6.4.5. Uncertainties in the assumed and measured parameters were considered via Monte Carlo simulations.

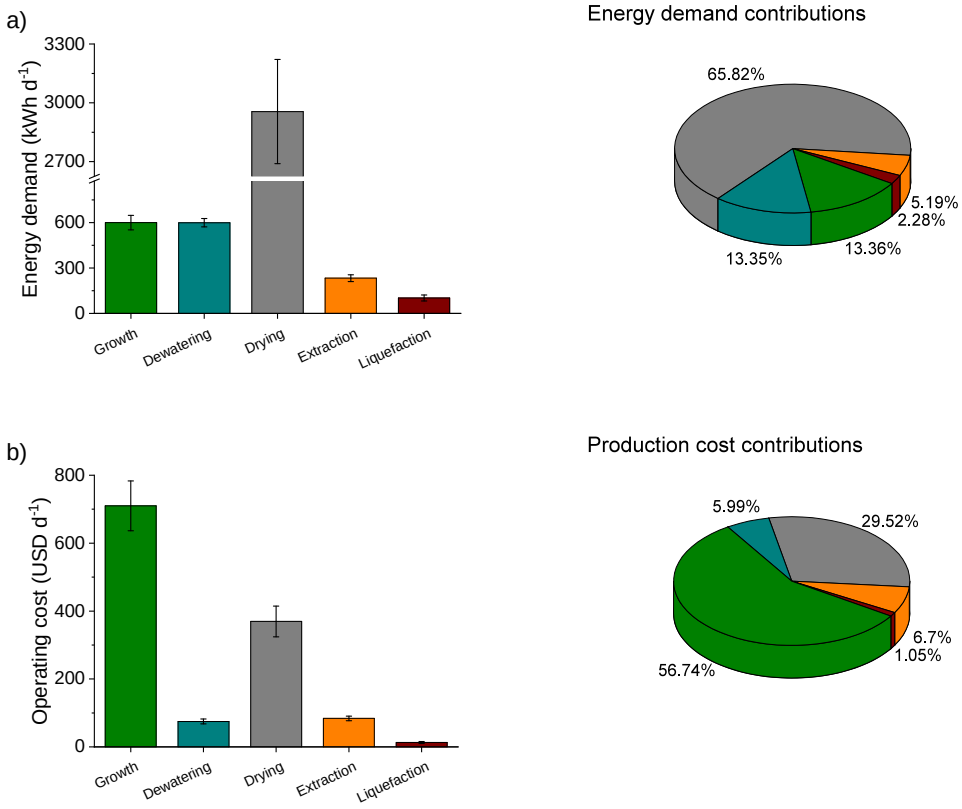

Figure 6.9: Process unit scale a) energy demand in kWh d^{-1} or % of the overall production energy as well as b) operating costs contribution in USD d^{-1} or % of the overall operation costs for industrial *D. salina* based β-carotene and glucose production. Error bars represent one standard deviation from the estimated average values based on Monte Carlo simulations.

The results of the energy and operating cost analysis for glucose production by mild HTL are depicted in Figure 6.9. With a consumption of 102 kWh d^{-1} the liquefaction needs less energy compared to all other process steps in the β-carotene production (see Figure 6.9 a). Only 2.3% of the overall energy is required to liquefy the remnant biomass. In detail, the production of one kg glucose consumes 0.74 ± 0.14 kWh energy. These results are in line with the production cost of glucose amounting to 0.09 ± 0.02 USD per kg glucose (see Figure 6.9 b). By avoiding harsh reaction con-

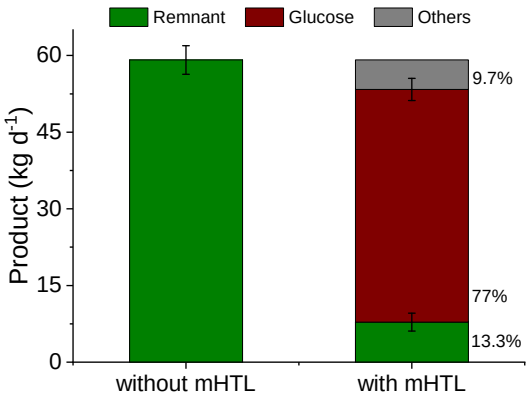

Figure 6.10: Influence of mild hydrothermal treatment on overall biomass exploitation. Error bars represent one standard deviation from the estimated average values based on Monte Carlo simulations.

ditions and the use of catalysts, an inexpensive by-product generation seems possible. Using the current market price of glucose derived from USDA (2016), a gross revenue of 34030 ± 3267 USD a^{-1} can be achieved for the annual glucose by-production. In contrast, the estimated production costs are calculated to be 4319 ± 909 USD a^{-1}.

However, it needs to be emphasized, that the gross revenue was calculated based on the price of glucose syrup. This assumption is optimistic since the product of the present work is a glucose containing aqueous solution. To achieve syrup consistency the evaporation of water is needed which would further raise the energy demand. Nevertheless, the results of the cultivation experiments reveal the successfully proven application of the glucose in the form of an aqueous solution without the need of further concentration into syrup. With respect to the biorefinery concept, Figure 6.10 highlights the high rate of remnant utilization. Here, it becomes obvious that the low valued biomass waste is mainly converted into valuable glucose. According to the results of the modeled β-carotene production process, a total production of 45.5 ± 2.2 t glucose per year can be achieved by liquefying the annual produced biomass remnant of 59.1 ± 2.8 t. Consequently, the by-product valorization using mild HTL seems to be highly beneficial for the overall process economics. With that, a holistic biorefinery concept with a more extensive exploitation of available biomass components appears feasible.

6.5 Conclusion

In the present work the potential of HTL to valorize remnant *D. salina* biomass was investigated. Mild process conditions of 100 °C and 0 min were found to be sufficient for a high biomass conversion of at least 85%. With a yield of more than 70%, glucose was the most abundant hydrolysis product in the aqueous phase. The monomer is the preferred carbon source of a numerous microorganisms, enabling its application for the production

of food, feed, pharmaceuticals and fuels. The glucose-rich aqueous phase was successfully utilized as organic carbon source in mixotrophic and heterotrophic cultivation of three microorganisms of biotechnologically relevance. Accordingly, liquefaction-derived glucose can be considered as valuable co-product of the β-carotene production process. The beneficial effect of the by-product on the overall process economics was clearly verified by the calculation of energy demand and operating costs. With these findings initial steps were done to realize a more economic and more sustainable multi-product bio-process based on *D. salina*.

7

Summary and perspectives

7.1 Concluding remarks

Currently, microalgae are intensively discussed as additional sources of biomass and valuable products that can complement agricultural biomass production. However, to become a viable alternative, the reduction of production costs is an envisaged aim of microalgae process design. Since 50-80% of the overall process costs are caused by the downstream processing (Molina Grima *et al.*, 2003), the present thesis aimed for the investigation of diverse process alternatives in the downstream route. Therefore, microalgal β-carotene production by *D. salina* was selected as a case study to assess the potential of innovative downstream technologies including flocculation, supercritical fluid extraction and by-product generation by mild hydrothermal liquefaction. The underlining evaluation approach provides the techno-economic analysis of the investigated technologies based on reliable data which have also been obtained in the course of the thesis.

For this purpose, a process model of the industrial β-carotene production by *D. salina* was developed in Chapter 3, integrating strain-dependent parameters from literature and industry. Uncertainties of the used parameters were considered by the application of Monte Carlo sampling. As a result, reference values of the operation costs, product yield and energy demand were identified for each processing unit within the production route. The reliability of the results was confirmed by the comparison with the economic data derived from the industrial *D. salina* production site in Israel. The annual process costs of 181,603 $\pm$ 19,330 USD a^{-1} as well as the biomass production cost calculated to be 17.13 $\pm$ 1.59 USD kg_{dw}^{-1} biomass are almost identical to the values reported from there (Ben-Amotz, 2008; Sun *et al.*, 2011). Accordingly, the model was found to be appropriate as reference case and working platform to assess alternative downstream routes regarding their techno-economic properties. In the sub-projects of the thesis this process model was modified or extended by the investigated downstream techniques.

Chapter 4 examined flocculation as potential preconcentration strategy for *D. salina*. Due to the high ionic culture medium, the surface potential of the alga is close to the range which allows self-aggregation. This hypothesis is supported by the results of the surface free energy calculation according to DLVO theory. With that, the preconditions for a gentle flocculation of the alga were rated as optimal. In preliminary experiments, the application of 0.3 mM $Al_2(SO_4)_3 \times 16H_2O$, 1 mM $FeCl_3 \times 6H_2O$, 20 mM NaOH and 3.4 mA cm^{-2} Al-electrolysis were selected as potential flocculation techniques to preconcentrate *D. salina*. The flocculation agent NaOH performed most efficient with a harvesting efficiency of about 93% which is comparable to that of the reference method centrifugation. Besides harvesting efficiencies and concentration factors, also the influence of flocculants on the reusability of the separated culture medium, the extractability of β-carotene and the biomass contamination were determined for each method. Among all analyzed flocculants, NaOH revealed the highest influence on further process steps. More precisely, the recycling of the separated culture medium was not feasible as well as the pigment extraction was hampered by the flocculant. These findings clearly demonstrate that a high efficiency of a certain method does not automatically result in a good performance within the overall process. Knowledge of the side-effects of the method on up- or downstream ones is essential prior to process installation. The results of the experimental study were incorporated in the extended process model to predict the operating costs and energy requirements for the diverse flocculation strategies. The simulation indicated a more energy-saving production of β-carotene from flocculated *D. salina* biomass compared to the use of conventional concentration by centrifugation. With regard to process economics and product yields, the conventional harvesting approach performed better than flocculation. Consequently, flocculation do not represents the method of choice for an effective and economic preconcentration within the β-carotene production route.

In Chapter 5 the conventional organic solvent extraction was compared to supercritical fluid extraction. Therefore, the method of Dean *et al.* (1995) was used to identify the theoretical potential of $scCO_2$ to solve β-carotene. Pilot scale experiments have shown the strong influence of the operating parameter T and p on the extraction results. Furthermore, the use of EtOH as polar co-solvent was clearly beneficial for the extraction results. By applying 70 °C, 500 bar and a co-solvent addition of 10%, comparable results to that of conventional solvent extraction were achieved. The calculation of the techno-economic properties of both extraction techniques revealed that $scCO_2$ is more energy consuming than conventional organic solvent extraction. However, product yields as well as the production costs reached equivalent values according to the simulation results. Consequently, this sub-project validates the high potential of $scCO_2$ extraction as green and sustainable alternative of conventional used hexane for the recovery of β-carotene from algal biomass. Based on the results of the present study as well as the less harmful character of $scCO_2$ and its co-solvent EtOH, the application of the extraction approach is highly recommended for installation in new production plants of *D. salina*.

A great potential of process optimization is attributed to the exploitation of the large quantity of biomass residuals in the β-carotene production process. Chapter 6 summarized possible ways of utilization. Here, mild hydrothermal liquefaction was found to be appropriate to valorize the pigment-extracted biomass. The biomass composition of the remnant possessed a carbohydrate fraction of more than 85 wt% which was mainly hydrolyzed into glucose during liquefaction. After the reaction, the monomer is dissolved in the aqueous phase. 100 °C was identified as optimal operating temperature to reach glucose yields of more than 70 wt% accompanied by relativity low energy inputs. Following the predictions of the extended process model, the application of a HTL process unit after pigment extraction significantly improves the overall process economics. The glucose-rich aqueous phase can be used for the production of biofuels or further high-value products by means of heterotrophic fermentation. Cultivation experiments of biotechnological relevant model organisms were used to demonstrate the wide spectrum of application of the HTL-product. To be more precise, the bacterium *E. coli*, the green microalga *C. vulgaris* as well as the yeast *S. cerevisiae* successfully utilized the glucose-rich aqueous phase as organic carbon source in their mixotrophic or heterotrophic cultivations. All in all, the valorization of industrial *D. salina* biomass remnant by glucose production was demonstrated for the first time. With the results of this thesis preliminary steps towards a more sustainable multi-product bio-process were done.

In conclusion, the outcomes of the thesis reveal the importance of a strain-dependent process assessment platform to evaluate the potential of upcoming techniques in microalgal biotechnology. Each species has its own properties affecting the respective processing steps within the production chain. By using only standardized numbers for the efficiencies of the individual process units, no reliable statement can be provided in terms of the economy and the yield of a certain process. In contrast, by applying exclusively strain-dependent parameter without the consideration of interlinkages between process units, the potential of an innovative approach can be overestimated. This was clearly indicated by the results of the NaOH flocculation. This preconcentration approach lead to high harvesting efficiencies making it relevant for application at the first glace. However, after consideration of the side-effects of the method it turned out, that the flocculant is not appropriate for the *D. salina* process. The new evaluation concept introduced in the thesis takes into account all these mentioned obstacles of experimental and techno-economic process assessment. With that, a general approach is provided for the reliable evaluation of the quality of an innovative technology in microalgae based production processes.

7.2 Future work

In the current work three downstream techniques were investigated regarding their potential of optimization in algal β-carotene production. Flocculation turned out to be not

appropriate for *D. salina* preconcentration. Since the industrial process is characterized be the low biomass concentration, further research and technical development are required to meet this particular challenge. Therefore, new concepts of preconcentration are needed for the reduction of the high energy cost caused by centrifugation. It might be advisable to examine the potential of chemical-free techniques, such as filtration, to address the problems of biomass and medium contamination. An interesting study in this direction was recently presented by Monte *et al.* (2018) using membrane filtration to reduce harvesting energy of industrial *D. salina* production by 45%.

Moreover, the drying step in the underlying process is the most energy consuming one which also holds true for other algal based processes. Ideally, the pigment extraction would be applicable to wet biomass to gain improved profitability by the elimination of the drying step. However, so far the extraction of wet biomass is difficult and extraction yields are far away from that reached by the extraction of dried one. The presence of water hampers the mass transfer and promotes the formation of undesired emulsion during the extraction process (Dong *et al.*, 2016). Nevertheless, there are few promising examinations demonstrating the potential of e.g. liquefied dimethyl ether or subcritical propane for the extraction of lipophilic compounds from wet algal biomass (Hoshino *et al.*, 2017; Seibert, 2012). However, further experimental efforts and economic analyzes are required to assess the feasibility of these options for algal β-carotene extraction.

Aside from mild hydrothermal liquefaction, there are diverse other potential options to valorize the residual biomass of *D. salina*. Thus, the defatted powder was tested as additive of gluten-free bread, fish sausages or chick-feed (Harvey, 2017). Moreover, a direct anaerobic digestion of the carbohydrate-rich remnant could be economical for the overall process. To keep processing cost small, the biorefinery concept should be provided with a minimum number of further downstream steps for by-product valorization (t Lam *et al.*, 2018). Therefore, it is advisable to focus on the by-product streams with a strong demand on the market under consideration of the added-value created in the process.

Regarding algal process assessment it would be helpful to establish a universal database, collecting strain-specific parameters for various promising microalgae to allow more realistic techno-economic predictions. For this purpose, the integration of large-scale data from running microalgae cultivation plants are essential to fairly evaluate the potential of new investigations. So far, industrial data are rarely published and industrial technologies are mainly protected by patent law making them difficult to access for research and development purposes. In addition, to compare the sustainability characters of competing techniques, the application of life cycle assessment should be integrated in the evaluation concept.

Appendix A

Supplementary material

A.1 Sedimentation behavior of *D. salina*

Simple sedimentation gravity was investigated in a jar test for the time course of five days. The preparation of the cells and the measurement procedure was done as described in 4.3.3.

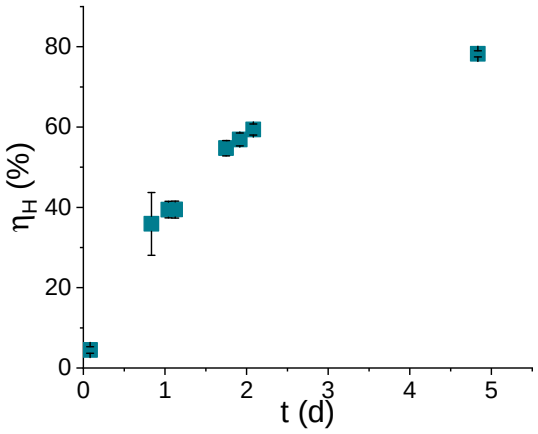

Figure A.1: Sedimentation efficiency of *D. salina* without the addition of flocculants. Experiments were conducted in duplicates. Error bars represent the deviation of the measurements from the average value.

A.2 Floc images

For the microscopic analysis of the flocs, samples were taken after the flocculation experiments described in 4.3.3.

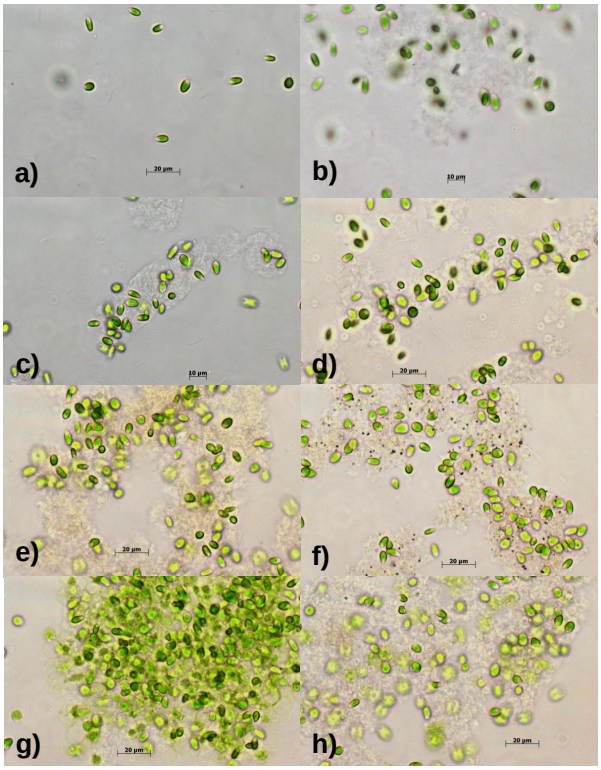

Figure A.2: Microscopic images of *D. salina* a) control cells and cells flocculated by b) electrolysis (5 min, 3.7 mA cm^{-1}), c) 0.3 mM $Al_2(SO_4)_3$, d) 1 mM $AlCl_3$, e) 1 mM $Fe_2(SO_4)_3$, f) 1 mM $FeCl_3$, g) 20 mM NaOH or h) 10 mM $Ca(OH)_2$.

A.3 Photochemical activity and cell vitality after flocculation

The photochemical activity of photosystem II (PSII) of *D. salina* was determined using pulse amplitude modulation (PAM) fluorometry (Dual-PAM-100, Walz, Germany) in order to investigate the cell stress induced by the harvesting procedure. For this purpose, 1.5 mL culture samples adjusted to 5x10^6 cells mL^{-1} were placed in a glass cuvette with 1 cm path length. Flocculated cells were decollated in the medium by resuspension, followed by a dark adaptation of 5 min at 26 °C and 150 rpm mixing frequency. The minimal (F_0) and maximum (F_m) fluorescence levels were measured using a measuring

radiation of 460 nm at 5 μE m^{-2} s^{-1} PAR (Photosynthetically active radiation), an actinic radiation of 635 nm at 166 μE m^{-2} s^{-1} and a saturating actinic excitation pulse of 635 nm at 2000 μE m^{-2} s^{-1} PAR for 0.5 s. The F_v/F_m value was calculated to quantify the maximum quantum yield of PSII $\Phi_{PSII,max}$ (biochemical efficiency of PSII) according to Butler (1978).

$$\Phi_{PSII,max} = \frac{F_v}{F_m} = \frac{F_m - F_0}{F_m} \tag{A.1}$$

Cell vitality was analyzed by flow cytometry applying the dyer fluorescein diacetate (FDA) (Hejazi *et al.*, 2004). Metabolically active cells convert the non-fluorescent FDA into green fluorescent fluorescein with the help of esterase enzymes. For the cell staining 20 μL of a FDA stock solution (2 mg mL^{-1} in acetone) was added to 1 mL of the cell suspension, mixed and incubated in the dark for 5 min at room temperature. Stained cells were analyzed by flow cytometry (Cyflow Space, Partec, Germany) with a blue argon solid state excitation laser (488 nm). To get reliable results at least 300000 particles were analyzed using a flow rate of 1 μL s^{-1} and 1.5 M NaCl solution as sheath fluid. The background signals were excluded in the analysis by considering only the particles with a red chlorophyll fluorescence emission signal. Data were acquired with FloMax software (Version 2.70, Partec, Germany). As negative control 1 mL of *D. salina* culture was heated for 5 min at 70 °C, stained and measured as described above. All results were normalized to the mean received signal strength of the control, non-flocculated cells.

Table A.1: Photosynthetic activity of photosystem II (PSII) and cells vitality of *D. salina* cells flocculated via electrolysis for 5 min at 3.4 mA cm^{-2}, the addition of 20 mM NaOH, the addition of 0.3 mM $Al_2(SO_4)_3$ or the addition of 1 mM $FeCl_3$. Experiments were conducted in duplicates. Errors represent the deviation of the measurements from the average value.

Method	**PSII activity**[a] (-)	**Cell vitality**[b] %
Control (positiv)	0.679 ± 0.003	100 ± 7.56
Control (negativ)	-	0.44
Electrolysis	0.657 ± 0.003	44.30 ± 4.08
NaOH	n.d.	64.31 ± 2.44
$Al_2(SO_4)_3$	0.693 ± 0.007	70.56 ± 0.23
$FeCl_3$	0.674 ± 0.005	60.30 ± 2.67

[a] measured by PAM fluorometry
[b] FDA-stained cells were detected by flow cytometry

A SUPPLEMENTARY MATERIAL

Bibliography

Anthony, R.J., Ellis, J.T., Sathish, A., Rahman, A., Miller, C.D. & Sims, R.C. (2013). Effect of coagulant/flocculants on bioproducts from microalgae. *Bioresource Technology*, **149**, 65–70.

Arvayo-Enriquez, H., Mondaca-Fernandez, I., Gortarez-Moroyoqui, P., Lopez-Cervantes, J. & Rodriguez-Ramirez, R. (2013). Carotenoids extraction and quantification: a review. *Analytical Methods*, **5**, 2916–2924.

Attard, T.M., McElroy, C.R. & Hunt, A.J. (2015). Economic assessment of supercritical CO_2 extraction of waxes as part of a maize stover biorefinery. *International Journal of Molecular Sciences*, **16**, 17546–17564.

Avron, A., Mordhay; Ben-Amotz (1980). Patent US 4199895: Production of glycerol, carotenes and algae meal.

Bailey Green, F., Bernstone, L.S., Lundquist, T.J. & Oswald, W.J. (1996). Advanced integrated wastewater pond systems for nitrogen removal. *Water Science and Technology*, **33**, 207–217.

Bajpai, R., Prokop, A. & Zappi, M. (2014). *Algal Biorefineries - Volume 1: Cultivation of Cells and Products*. Springer.

Baker, C.G.J. & McKenzie, K.A. (2005). Energy consumption of industrial spray dryers. *Drying Technology*, **23**, 365–386.

Barry, A., Wolfe, A., English, C., Ruddick, C. & Lambert, D. (2016). National algal biofuels technology review. Report.

Baumgardt, F.J.L., Filho, A.Z., Brandalize, M.V., da Costa, D.C., Antoniosi Filho, N.R., Abreu, P.C.O.V., Corazza, M.L. & Ramos, L.P. (2016). Lipid content and fatty acid profile of *Nannochloropsis oculata* before and after extraction with conventional solvents and/or compressed fluids. *The Journal of Supercritical Fluids*, **108**, 89–95.

Ben-Amotz, A. (1999). *Dunaliella β-carotene. From science to commerce*, vol. 1 of *Cellular Origin and Life in Extreme Habitats*, book section 31, 399–410. Kluwer Academic Publishers, Dordrecht.

Ben-Amotz, A. (2008). Bio-fuel and CO_2 capture by marine microalgae. In *Algae Biomass Summit. Seattle, WA, USA*, 1–84.

BIBLIOGRAPHY

Ben-Amotz, A. & Avron, M. (1983). On the factors which determine massive beta-carotene accumulation in the halotolerant alga *Dunaliella bardawil*. *Plant Physiology*, **72**, 593–597.

Ben-Amotz, A. & Avron, M. (1989). *The biotechnology of mass culturing Dunaliella for products of commercial interest*, 91 – 114. Longman Scientific and Technical, New York.

Ben-Amotz, A. & Avron, M. (1990). The biotechnology of cultivating the halotolerant alga *Dunaliella*. *Trends in Biotechnology*, **8**, 121–126.

Ben-Amotz, A. & Mori, N. (2014). Patent US 20120288519 A1: Method for producing β-carotene rich *Dunaliella* powder.

Ben-Amotz, A., Shaish, A. & Avron, M. (1991). The biotechnology of cultivating *Dunaliella* for production of β-carotene rich algae. *Bioresource Technology*, **38**, 233–235.

Ben-Amotz, A., Polle, J. & Subba, R.D. (2009). *The Alga Dunaliella: Biodiversity, Physiologoy, Genomics and Biotechnology*. Science Publishers, Enfield, 1st edn.

Benemann, J. (2008). Overview: Algae oil to biofuels. In *NREL-AFOSR Workshop, Algal oil for Jet Fuel Production*, 63.

Benemann, J. & Oswald, W. (1996). Systems and economic analysis of microalgae ponds for conversion of CO_2 to biomass. Final report. Report.

Benemann, J., Woertz, I. & Lundquist, T. (2011). A techno-economic analysis of open pond microalgae biofuels production. In *First International Conference on Algal Biomass, Biofuel & Bioproducts*, 44.

Besson, A. & Guiraud, P. (2013). High-pH-induced flocculation - flotation of the hypersaline microalga *Dunaliella salina*. *Bioresource Technology*, **147**, 464–470.

Biller, P. & Ross, A.B. (2011). Potential yields and properties of oil from the hydrothermal liquefaction of microalgae with different biochemical content. *Bioresource Technology*, **102**, 215–225.

Biller, P., Ross, A.B., Skill, S.C., Lea-Langton, A., Balasundaram, B., Hall, C., Riley, R. & Llewellyn, C.A. (2012). Nutrient recycling of aqueous phase for microalgae cultivation from the hydrothermal liquefaction process. *Algal Research*, **1**, 70–76.

Boie, W. (1953). Fuel technology calculations. *Energietechnik*, **3**, 309–316.

Borges, L., Caldas, S., Montes D'Oca, M.G. & Abreu, P.C. (2016). Effect of harvesting processes on the lipid yield and fatty acid profile of the marine microalga *Nannochloropsis oculata*. *Aquaculture Reports*, **4**, 164–168.

Borowitzka, L.J. & Borowitzka, M.A. (1990). Commercial production of β-carotene by *Dunaliella salina* in open ponds. *Bulletin of Marine Science*, **47**, 244–252.

Borowitzka, M.A. (2013). High-value products from microalgae-their development and commercialisation. *Journal of Applied Phycology*, **25**, 743–756.

Bos, R., van der Mei, H.C. & Busscher, H.J. (1999). Physico-chemistry of initial microbial adhesive interactions - its mechanisms and methods for study. **23**, 179–230.

Brady, P.V., Pohl, P.I. & Hewson, J.C. (2014). A coordination chemistry model of algal autoflocculation. *Algal Research*, **5**, 226–230.

Brown, T.M., Duan, P. & Savage, P.E. (2010). Hydrothermal liquefaction and gasification of *Nannochloropsis sp. Energy & Fuels*, **24**, 3639–3646.

Brunner, G. (1983). Selectivity of supercritical compounds and entrainers with respect to model substances. *Fluid Phase Equilibria*, **10**, 289–298.

Brunner, G. (1994). *Gas extraction. An introduction to fundamentals of supercritical fluids and the application to separation processes*. Springer, New York.

Brunner, G. (2005). Supercritical fluids: technology and application to food processing. *Journal of Food Engineering*, **67**, 21–33.

Buehler, W., Dinjus, E., Ederer, H.J., Kruse, A. & Mas, C. (2002). Ionic reactions and pyrolysis of glycerol as competing reaction pathways in near- and supercritical water. *The Journal of Supercritical Fluids*, **22**, 37–53.

Busscher, H.J., Weerkamp, A.H., van der Mei, H.C., van Pelt, A.W., de Jong, H.P. & Arends, J. (1984). Measurement of the surface free energy of bacterial cell surfaces and its relevance for adhesion. *Applied and Environmental Microbiology*, **48**, 980–983.

Bustamante, A., Roberts, P., Aravena, R. & del Valle, J. (2011). Supercritical extraction of astaxanthin from *Haematococcus pluvialis* using ethanol-modified CO_2, experiments and modelling. In *11th International Conference of Engineering and Food*.

Butler, W.L. (1978). *Energy distribution in the photochemical apparatus of photosynthesis*.

Carriquiry, M.A., Du, X. & Timilsina, G.R. (2011). Second generation biofuels: Economics and policies. *Energy Policy*, **39**, 4222–4234.

Casas Cardoso, L., Mantell Serrano, C., Rodríguez Rodríguez, M., Martínez de la Ossa, E.J. & Lubián, L.M. (2012). Extraction of carotenoids and fatty acids from microalgae using supercritical technology. *American Journal of Analytical Chemistry*, **3**, 877–883.

Castrillo, M., Lucas-Salas, L.M., Rodríguez-Gil, C. & Martínez, D. (2013). High pH-induced flocculation-sedimentation and effect of supernatant reuse on growth rate and lipid productivity of *Scenedesmus obliquus* and *Chlorella vulgaris*. *Bioresource Technology*, **128**, 324–329.

Chatsungnoen, T. & Chisti, Y. (2016). Harvesting microalgae by flocculation-sedimentation. *Algal Research*, **13**, 271–283.

Chaumont, D. (1993). Biotechnology of algal biomass production: a review of systems for outdoor mass culture. *Journal of Applied Phycology*, **5**, 593–604.

Chemat, F. & Abert Vian, M. (2014). *Alternative solvents for natural products extraction*. Green Chemistry and Sustainable Technology, Springer-Verlag, Berlin Heidelberg.

Chen, L., Wang, C., Wang, W. & Wei, J. (2013). Optimal conditions of different flocculation methods for harvesting *Scenedesmus sp.* cultivated in an open-pond system. *Bioresource Technology*, **133**, 9–15.

BIBLIOGRAPHY

Chen, W.H., Lin, B.J., Huang, M.Y. & Chang, J.S. (2015). Thermochemical conversion of microalgal biomass into biofuels: A review. *Bioresource Technology*, **184**, 314–327.

Chen, W.T., Zhang, Y., Zhang, J., Yu, G., Schideman, L.C., Zhang, P. & Minarick, M. (2014). Hydrothermal liquefaction of mixed-culture algal biomass from wastewater treatment system into bio-crude oil. *Bioresource Technology*, **152**, 130–139.

Chidambara Murthy, K. (2005). *Production of β-carotene from cultured Dunaliella sp. and evaluation of biological activities*. Phd thesis.

Choi, J.H., Keum, K.C. & Lee, S.Y. (2006). Production of recombinant proteins by high cell density culture of *Escherichia coli*. *Chemical Engineering Science*, **61**, 876–885.

Craft, N.E. & Soares, J.H. (1992). Relative solubility, stability, and absorptivity of lutein and beta-carotene in organic solvents. *Journal of Agricultural and Food Chemistry*, **40**, 431–434.

Şirin, S., Clavero, E. & Salvadò, J. (2013). Potential pre-concentration methods for *Nannochloropsis gaditana* and a comparative study of pre-concentrated sample properties. *Bioresource Technology*, **132**, 293–304.

Cuellar-Bermudez, S.P., Aguilar-Hernandez, I., Cardenas-Chavez, D.L., Ornelas-Soto, N., Romero-Ogawa, M.A. & Parra-Saldivar, R. (2015). Extraction and purification of high-value metabolites from microalgae: essential lipids, astaxanthin and phycobiliproteins. *Microbial Biotechnology*, **8**, 190–209.

Curtain, C.C. & Snook, H. (1983). Patent US 4554390: Method for harvesting algae.

Daneshvar, S., Salak, F., Ishii, T. & Otsuka, K. (2012). Application of subcritical water for conversion of macroalgae to value-added materials. *Industrial & Engineering Chemistry Research*, **51**, 77–84.

Danielski, L., Campos, L.M.A.S., Bresciani, L.F.V., Hense, H., Yunes, R.A. & Ferreira, S.R.S. (2007). Marigold (*Calendula officinalis L.*) oleoresin: Solubility in $scCO_2$ and composition profile. *Chemical Engineering and Processing: Process Intensification*, **46**, 99–106.

Das, D. (2015). *Algal Biorefinery: An Integrated Approach*, vol. 1. Springer-Verlag GmbH.

Davis, R., Aden, A. & Pienkos, P.T. (2011). Techno-economic analysis of autotrophic microalgae for fuel production. *Applied Energy*, **88**, 3524–3531.

Dean, J.R., Kane, M., Khundker, S., Dowle, C., Tranter, R.L. & Jones, P. (1995). Estimation and determination of steroid solubility in supercritical carbon dioxide. *The Analyst*, **120**, 2153–2157.

Del Campo, J.A., García-González, M. & Guerrero, M. (2007). Outdoor cultivation of microalgae for carotenoid production: current state and perspectives. *Applied Microbiology and Biotechnology*, **74**, 1163–1174.

Delrue, F., Setier, P.A., Sahut, C., Cournac, L., Roubaud, A., Peltier, G. & Froment, A.K. (2012). An economic, sustainability, and energetic model of biodiesel production from microalgae. *Bioresource Technology*, **111**, 191–200.

Delrue, F., Li-Beisson, Y., Setier, P.A., Sahut, C., Roubaud, A., Froment, A.K. & Peltier, G. (2013). Comparison of various microalgae liquid biofuel production pathways based on energetic, economic and environmental criteria. *Bioresource Technology*, **136**, 205–212.

Denery, J.R., Dragull, K., Tang, C.S. & Li, Q.X. (2004). Pressurized fluid extraction of carotenoids from *Haematococcus pluvialis* and *Dunaliella salina* and kavalactones from *Piper methysticum*. *Analytica Chimica Acta*, **501**, 175–181.

Dias Ribeiro, B., Weingart Barreto, D. & Zarur Coelho, M.A. (2011). Technological aspects of β-carotene production. *Food and Bioprocess Technology*, **4**, 693–701.

Dierkes, H., Steinhagen, V., Bork, M., Luetge, C. & Knez, Z. (2011). Patent US 20110183403 A1: Cell disruption of plant and animal raw materials by a combination of automization process with decompression processes for selective extraction and separation of interacellular valuable substances.

Dong, T., Knoshaug, E.P., Pienkos, P.T. & Laurens, L.M.L. (2016). Lipid recovery from wet oleaginous microbial biomass for biofuel production: A critical review. *Applied Energy*, **177**, 879–895.

Duan, J. & Gregory, J. (2003). Coagulation by hydrolysing metal salts. *Advances in Colloid and Interface Science*, **100-102**, 475–502.

Eldridge, R.J., Hill, D.R.A. & Gladman, B.R. (2012). A comparative study of the coagulation behaviour of marine microalgae. *Journal of Applied Phycology*, **24**, 1667–1679.

Farid, M.S., Shariati, A., Badakhshan, A. & Anvaripour, B. (2013). Using nano-chitosan for harvesting microalga *Nannochloropsis sp. Bioresource Technology*, **131**, 555–559.

Farooq, W., Moon, M., Ryu, B.g., Suh, W.I., Shrivastav, A., Park, M.S., Mishra, S.K. & Yang, J.W. (2015). Effect of harvesting methods on the reusability of water for cultivation of *Chlorella vulgaris*, its lipid productivity and biodiesel quality. *Algal Research*, **8**, 1–7.

Fedors, R.F. (1974). A method for estimating both the solubility parameters and molar volumes of liquids. *Polymer Engineering & Science*, **14**, 147–154.

Feroiu, V., Sima, S. & Geană, D. (2013). High pressure phase equilibrium in carbon dioxide+ethanol system. *UPB Scientific Bulletin*, **75**, 53–62.

Frank, E.D., Elgowainy, A., Han, J. & Wang, Z. (2013). Life cycle comparison of hydrothermal liquefaction and lipid extraction pathways to renewable diesel from algae. *Mitigation and Adaptation Strategies for Global Change*, **18**, 137–158.

Gai, C., Zhang, Y., Chen, W.T., Zhang, P. & Dong, Y. (2015a). An investigation of reaction pathways of hydrothermal liquefaction using *Chlorella pyrenoidosa* and *Spirulina platensis*. *Energy Conversion and Management*, **96**, 330–339.

Gai, C., Zhang, Y., Chen, W.T., Zhou, Y., Schideman, L., Zhang, P., Tommaso, G., Kuo, C.T. & Dong, Y. (2015b). Characterization of aqueous phase from the hydrothermal liquefaction of *Chlorella pyrenoidosa*. *Bioresource Technology*, **184**, 328–335.

Gao, S., Du, M., Tian, J., Yang, J., Yang, J., Ma, F. & Nan, J. (2010). Effects of chloride ions on electro-coagulation-flotation process with aluminum electrodes for algae removal. *Journal of Hazardous Materials*, **182**, 827–834.

Garcia Alba, L., Torri, C., Samorí, C., van der Spek, J., Fabbri, D., Kersten, S.R.A. & Brilman, D.W.F. (2012). Hydrothermal treatment (HTT) of microalgae: Evaluation of the process as conversion method in an algae biorefinery concept. *Energy & Fuels*, **26**, 642–657.

García-Pérez, J.S., Beuckels, A., Vandamme, D., Depraetere, O., Foubert, I., Parra, R. & Muylaert, K. (2014). Influence of magnesium concentration, biomass concentration and pH on flocculation of *Chlorella vulgaris*. *Algal Research*, **3**, 24–29.

Gavish, N. & Promislow, K. (2016). Dependence of the dielectric constant of electrolyte solutions on ionic concentration. *Physical review E*, **94**, 1–5.

Godwin, C.M., Hietala, D.C., Lashaway, A.R., Narwani, A., Savage, P.E. & Cardinale, B.J. (2017). Algal polycultures enhance coproduct recycling from hydrothermal liquefaction. *Bioresource Technology*, **224**, 630–638.

Gong, X., Zhang, B., Zhang, Y., Huang, Y. & Xu, M. (2014). Investigation on pyrolysis of low lipid microalgae *Chlorella vulgaris* and *Dunaliella salina*. *Energy and Fuels*, **28**, 95–103.

Griehl, C. & Bieler, S. (2011). Algen: Rohstoffe für Gesundheit, Schoenheit und Energie. *Nachrichten aus der Chemie*, **59**, 942–947.

Guedes, A.C., Amaro, H.M. & Malcata, F.X. (2011). Microalgae as sources of high added-value compounds-a brief review of recent work. *Biotechnology Progress*, **27**, 597–613.

Guo, Y., Yeh, T., Song, W., Xu, D. & Wang, S. (2015). A review of bio-oil production from hydrothermal liquefaction of algae. *Renewable and Sustainable Energy Reviews*, **48**, 776–790.

Hara, K.Y., Araki, M., Okai, N., Wakai, S., Hasunuma, T. & Kondo, A. (2014). Development of bio-based fine chemical production through synthetic bioengineering. *Microbial Cell Factories*, **13**, 1–18.

Harun, R., Danquah, M.K. & Forde, G.M. (2010a). Microalgal biomass as a fermentation feedstock for bioethanol production. *Journal of Chemical Technology and Biotechnology*, **85**, 199–203.

Harun, R., Singh, M., Forde, G.M. & Danquah, M.K. (2010b). Bioprocess engineering of microalgae to produce a variety of consumer products. *Renewable and Sustainable Energy Reviews*, **14**, 1037–1047.

Harvey, P.J. (2017). From development to demo: A sustainable *Dunaliella* biorefinery. In *Algae Biorefineries for Europe*.

Hejazi, M.A., Holwerda, E. & Wijffels, R.H. (2004). Milking microalga *Dunaliella salina* for β-carotene production in two-phase bioreactors. *Biotechnol Bioeng*, **85**, 475–81, hejazi, M A Holwerda, E Wijffels, R H eng Comparative Study Evaluation Studies Research Support, Non-U.S. Gov't 2004/02/05 05:00 Biotechnol Bioeng. 2004 Mar 5;85(5):475-81.

Henderson, R., Parsons, S. & Jefferson, B. (2006). Successful removal of algae through the control of zeta potential. *Separation Science and Technology*, **43**, 1653–1666.

Herrero, M., Jaime, L., Martín-Álvarez, P.J., Cifuentes, A. & Ibáñez, E. (2006). Optimization of the extraction of antioxidants from *Dunaliella salina* microalga by pressurized liquids. *Journal of Agricultural and Food Chemistry*, **54**, 5597–5603.

Ho, T.Y., Quigg, A., Finkel, Z.V., Milligan, A.J., Wyman, K., Falkowski, P.G. & Morel, F.M.M. (2003). The elemental composition of some marine phytoplankton. *Journal of Phycology*, **39**, 1145–1159.

Hognon, C., Delrue, F. & Boissonnet, G. (2015). Energetic and economic evaluation of *Chlamydomonas reinhardtii* hydrothermal liquefaction and pyrolysis through thermochemical models. *Energy*, **93**, 31–40.

Hong, Y. & Brown, D.G. (2006). Cell surface acid-base properties of *Escherichia coli* and *Bacillus brevis* and variation as a function of growth phase, nitrogen source and C:N ratio. *Colloids and Surfaces B: Biointerfaces*, **50**, 112–119.

Horiuchi, J.I., Ohba, I., Tada, K., Kobayashi, M., Kanno, T. & Kishimoto, M. (2003). Effective cell harvesting of the halotolerant microalga *Dunaliella tertiolecta* with pH control. *Journal of Bioscience and Bioengineering*, **95**, 412–415.

Hoshino, R., Ogawa, M., Murakami, K., Wahyudiono, Kanda, H. & Goto, M. (2017). Extraction of lipids from wet *Arthrospira platensis* by liquefied dimethyl ether. *Solvent Extraction Research and Development*, **24**, 47–60.

Hu, Y., Feng, S., Yuan, Z., Xu, C. & Bassi, A. (2017). Investigation of aqueous phase recycling for improving bio-crude oil yield in hydrothermal liquefaction of algae. *Bioresource Technology*, **239**, 151–159.

Ibañez, E. & Cifuentes, A. (2013). Benefits of using algae as natural sources of functional ingredients. *Journal of the Science of Food and Agriculture*, **93**, 703–709.

Illés, V., Daood, H., Biacs, P., Gnayfeed, M. & Mészáros, B. (1999). Supercritical CO_2 and subcritical propane extraction of spice red pepper oil with special regard to carotenoid and tocopherol content. *Journal of Chromatographic Science*, **37**, 345–352.

Ishida, B.K. & Chapman, M.H. (2009). Carotenoid extraction from plants using a novel, environmentally friendly solvent. *Journal of Agricultural and Food Chemistry*, **57**, 1051–1059.

Jeevan Kumar, S.P., Vijay Kumar, G., Dash, A., Scholz, P. & Banerjee, R. (2017). Sustainable green solvents and techniques for lipid extraction from microalgae: A review. *Algal Research*, **21**, 138–147.

Jena, U., Das, K.C. & Kastner, J.R. (2011a). Effect of operating conditions of thermochemical liquefaction on biocrude production from *Spirulina platensis*. *Bioresource Technology*, **102**, 6221–6229.

Jena, U., Vaidyanathan, N., Chinnasamy, S. & Das, K.C. (2011b). Evaluation of microalgae cultivation using recovered aqueous co-product from thermochemical liquefaction of algal biomass. *Bioresource Technology*, **102**, 3380–3387.

BIBLIOGRAPHY

Khoo, H.H., Koh, C.Y., Shaik, M.S. & Sharratt, P.N. (2013). Bioenergy co-products derived from microalgae biomass via thermochemical conversion - Life cycle energy balances and CO_2 emissions. *Bioresource Technology*, **143**, 298–307.

Kim, S.S., Ly, H.V., Kim, J., Lee, E.Y. & Woo, H.C. (2015). Pyrolysis of microalgae residual biomass derived from *Dunaliella tertiolecta* after lipid extraction and carbohydrate saccharification. *Chemical Engineering Journal*, **263**, 194–199.

Kiran, E., Debenedetti, P.G. & Peters, C.J. (2000). *Supercritical Fluids: Fundamentals and Applications*. Nato Science Series E, Kluwer Academic Publishers, Netherlands, 1st edn.

Kirk, J.T. (1994). *Light and Photosynthesis in Aquatic Ecosystems*, vol. 1. Cambridge University Press.

Kitada, K., Machmudah, S., Sasaki, M., Goto, M., Nakashima, Y., Kumamoto, S. & Hasegawa, T. (2009). Supercritical CO_2 extraction of pigment components with pharmaceutical importance from *Chlorella vulgaris*. *Journal of Chemical Technology & Biotechnology*, **84**, 657–661.

Klamt, A. (1995). Conductor-like screening model for real solvents: A new approach to the quantitative calculation of solvation phenomena. *The Journal of Physical Chemistry*, **99**, 2224–2235.

Knez Hrnčič, M., Škerget, M. & Knez, v. (2012). Sustainable processes using sub-and super critical fluids. In *Procedia Engineering*, vol. 42, 1788–1795.

Koller, M., Salerno, A., Tuffner, P., Koinigg, M., Boechzelt, H., Schober, S., Pieber, S., Schnitzer, H., Mittelbach, M. & Braunegg, G. (2012). Characteristics and potential of micro algal cultivation strategies: a review. *Journal of Cleaner Production*, **37**, 377–388.

Kwon, O.M., Kim, D.H., Kim, S.K. & Jeong, G.T. (2016). Production of sugars from macro-algae *Gracilaria verrucosa* using combined process of citric acid-catalyzed pretreatment and enzymatic hydrolysis. *Algal Research*, **13**, 293–297.

Kyriakopoulou, K., Papadaki, S. & Krokida, M. (2015). Life cycle analysis of β-carotene extraction techniques. *Journal of Food Engineering*, **167**, 51–58.

Lamers, P.P., van de Laak, C.C.W., Kaasenbrood, P.S., Lorier, J., Janssen, M., De Vos, R.C.H., Bino, R.J. & Wijffels, R.H. (2010). Carotenoid and fatty acid metabolism in light-stressed *Dunaliella salina*. *Biotechnology and Bioengineering*, **106**, 638–648.

Li, M. & Borodina, I. (2015). Application of synthetic biology for production of chemicals in yeast *Saccharomyces cerevisiae*. *FEMS Yeast Research*, **15**, 1–12.

Lichtenthaler, H.K. (2001). *Chlorophylls and Carotenoids: Measurement and Characterization by UV-VIS Spectroscopy*. Current Protocols in Food Analytical Chemistry, John Wiley & Sons, Inc.

Lin, J.H., Lee, D.J. & Chang, J.S. (2015). Lutein production from biomass: Marigold flowers versus microalgae. *Bioresource Technology*, **184**, 421–428.

Liss, S., Milligan, T.G., Droppo, I. & Leppard, G. (2005). *Methods for analyzing floc properties*. CRC Press.

Liu, X., Saydah, B., Eranki, P., Colosi, L.M., Greg Mitchell, B., Rhodes, J. & Clarens, A.F. (2013). Pilot-scale data provide enhanced estimates of the life cycle energy and emissions profile of algae biofuels produced via hydrothermal liquefaction. *Bioresource Technology*, **148**, 163–171.

López Barreiro, D., Prins, W., Ronsse, F. & Brilman, W. (2013). Hydrothermal liquefaction (HTL) of microalgae for biofuel production: State of the art review and future prospects. *Biomass and Bioenergy*, **53**, 113–127.

López Barreiro, D., Samorí, C., Terranella, G., Hornung, U., Kruse, A. & Prins, W. (2014). Assessing microalgae biorefinery routes for the production of biofuels via hydrothermal liquefaction. *Bioresource Technology*, **174**, 256–265.

López Barreiro, D., Bauer, M., Hornung, U., Posten, C., Kruse, A. & Prins, W. (2015). Cultivation of microalgae with recovered nutrients after hydrothermal liquefaction. *Algal Research*, **9**, 99–106.

Lowry, O.H., Rosebrough, N.J., Farr, A.L. & Randall, R.J. (1951). Protein measurement with the folin phenol reagent. *Journal of Biological Chemistry*, **193**, 265–275.

Lum, K.K., Kim, J. & Lei, X.G. (2013). Dual potential of microalgae as a sustainable biofuel feedstock and animal feed. *Journal of Animal Science and Biotechnology*, **4**, 53–53.

Lundquist, T.J., Woertz, I.C., Quinn, N. & Benemann, J.R. (2010). A realistic technology and engineering assessment of algae biofuel production. *Energy Biosciences Institute*, 178.

Ma, S., Zhou, K., Yang, K. & Lin, D. (2015). Heteroagglomeration of oxide nanoparticles with algal cells: effects of particle type, ionic strength and pH. *Environmental Science & Technology*, **49**, 932–939.

Machmudah, S., Shotipruk, A., Goto, M., Sasaki, M. & Hirose, T. (2006). Extraction of astaxanthin from *Haematococcus pluvialis* using supercritical CO_2 and ethanol as entrainer. *Industrial & Engineering Chemistry Research*, **45**, 3652–3657.

Macías-Sánchez, M.D., Mantell, C., Rodríguez, M., Martínez de la Ossa, E., Lubián, L.M. & Montero, O. (2007). Supercritical fluid extraction of carotenoids and chlorophyll a from *Synechococcus sp. The Journal of Supercritical Fluids*, **39**, 323–329.

Macías-Sánchez, M.D., Mantell, C., Rodríguez, M., Martínez de la Ossa, E., Lubián, L.M. & Montero, O. (2009a). Comparison of supercritical fluid and ultrasound-assisted extraction of carotenoids and chlorophyll a from *Dunaliella salina*. *Talanta*, **77**, 948–952.

Macías-Sánchez, M.D., Serrano, C.M., Rodríguez, M.R. & Martínez de la Ossa, E. (2009b). Kinetics of the supercritical fluid extraction of carotenoids from microalgae with CO_2 and ethanol as cosolvent. *Chemical Engineering Journal*, **150**, 104–113.

Mäki-Arvela, P., Hachemi, I. & Murzin, D.Y. (2014). Comparative study of the extraction methods for recovery of carotenoids from algae: extraction kinetics and effect of different extraction parameters. *Journal of Chemical Technology & Biotechnology*, **89**, 1607–1626.

BIBLIOGRAPHY

Marcilla, A., Catalá, L., García-Quesada, J.C., Valdés, F.J. & Hernández, M.R. (2013). A review of thermochemical conversion of microalgae. *Renewable and Sustainable Energy Reviews*, **27**, 11–19.

Martienssen, M. (2001). *Leistungen immobilisierter Mikroorganismen bei der Eliminierung von Umweltschadstoffen*. Habilitation thesis.

Martínez, J.L. (2008). *Supercritical Fluid Extraction of Nutraceuticals and Bioactive Compounds*. CRC Press, Boca Raton.

Masarin, F., Cedeno, F.R.P., Chavez, E.G.S., de Oliveira, L.E., Gelli, V.C. & Monti, R. (2016). Chemical analysis and biorefinery of red algae *Kappaphycus alvarezii* for efficient production of glucose from residue of carrageenan extraction process. *Biotechnology for Biofuels*, **9**, 122.

Mata, T.M., Martins, A.A. & Caetano, N.S. (2010). Microalgae for biodiesel production and other applications: A review. *Renewable and Sustainable Energy Reviews*, **14**, 217–232.

Mendes, R.L., Fernandes, H.L., Coelho, J.P., Reis, E.C., Cabral, J.M.S., Novais, J.M. & Palavra, A.F. (1995). Supercritical CO_2 extraction of carotenoids and other lipids from *Chlorella vulgaris*. *Food Chemistry*, **53**, 99–103.

Meullemiestre, A., Breil, C., Maryline, A.V. & Chemat, F. (2015). *Modern Techniques and Solvents for the Extraction of Microbial Oils*. SpringerBriefs in Molecular Science, Springer.

Mezzomo, N. & Ferreira, S.R.S. (2016). Carotenoids functionality, sources, and processing by supercritical technology: A review. *Journal of Chemistry*, **2016**, 16.

Minowa, T., Yokoyama, S.y., Kishimoto, M. & Okakura, T. (1995). Oil production from algal cells of *Dunaliella tertiolecta* by direct thermochemical liquefaction. *Fuel*, **74**, 1735–1738.

Mixson, S., Stikeleather, L., Simmons, I., OttoD, Wilson, C. & Burkholder, J. (2014). pH-induced flocculation, indirect electrocoagulation, and hollow fiber filtration techniques for harvesting the saltwater microalga *Dunaliella*. *Journal of Applied Phycology*, 1–9.

Mobin, S. & Alam, F. (2017). Some promising microalgal species for commercial applications: A review. *Energy Procedia*, **110**, 510–517.

Molina Grima, E., Belarbi, E.H., Acién Fernández, F.G., Robles Medina, A. & Chisti, Y. (2003). Recovery of microalgal biomass and metabolites: process options and economics. *Biotechnology Advances*, **20**, 491–515.

Monte, J., Sá, M., Galinha, C.F., Costa, L., Hoekstra, H., Brazinha, C. & Crespo, J.G. (2018). Harvesting of *Dunaliella salina* by membrane filtration at pilot scale. *Separation and Purification Technology*, **190**, 252–260.

Morales-Sánchez, D., Martinez-Rodriguez, O.A. & Martinez, A. (2017). Heterotrophic cultivation of microalgae: production of metabolites of commercial interest. *Journal of Chemical Technology & Biotechnology*, **92**, 925–936.

Moulton, T.P., Sommer, T.R., Burford, M.A. & Borowitzka, L.J. (1987). *Competition between Dunaliella species at high salinity*, vol. 41 of *Developments in Hydrobiology*, book section 15, 107–116. Springer Netherlands.

Mukhopadhyay, M. (2009). Extraction and processing with supercritical fluids. *Journal of Chemical Technology & Biotechnology*, **84**, 6–12.

Nelson, M., Zhu, L., Thiel, A., Wu, Y., Guan, M., Minty, J., Wang, H.Y. & Lin, X.N. (2013). Microbial utilization of aqueous co-products from hydrothermal liquefaction of microalgae *Nannochloropsis oculata*. *Bioresource Technology*, **136**, 522–528.

NIST (2016). Webbook, Thermophysical properties of fluid systems (date of access 07.07.2016).

Nobre, B., Marcelo, F., Passos, R., Beirao, L., Palavra, A., Gouveia, L. & Mendes, R. (2006). Supercritical carbon dioxide extraction of astaxanthin and other carotenoids from the microalga *Haematococcus pluvialis*. *European Food Research and Technology*, **223**, 787–790.

Nowicki, A., Pinder, A., Kern, S. & Daniel, G. (2009). Resource condition report for a significant Western Australian Wetland: Hutt lagoon. Unpublished report, Dept. of Environment & Conservation.

Orfield, N.D., Fang, A.J., Valdez, P.J., Nelson, M.C., Savage, P.E., Lin, X.N. & Keoleian, G.A. (2014). Life cycle design of an algal biorefinery featuring hydrothermal liquefaction: Effect of reaction conditions and an alternative pathway including microbial regrowth. *ACS Sustainable Chemistry & Engineering*, **2**, 867–874.

Orosz, M.S. & Forney, D. (2008). A comparison of algae to biofuel conversion pathways for energy storage off-grid. Report 2.62, Massachusetss Institute of Technology.

Ozkan, A. (2012). *Development of a Novel Algae Biofilm Photobioreactor for Biofuel Production*. Phd thesis.

Ozkan, A. & Berberoglu, H. (2013). Physico-chemical surface properties of microalgae. *Colloids and Surfaces B: Biointerfaces*, **112**, 287–293.

Palma, M., Barbero, G., Piñeiro, Z., Liazid, A., Barroso, C., Rostagno, M., Prado, J. & Meireles, M. (2013). *Extraction of Natural Products: Principles and Fundamental Aspects*, 58–86. Cambridge Royal Society of Chemistry, Dorchester.

Panesar, P.S., Panesar, R., Singh, R.S. & Bera, M.B. (2007). Permeabilization of yeast cells with organic solvents for β-galactosidase activity. *Research Journal of Microbiology*, **2**, 34–41.

Papazi, A., Makridis, P. & Divanach, P. (2010). Harvesting *Chlorella minutissima* using cell coagulants. *Journal of Applied Phycology*, **22**, 349–355.

Parliament, E. (2009). Directive 2009/32/EC of the european parliament and of the council of 23 april 2009 on the approximation of the laws of the member states on extraction solvents used in the production of foodstuffs and food ingredients. *Official Journal of the European Union*, **141**, 3–11.

BIBLIOGRAPHY

Pervez, S., Aman, A., Iqbal, S., Siddiqui, N.N. & Qader, S.A.U. (2014). Saccharification and liquefaction of cassava starch: an alternative source for the production of bioethanol using amylolytic enzymes by double fermentation process. *BMC Biotechnology*, **14**, 1–10.

Peterson, A.A., Vogel, F., Lachance, R.P., Froling, M., Antal, J.M.J. & Tester, J.W. (2008). Thermochemical biofuel production in hydrothermal media: A review of sub- and supercritical water technologies. *Energy & Environmental Science*, **1**, 32–65.

Petrick, I., Dombrowski, L., Kroeger, M., Beckert, T., Kuchling, T. & Kureti, S. (2013). Algae biorefinery - material and energy use of algae. Report, DBFZ Deutsches Biomasseforschungszentrum.

Pham, M., Schideman, L., Scott, J., Rajagopalan, N. & Plewa, M.J. (2013). Chemical and biological characterization of wastewater generated from hydrothermal liquefaction of *Spirulina*. *Environmental Science & Technology*, **47**, 2131–2138.

Piechocki, J., Zdanis, D., Norris, L. & Rakitsky, W. (2011). Patent: US20110256282 Lipid-rich microalgal flour food compositions.

Pirwitz, K., Flassig, R.J., Rihko-Struckmann, L.K. & Sundmacher, K. (2015a). Energy and operating cost assessment of competing harvesting methods fo *D. salina* in a β-carotene production process. *Algal Research*, **12**, 161–169.

Pirwitz, K., Rihko-Struckmann, L. & Sundmacher, K. (2015b). Comparison of flocculation methods for harvesting *Dunaliella*. *Bioresource Technology*, **196**, 145–152.

Pirwitz, K., Rihko-Struckmann, L. & Sundmacher, K. (2016). Valorization of the aqueous phase obtained from hydrothermally treated *Dunaliella salina* remnant biomass. *Bioresource Technology*, **219**, 64–71.

Pittman, J.K., Dean, A.P. & Osundeko, O. (2011). The potential of sustainable algal biofuel production using wastewater resources. *Bioresource Technology*, **102**, 17–25.

Plaza, M., Herrero, M., Cifuentes, A. & Ibáñez, E. (2009). Innovative natural functional ingredients from microalgae. *Journal of Agricultural and Food Chemistry*, **57**, 7159–7170.

Polikovsky, M., Fernand, F., Sack, M., Frey, W., MÃijller, G. & Golberg, A. (2016). Towards marine biorefineries: Selective proteins extractions from marine macroalgae *Ulva* with pulsed electric fields. *Innovative Food Science & Emerging Technologies*, **37**, 194–200.

Polle, J.E., Niyogi, K.K. & Melis, A. (2001). Absence of lutein, violaxanthin and neoxanthin affects the functional chlorophyll antenna size of photosystem-II but not that of photosystem-I in the green alga *Chlamydomonas reinhardtii*. *Plant Cell Physiology*, **42**, 482–491.

Posten, C. & Schaub, G. (2009). Microalgae and terrestrial biomass as source for fuels-a process view. *Journal of Biotechnology*, **142**, 64–69.

Potts, W.T. (1987). Patent AU-A-69260/87: Extraction of carotenoids from algae of the genus *Dunaliella*.

Pulz, O. & Gross, W. (2004). Valuable products from biotechnology of microalgae. *Applied Microbiology and Biotechnology*, **65**, 635–648.

Qadariyah, L., Mahfud, Sumarno, Machmudah, S., Wahyudiono, Sasaki, M. & Goto, M. (2011). Degradation of glycerol using hydrothermal process. *Bioresource Technology*, **102**, 9267–9271.

Quinn, J.C. & Davis, R. (2015). The potentials and challenges of algae based biofuels: A review of the techno-economic, life cycle, and resource assessment modeling. *Bioresource Technology*, **184**, 444–452.

Ramos, A.A., Polle, J., Tran, D., Cushman, J., EonSeon, J. & Varela, J.C. (2011). The unicellular green alga *Dunaliella salina Teod.* as a model for abiotic stress tolerance: genetic advances and future perspectives. *Algae*, **26**, 3–20.

Ribeiro, L.A. & Silva, P.P.d. (2013). Surveying techno-economic indicators of microalgae biofuel technologies. *Renewable and Sustainable Energy Reviews*, **25**, 89–96.

Richardson, J.W., Johnson, M.D. & Outlaw, J.L. (2012). Economic comparison of open pond raceways to photo bio-reactors for profitable production of algae for transportation fuels in the southwest. *Algal Research*, **1**, 93–100.

Richmond, A. (2007). *Handbook of microalgal culture biotechnology and applied phycology*. Blackwell Science, Oxford.

Rihko-Struckmann, L.K., Molnar, M., Pirwitz, K., Fachet, M., McBride, K., Zinser, A. & Sundmacher, K. (2017). Recovery and separation of carbohydrate derivatives from the lipid extracted alga *Dunaliella* by mild liquefaction. *ACS Sustainable Chemistry and Engineering*, **5**, 588–595.

Rizvi, S.S.H. (2010). *Separation, Extraction and Concentration Processes in the Food, Beverage and Nutraceutical Industries, 1st Edition*. Woodhead Publishing Series in Food Science, Technology and Nutrition, Woodhead Publishing.

Rizwan, M., Lee, J.H. & Gani, R. (2015). Optimal design of microalgae-based biorefinery: Economics, opportunities and challenges. *Applied Energy*, **150**, 69–79.

Rosa, P.T.V. & Meireles, M.A.A. (2005). Rapid estimation of the manufacturing cost of extracts obtained by supercritical fluid extraction. *Journal of Food Engineering*, **67**, 235–240.

Ruane, M. (1974). Patent AU 1974072395 b: Extraction of caroteniferous materials from algae.

Ruen-ngam, D., Shotipruk, A., Pavasant, P., Machmudah, S. & Goto, M. (2012). Selective extraction of lutein from alcohol treated *Chlorella vulgaris* by supercritical CO_2. *Chemical Engineering & Technology*, **35**, 255–260.

Rwehumbiza, V.M., Harrison, R. & Thomsen, L. (2012). Alum-induced flocculation of preconcentrated *Nannochloropsis salina*: Residual aluminium in the biomass, fames and its effects on microalgae growth upon media recycling. *Chemical Engineering Journal*, **200**, 168–175.

Sathish, A., Marlar, T. & Sims, R.C. (2015). Optimization of a wet microalgal lipid extraction procedure for improved lipid recovery for biofuel and bioproduct production. *Bioresource Technology*, **193**, 15–24.

BIBLIOGRAPHY

Schlesinger, A., Eisenstadt, D., Bar-Gil, A., Carmely, H., Einbinder, S. & Gressel, J. (2012). Inexpensive non-toxic flocculation of microalgae contradicts theories; overcoming a major hurdle to bulk algal production. *Biotechnology Advances*, **30**, 1023–1030.

Seibert, A. (2012). *Entwicklung eines Verfahrens zur Gewinnung von EPA-Ethylestern aus Phaeodactylum tricornutum mit überkritischen Fluiden*. Phd thesis.

Seo, Y.H., Sung, M., Kim, B., Oh, Y.K., Kim, D.Y. & Han, J.I. (2015). Ferric chloride based downstream process for microalgae based biodiesel production. *Bioresource Technology*, **181**, 143–147.

Shakya, R., Adhikari, S., Mahadevan, R., Shanmugam, S.R., Nam, H., Hassan, E.B. & Dempster, T.A. (2017). Influence of biochemical composition during hydrothermal liquefaction of algae on product yields and fuel properties. *Bioresource Technology*, **243**, 1112–1120.

Shariaty-Niassar, M., Aminzadeh, B., Azadi, P. & Soltanali, S. (2009). Economic evaluation of herb extraction using supercritical fluid. *Chemical Industry and Chemical Engineering Quarterly*, **15**, 143–148.

Spolaore, P., Joannis-Cassan, C., Duran, E. & Isambert, A. (2006). Commercial applications of microalgae. *Journal of Bioscience and Bioengineering*, **101**, 87–96.

Srokol, Z., Bouche, A.G., van Estrik, A., Strik, R.C.J., Maschmeyer, T. & Peters, J.A. (2004). Hydrothermal upgrading of biomass to biofuel; studies on some monosaccharide model compounds. *Carbohydrate Research*, **339**, 1717–1726.

Stahl, E., Quirin, K. & Gerard, D. (1987). *Verdichtete Gase zur Extraktion und Raffination*. Springer Berlin Heidelberg.

Stanier, R.Y., Kunisawa, R., Mandel, M. & Cohen-Bazire, G. (1971). Purification and properties of unicellular blue-green algae (order *Chroococcales*). *Bacteriological Reviews*, **35**, 171–205.

Sukenik, A. & Shelef, G. (1984). Algal autoflocculation-verification and proposed mechanism. *Biotechnology and Bioengineering*, **26**, 142–147.

Sun, A., Davis, R., Starbuck, M., Ben-Amotz, A., Pate, R. & Pienkos, P.T. (2011). Comparative cost analysis of algal oil production for biofuels. *Energy*, **36**, 5169–5179.

Surendranath, R., Ganga, M., Jawaharlal, M. & Anitha, K. (2016). Extraction and quantification of marigold lutein using different solvent systems. *International Journal of Pharmaceutical Sciences Review and Research*, **37**, 187–191.

t Lam, G.P., Vermue, M.H., Eppink, M.H.M., Wijffels, R.H. & van den Berg, C. (2018). Multi-product microalgae biorefineries: From concept towards reality. *Trends in Biotechnology*, **36**, 216–227.

Tafreshi, H.A. & Shariati, M. (2009). *Dunaliella* biotechnology: methods and applications. *Journal of Applied Microbiology*, **107**, 14–35.

Talisic, G.C., Yumang, A.N. & Salta, M.T.S. (2012). Supercritical fluid extraction of β-carotene from *D. salina* algae using C_2H_6 and C_2H_2. In *International Conference on Geological and Environmental Sciences IPCBEE*, vol. 3, 30–34.

Tang, Y.C. & Chen, B.H. (2000). Pigment change of freeze-dried carotenoid powder during storage. *Food Chemistry*, **69**, 11–17.

Taungbodhitham, A.K., Jones, G.P., Wahlqvist, M.L. & Briggs, D.R. (1998). Evaluation of extraction method for the analysis of carotenoids in fruits and vegetables. *Food Chemistry*, **63**, 577–584.

Teodoresco, E. (1905). *Organisation et développement du Dunaliella, nouveau genre de Volvocacée-Polyblepharidée.*, 215–232.

Toor, S.S., Rosendahl, L. & Rudolf, A. (2011). Hydrothermal liquefaction of biomass: A review of subcritical water technologies. *Energy*, **36**, 2328–2342.

Toor, S.S., Reddy, H., Deng, S., Hoffmann, J., Spangsmark, D., Madsen, L.B., Holm-Nielsen, J.B. & Rosendahl, L.A. (2013). Hydrothermal liquefaction of *Spirulina* and *Nannochloropsis salina* under subcritical and supercritical water conditions. *Bioresource Technology*, **131**, 413–419.

Uduman, N., Qi, Y., Danquah, M.K., Forde, G.M. & Hoadley, A. (2010). Dewatering of microalgal cultures: A major bottleneck to algae-based fuels. *Journal of Renewable and Sustainable Energy*, **2**, 1–15.

Uduman, N., Bourniquel, V., Danquah, M.K. & Hoadley, A.F.A. (2011). A parametric study of electrocoagulation as a recovery process of marine microalgae for biodiesel production. *Chemical Engineering Journal*, **174**, 249–257.

USDA (2016). United States Department of Agriculture; Sugar and Sweeteners Yearbook Tables; http://www.ers.usda.gov/datafiles/ sugar_and_sweeteners_yearbook_tables/ world_and_us_sugar_and_corn_sweetener_prices/ table07.xls.

van Oss, C.J. (1995). Hydrophobicity of biosurfaces - origin, quantitative determination and interaction energies. *Colloids and Surfaces B: Biointerfaces*, **5**, 91–110.

Vandamme, D., Pontes, S.C.V., Goiris, K., Foubert, I., Pinoy, L.J.J. & Muylaert, K. (2011). Evaluation of electro-coagulation-flocculation for harvesting marine and freshwater microalgae. *Biotechnology and Bioengineering*, **108**, 2320–2329.

Vandamme, D., Foubert, I., Fraeye, I., Meesschaert, B. & Muylaert, K. (2012). Flocculation of *Chlorella vulgaris* induced by high pH: Role of magnesium and calcium and practical implications. *Bioresource Technology*, **105**, 114–119.

Vandamme, D., Foubert, I. & Muylaert, K. (2013). Flocculation as a low-cost method for harvesting microalgae for bulk biomass production. *Trends in Biotechnology*, **31**, 233–239.

Vandamme, D., Muylaert, K., Fraeye, I. & Foubert, I. (2014). Floc characteristics of *Chlorella vulgaris*: Influence of flocculation mode and presence of organic matter. *Bioresource Technology*, **151**, 383–387.

Vandamme, V. (2013). *Flocculation based harvesting processes for microalgae biomass production.* Phd thesis.

VDI (2013). *VDI-Wärmeatlas der VDI-Gesellschaft Verfahrenstechnik und Chemieingenieurwesen.* Springer-Verlag, Berlin Heidelberg.

BIBLIOGRAPHY

Verrecht, B., Maere, T., Nopens, I., Brepols, C. & Judd, S. (2010). The cost of a large-scale hollow fibre MBR. *Water Research*, **44**, 5274–5283.

Wan, C., Alam, M.A., Zhao, X.Q., Zhang, X.Y., Guo, S.L., Ho, S.H., Chang, J.S. & Bai, F.W. (2014). Current progress and future prospect of microalgal biomass harvest using various flocculation technologies. *Bioresource Technology*, **184**.

Wang, B., Lan, C.Q. & Horsman, M. (2012). Closed photobioreactors for production of microalgal biomasses. *Biotechnology Advances*, **30**, 904–912.

Watanabe, M., Iida, T. & Inomata, H. (2006). Decomposition of a long chain saturated fatty acid with some additives in hot compressed water. *Energy Conversion and Management*, **47**, 3344–3350.

Weschler, M.K., Barr, W.J., Harper, W.F. & Landis, A.E. (2014). Process energy comparison for the production and harvesting of algal biomass as a biofuel feedstock. *Bioresource Technology*, **153**, 108–115.

Wijffels, R.H., Barbosa, M.J. & Eppink, M.H. (2010). Microalgae for the production of bulk chemicals and biofuels. *Biofuels, Bioproducts and Biorefining*, **4**, 287–295.

Williams, P.J.L.B. & Laurens, L.M.L. (2010). Microalgae as biodiesel & biomass feedstocks: Review & analysis of the biochemistry, energetics & economics. *Energy & Environmental Science*, **3**, 554–590.

Wu, Z., Zhu, Y., Huang, W., Zhang, C., Li, T., Zhang, Y. & Li, A. (2012). Evaluation of flocculation induced by pH increase for harvesting microalgae and reuse of flocculated medium. *Bioresource Technology*, **110**, 496–502.

Xu, L., Brilman, D.W.F., Withag, J.A.M., Brem, G. & Kersten, S. (2011). Assessment of a dry and a wet route for the production of biofuels from microalgae: Energy balance analysis. *Bioresource Technology*, **102**, 5113–5122.

Yaakob, Z., Ali, E., Zainal, A., Mohamad, M. & Takriff, M.S. (2014). An overview: biomolecules from microalgae for animal feed and aquaculture. *Journal of Biological Research*, **21**, 6.

Yang, C., Jia, L., Chen, C., Liu, G. & Fang, W. (2011). Bio-oil from hydro-liquefaction of *Dunaliella salina* over Ni/REHY catalyst. *Bioresource Technology*, **102**, 4580–4584.

Yang, W., Li, X., Li, Z., Tong, C. & Feng, L. (2015). Understanding low-lipid algae hydrothermal liquefaction characteristics and pathways through hydrothermal liquefaction of algal major components: Crude polysaccharides, crude proteins and their binary mixtures. *Bioresource Technology*, **196**, 99–108.

Yang, Y.F., Feng, C.P., Inamori, Y. & Maekawa, T. (2004). Analysis of energy conversion characteristics in liquefaction of algae. *Resources, Conservation and Recycling*, **43**, 21–33.

Yen, H.W., Chiang, W.C. & Sun, C.H. (2012). Supercritical fluid extraction of lutein from *Scenedesmus* cultured in an autotrophical photobioreactor. *Journal of the Taiwan Institute of Chemical Engineers*, **43**, 53–57.

Yen, H.W., Yang, S.C., Chen, C.H., Jesisca & Chang, J.S. (2015). Supercritical fluid extraction of valuable compounds from microalgal biomass. *Bioresource Technology*, **184**, 291–296.

Yu, G., Zhang, Y., Schideman, L., Funk, T.L. & Wang, Z. (2011). Hydrothermal liquefaction of low lipid content microalgae into bio-crude oil. *Transactions of the Asabe*, **54**, 239–246.

Zenouzi, A., Ghobadian, B., Hejazi, M. & Rahnemoon, P. (2013). Harvesting of microalgae *Dunaliella salina* using electroflocculation. *Journal of Agricultural Science and Technology*, **15**, 879–887.

Zhan, J., Rong, J. & Wang, Q. (2017). Mixotrophic cultivation, a preferable microalgae cultivation mode for biomass/bioenergy production, and bioremediation, advances and prospect. *International Journal of Hydrogen Energy*, **42**, 8505–8517.

Zhou, D., Zhang, L., Zhang, S., Hongbo, F. & Chen, J. (2010). Hydrothermal liquefaction of macroalgae *Enteromorpha prolifera* to bio-oil. *Energy & Fuels*, **24**, 4054–4061.

Zhu, L. (2014). The combined production of ethanol and biogas from microalgal residuals to sustain microalgal biodiesel: A theoretical evaluation. *Biofuels, Bioproducts and Biorefining*, **8**, 7–15.

Publications and Statements on Authorship

Peer-reviewed contributions

1. R. Sadegh-Vaziri, **K. Ludwig**, K. Sundmacher, M.U. Babler: Mechanisms behind overshoots in mean cluster size profiles in aggregation-breakup processes, *Journal of Colloid and Interface Science*, submitted (01/2018).
   K. Ludwig provided experimental data and revised the manuscript.

2. L. Rihko-Struckmann, M. Molnar, **K. Pirwitz**, M.Fachet, K. McBride, A. Zinser, K. Sundmacher: Recovery and separation of carbohydrate derivatives from the lipid extracted alga *Dunaliella* by mild liquefaction, *ACS Sustainable Chemistry and Engineering*, 2017, 5:488-495.
   K. Ludwig (née Pirwitz) provided experimental data and revised the manuscript.

3. **K. Pirwitz**, L. Rihko-Struckmann, K. Sundmacher: Valorization of the aqueous phase obtained from hydrothermally treated *Dunaliella salina* remnant biomass, *Bioresource Technology*, 2016, 219:64-71.
   K. Ludwig carried out the experiments and techno-economic calculations, analyzed the data and wrote the manuscript.

4. **K. Pirwitz**, R. J. Flassig, L. Rihko-Struckmann, K. Sundmacher: Energy and operating cost assessment of competing harvesting methods for *D. salina* in a β-carotene production process, *Algal Research*, 2015, 12:161-169.
   K. Ludwig developed the process model, carried out the experiments and techno-economic calculation, analyzed the data and wrote the manuscript.

5. **K. Pirwitz**, L. Rihko-Struckmann, K. Sundmacher: Comparison of flocculation methods for harvesting *Dunaliella*, *Bioresource Technology*, 2015, 196:145-152.
   K. Ludwig carried out the experiments, analyzed the data and wrote the manuscript.

Conference contributions

1. **K. Pirwitz**, L. Rihko-Struckmann, K. Sundmacher: Valorization of the aqueous phase from hydrothermally treated remnant biomass of *Dunaliella salina*, *3st Young Algaeneers Symposium*, Qawra, Malta, 23 - 26 April, 2016. (Oral presentation).

2. **K. Pirwitz**, L. Rihko-Struckmann, K. Sundmacher: Valorization of the aqueous phase from hydrothermally treated remnant biomass of *Dunaliella salina*, *European Networks Conference on Algal and Plant Photosynthesis (ENCAPP)*, Qawra, Malta, 26 - 29 April, 2016. (Poster presentation).

3. **K. Pirwitz**, L. Rihko-Struckmann, K. Sundmacher: Analysis of physicochemical properties of *D. salina* to assess flocculation. *10th European Congress of Chemical Engineering (ECCE) and 3rd European Congress of Applied Biotechnology (ECAB)*, Nice, France, 27 September - 1 October, 2015. (Poster presentation).

4. L. Rihko-Struckmann, **K. Pirwitz**, U. Karani, M. Molnar, R.-J. Flassig, K. Sundmacher: Mild hydrothermal liquefaction of *Dunaliella salina* for the recovery and extraction of valuable microalgal ingredients. *10th European Congress of Chemical Engineering (ECCE) and 3rd European Congress of Applied Biotechnology (ECAB)*, Nice, France, 27 September - 1 October, 2015. (Oral presentation).

5. **K. Pirwitz**, L. Rihko-Struckmann, K. Sundmacher: Investigation of different flocculation methods for *Dunaliella sp*,*4th International Conference on Algal Biomass, Biofuels and Bioproducts*, San Diego, California, United States, 7 - 10 June, 2015. (Oral presentation).

6. **K. Pirwitz**, L. Rihko-Struckmann, K. Sundmacher: Process analysis of β-carotene production by D. salina, *4th International Conference on Algal Biomass, Biofuels and Bioproducts*, Santa Fe, New Mexico, United States, 15 - 18 June, 2014. (Poster presentation).

7. **K. Pirwitz**, L. Rihko-Struckmann, K. Sundmacher: Investigation of a multi-stage production system with photosynthetic microorganisms, *2nd Young Algaeneers Symposium*, Montpellier/Narbonne, France, 3 - 5 April, 2014. (Oral presentation).

8. **K. Pirwitz**, L. Rihko-Struckmann, K. Sundmacher: Establishment of a multi-stage production system with photosynthetic microorganisms,

AlgnChem, Montpellier, France, 31 March - 3 April, 2014. (Oral presentation).

9. **K. Pirwitz**, L. Rihko-Struckmann, K. Sundmacher: Establishment of a multi-stage production system with photosynthetic organisms, *9th European Congress of Chemical Engineering (ECCE) and 2nd European Congress of Applied Biotechnology (ECAB)*, The Hague, The Netherlands, 21 - 25 April, 2013. (Poster presentation).

10. **K. Pirwitz**, H. Grammel, L. Rihko-Struckmann, K. Sundmacher: Analysis of dynamic interactions of a coculture of green algae and purple nonsulfur bacteria, *1st Young Algaeneers Symposium*, Wageningen, The Netherlands, 14 - 16 June, 2012. (Poster presentation).

Student Assistance

Supervised theses

1. T. Fläschel: *Untersuchung des Einflusses externer Parameter auf die Produktbildung der Grünalge Chlamydomonas reinhardtii unter Schwefelentzug* (Bachelor thesis, 2013, Biosystemtechnik)
2. K. Eilers: *Untersuchung des Einflusses algaler Moleküle auf ein bakterielles Quorum Sensing System* (Bachelor thesis, 2013, Biosystemtechnik)
3. A. Eichel: *Entwicklung eines Ernteverfahrens für die Mikroalge Dunaliella salina* (Bachelor thesis, 2014, Biosystemtechnik)
4. T. Lau: *Entwicklung eines Flockungsverfahrens für die Mikroalge Dunaliella bardawil* (Master thesis, 2015, Biosystemtechnik)
5. N. Hellmond: *Hydrothermale Verflüssigung von Algenrestbiomasse* (Bachelor thesis, 2015, Biosystemtechnik)

Declaration

I herewith declare that I have produced this work without the prohibited assistance of third parties and without making use of aids other than those specified; notions taken over directly or indirectly from other sources have been identified as such.

This thesis has not previously been presented in identical or similar form to any other German or foreign examination board.

Halle, March, 28th 2018

Erklärung

Ich erkläre hiermit, dass ich die vorliegende Arbeit ohne unzulässige Hilfe Dritter und ohne Benutzung anderer als der angegebenen Hilfsmittel angefertigt habe. Die aus fremden Quellen direkt oder indirekt übernommenen Gedanken sind als solche kenntlich gemacht.

Insbesondere habe ich nicht die Hilfe einer kommerziellen Promotionsberatung in Anspruch genommen. Dritte haben von mir weder unmittelbar noch mittelbar geldwerte Leistungen für Arbeiten erhalten, die im Zusammenhang mit dem Inhalt der vorgelegten Dissertation stehen.

Die Arbeit wurde bisher weder im Inland noch im Ausland in gleicher oder ähnlicher Form als Dissertation eingereicht und ist als Ganzes auch noch nicht veröffentlicht.

Halle, March, 28th 2018